# Liquid biopsies of solid tumors: Non-small-cell lung and Pancreatic cancer

by

Madumali Kalubowilage

B.Sc., University of Colombo, Sri Lanka, 2011

AN ABSTRACT OF A DISSERTATION

submitted in partial fulfillment of the requirements for the degree

DOCTOR OF PHILOSOPHY

Department of Chemistry
College of Arts and Sciences

KANSAS STATE UNIVERSITY
Manhattan, Kansas

2017

# Abstract

Cancer is a group of diseases that are characterized by uncontrolled growth and spread of cells. In order to treat cancer successfully, it is important to diagnose cancers in their early stages, because survival often depends on the stage of cancer detection. For that purpose, highly sensitive and selective methods must be developed, taking advantage of suitable biomarkers. The expression levels of proteases differ from one cancer type to the other, because different cancers arise from different cell types. According to the literature, there are significant differences between the protease expression levels of cancer patients and healthy people, because solid tumors rely on proteases for survival, angiogenesis and metastasis.

Development of fluorescence-based nanobiosensors for the early detection of pancreatic cancer and non-small-cell lung cancer is discussed in this thesis. The nanobiosensors are capable of detecting protease/arginase activities in serum samples over a broad range. The functionality of the nanobiosensor is based on Förster resonance energy transfer and surface energy transfer mechanisms.

The nanobiosensors for protease detection feature dopamine-coated $Fe/Fe_3O_4$ nanoparticles, consensus (cleavage) peptide sequences, meso-tetra(4-carboxyphenyl)porphine (TCPP), and cyanine 5.5. The consensus peptide sequences were synthesized by solid-supported peptide synthesis. In this thesis, improved consensus sequences were used, which permit faster synthesis and higher signal intensities. TCPP, which is the fluorophore of the nanoplatform, was connected to the N-terminal end of the oligopeptides while it was still on the resin. After the addition of TCPP, the TCPP-oligopeptide was cleaved off the resin and linked to the primary amine groups of $Fe/Fe_3O_4$-bound via a stable amide bond.

In the presence of a particular protease, the consensus sequences attached to the nanoparticle can be cleaved and release TCPP to the aqueous medium. Upon releasing the dye, the emission intensity increases significantly and can be detected by fluorescence spectroscopy or, similarly, by using a fluorescence plate reader. In sensing of arginase, posttranslational modification of the peptide sequence will occur, transforming arginine to ornithine. This changes the conformational dynamics of the oligopeptide tether, leading to the increase of the TCPP signal. This is a highly selective technology, which has a very low limit of detection (LOD) of $1 \times 10^{-16}$ $molL^{-1}$ for proteases and arginase.

The potential of this nanobiosensor technology to detect early pancreatic and lung cancer was demonstrated by using serum samples, which were collected from patients who have been diagnosed with pancreatic cancer and non-small cell lung cancer at the South Eastern Nebraska Cancer Center (lung cancer) and the University of Kansas Cancer Center (pancreatic cancer). As controls, serum samples collected from healthy volunteers were analyzed.

In pancreatic cancer detection, the protease/arginase signature for the detection of pancreatic adenocarcinomas in serum was identified. It comprises arginase, MMPs -1, - 3, and -9, cathepsins -B and -E, urokinase plasminogen activator, and neutrophil elastase.

For lung cancer detection, the specificity and sensitivity of the nanobiosensors permit the accurate measurements of the activities of nine signature proteases in serum samples. Cathepsin -L and MMPs-1, -3, and -7 permit detecting non-small-cell lung-cancer at stage 1.

# Liquid biopsies of solid tumors: Non-small-cell lung and Pancreatic cancer

by

Madumali Kalubowilage

B.Sc., University of Colombo, Sri Lanka, 2011

A DISSERTATION

submitted in partial fulfillment of the requirements for the degree

DOCTOR OF PHILOSOPHY

Department of Chemistry
College of Arts and Sciences

KANSAS STATE UNIVERSITY
Manhattan, Kansas

2017

Approved by:

Major Professor
Stefan H. Bossmann

# Copyright

© Madumali Kalubowilage 2017.

# Abstract

Cancer is a group of diseases that are characterized by uncontrolled growth and spread of cells. In order to treat cancer successfully, it is important to diagnose cancers in their early stages, because survival often depends on the stage of cancer detection. For that purpose, highly sensitive and selective methods must be developed, taking advantage of suitable biomarkers. The expression levels of proteases differ from one cancer type to the other, because different cancers arise from different cell types. According to the literature, there are significant differences between the protease expression levels of cancer patients and healthy people, because solid tumors rely on proteases for survival, angiogenesis and metastasis.

Development of fluorescence-based nanobiosensors for the early detection of pancreatic cancer and non-small-cell lung cancer is discussed in this thesis. The nanobiosensors are capable of detecting protease/arginase activities in serum samples over a broad range. The functionality of the nanobiosensor is based on Förster resonance energy transfer and surface energy transfer mechanisms.

The nanobiosensors for protease detection feature dopamine-coated $Fe/Fe_3O_4$ nanoparticles, consensus (cleavage) peptide sequences, meso-tetra(4-carboxyphenyl)porphine (TCPP), and cyanine 5.5. The consensus peptide sequences were synthesized by solid-supported peptide synthesis. In this thesis, improved consensus sequences were used, which permit faster synthesis and higher signal intensities. TCPP, which is the fluorophore of the nanoplatform, was connected to the N-terminal end of the oligopeptides while it was still on the resin. After the addition of TCPP, the TCPP-oligopeptide was cleaved off the resin and linked to the primary amine groups of $Fe/Fe_3O_4$-bound via a stable amide bond.

In the presence of a particular protease, the consensus sequences attached to the nanoparticle can be cleaved and release TCPP to the aqueous medium. Upon releasing the dye, the emission intensity increases significantly and can be detected by fluorescence spectroscopy or, similarly, by using a fluorescence plate reader. In sensing of arginase, posttranslational modification of the peptide sequence will occur, transforming arginine to ornithine. This changes the conformational dynamics of the oligopeptide tether, leading to the increase of the TCPP signal. This is a highly selective technology, which has a very low limit of detection (LOD) of $1 \times 10^{-16}$ $molL^{-1}$ for proteases and arginase.

The potential of this nanobiosensor technology to detect early pancreatic and lung cancer was demonstrated by using serum samples, which were collected from patients who have been diagnosed with pancreatic cancer and non-small cell lung cancer at the South Eastern Nebraska Cancer Center (lung cancer) and the University of Kansas Cancer Center (pancreatic cancer). As controls, serum samples collected from healthy volunteers were analyzed.

In pancreatic cancer detection, the protease/arginase signature for the detection of pancreatic adenocarcinomas in serum was identified. It comprises arginase, MMPs -1, - 3, and -9, cathepsins -B and -E, urokinase plasminogen activator, and neutrophil elastase.

For lung cancer detection, the specificity and sensitivity of the nanobiosensors permit the accurate measurements of the activities of nine signature proteases in serum samples. Cathepsin -L and MMPs-1, -3, and -7 permit detecting non-small-cell lung-cancer at stage 1.

# Table of Contents

# List of Figures

# List of Tables

# Acknowledgements

I would first like to express my sincere gratitude to my major research advisor and mentor, Prof. Stefan H. Bossmann, for his guidance, continuous support and encouragement throughout my PhD program. I am very grateful for him for sharing his valuable knowledge, experience, patience and suggestions throughout the last few years. His advices in research as well as in real life have been helped me to build up myself and to overcome every hard time I had during this time period. I am so grateful for him for the support and the freedom provided for me throughout my PhD program and it is a great honor to work with such an exceptional scientist and a great human being.

Besides my advisor, I would like to especially acknowledge the rest of my PhD committee: Prof. Daniel Higgins, Prof. Deryl Troyer, Prof. Christopher Culbertson and outside chairperson Prof. William Hageman for their valuable time and support.

A special thank goes to Mrs. Katharine Bossmann for being a kind, supportive and loving friend throughout the years. I highly appreciate your support, love and care given for me all the time.

I would like to acknowledge Dr. Thilani Samarakoon for her valuable advices, support and time given and for sharing her research experience with me to initiate my research in the lab and for being a great friend throughout the time. Also a special thank goes to both present and past Bossmann group members for their help and support, especially to Dr. Hongwang Wang and Dr. Sebastian Wendel.

I also extend my acknowledgements to Prof. Daniel Higgins and Prof. Emily McLaurin for allowing me to use their resources and Prof. Gary Gadbury for the contribution on statistical analysis.

I also would like to acknowledge my collaborators: Prof. Deryl L. Troyer, Department of Anatomy and Physiology, Kansas State University for his guidance in all questions related to cancer biology; Prof. Christopher Culbertson, Department of Chemistry, Kansas State University for his valuable advices.

My sincere thanks go to the graduate faculty, non-graduate faculty, staff and all the colleagues in Department of Chemistry. It was a great pleasure and a valuable opportunity to work with such talented people.

I am grateful to all the family and friends here in United States and Sri Lanka and especially to Ravithree Senanayake, Medha Gunaratne, Dr. Dinusha Udukala, Dr. Dhanushi Welideniya and Dr. Gayani Pallewela for their loving and caring friendship.

Last but not least, my deepest gratitude goes to my mother, my grandma, my aunt, my sister and brother for all the sacrifices that they have made on my behalf and for their unconditional love and support.

I am forever indebted to my late father and grandpa for their unconditional love, care and support given for my life and for showing me the path to become who I am today. Your memory will be eternal.

# Dedication

*To my loving Mom, Grandma, Aunt, Sister and Brother*

*for their unconditional love and continuous support*

*And*

*To the memory of*

*my loving Dad and Grandpa!*

# Preface

Since I joined the group of Prof. Dr. Stefan Bossmann in 2013, my graduate research was concerned with the development of nanobiosensors for the detection of proteases, kinases, and cytokines, with a special emphasis on liquid biopsies.

My research has resulted in three accepted/published and two submitted publications:

1. Patabadige, D. E. W.; Sadeghi, J.; Kalubowilage, M.; Bossmann, S. H.; Culbertson, A. H.; Latifi, H.; Culbertson, C. T., Integrating Optical Fiber Bridges in Microfluidic Devices to Create Multiple Excitation/Detection Points for Single Cell Analysis. *Anal. Chem.* **2016,** *88* (20), 9920-9925.
2. Voelz, B. E.; Kalubowilage, M.; Bossmann, S. H.; Troyer, D. L.; Chebel, R. C.; Mendonca, L. G. D., Associations between concentrations of arginase or matrix metalloproteinase-8 (MMP-8) and metritis in periparturient dairy cattle *Reproductive Biology and Endocrinology* **2016,** *accepted.*
3. Maroto, R.; Zhao, Y.; Jamaluddin, M.; Popov, V. L.; Wang, H.; Kalubowilage, M.; Zhang, Y.; Luisi, J.; Sun, H.; Culbertson, C. T.; Bossmann, S. H.; Motamedi, M.; Brasier, A. R., Effects of storage conditions on airway exosome integrity for diagnostic and functional analyses. *Journal of Extracellular Vesicles* **2017,** *accepted*.

My thesis is focusing on the research that is reported in the following manuscripts, where I am either first author or one of the equally contributing authors.

4. Udukala, D.; Wendel, S.; Kalubowilage, M.; Wang, H.; Malalasekera, A. P.; Yapa, A. S.; Toledo, Y.; Ortega, R.; Maynez, P.; Bossmann, L.; Janik, K.; Gadbury, G.; Troyer, D. L.; Bossmann, S. H., Early Detection of Non-Small-Cell Lung Cancer in Liquid Biopsies by Ultrasensitive Fluorescence Nanobiosensors. *ACS Nano* **2017,** *submitted*.
5. Kalubowilage, M.; Malalasekera, A.; Covarrubias-Zambrano, O.; Wendel, S. O.; Wang, H.; Yapa, A. S.; Chlebanowski, L.; Toledo, Y.; Ortega, R.; Janik, K.; Gadbury, G.; Kasi, A.; Williamson, S.; Troyer, D. L.; Bossmann, S. H., Early Detection of Pancreatic Cancers in Liquid Biopsies by Ultrasensitive Fluorescence Nanobiosensors. *Nanomedicine NBM* **2017,** *submitted*.

In the research that is reported in both manuscripts, I have synthesized and purified peptide sequences and have assembled, purified, and characterized functional nanobiosensors. Furthermore, I have designed and carried out the fluorescence plate reader experiments, which led to the data reported here. I was a member of the team that did the data analysis.

I would like to thank Dr. Hongwang Wang for synthesizing the $Fe/Fe_3O_4$-nanoparticles, Dr. Malalasekera for the development of the arginase sensor and design of fluorescence plate reader experiments, Prof. Dr. Gary Gadbury, Dr. Sebastian Wendel and Ms. Obdulia Covarrubias-Zambrano for their help with the statistical data analysis and gene expression analysis, Dr. Dinusha Udukala, Ms. Asanka Yapa, Ms. Lauren Chlebanowski, Ms. Obdulia Covarrubias-Zambrano, Ms. Yubisela Toledo, Ms. Raquel Ortega, Ms. Pamela Maynez, and Ms. Leonie Bossmann for their synthetic contributions, and Ms. Katharine Janik-Bossmann for her help with the software and the use of the English language.

My thanks go to Prof. Anup Kasi, MD and Prof. Stephen Williamson, MD, as well as the staff of the Southeastern Nebraska Cancer Center, for the serum samples. I extend my thanks to

Prof. Dr. Deryl L. Troyer for his guidance in all questions related to cancer biology and the practical art of working with blood samples.

Finally, I would like to acknowledge my major research advisor and mentor, Dr. Stefan H. Bossmann, for sharing his knowledge, experience, suggestions and the support given to make these projects successful.

# Chapter 1 - Biochemical Foundations of Diagnosing Solid Tumors in Lung and Pancreas by Means of Liquid Biopsies

## 1.1 Introduction

Cancer is a group of diseases that are characterized by an uncontrolled growth and spread of cells. Cancer can develop anywhere in the human body, and produce large number of cells. In a healthy human body, cells normally grow up and divide in order to make new cells according to the body's needs. If these cells are damaged or aged, they die and new cells replace them. This process runs as a cycle. When a cancer starts to develop, cells become more and more abnormal. With the development of cancer, new cells develop even if they are not required and old cells, which are supposed to die, survive their damages and become virtually immortal. The unstoppable division of cells form cell growths called tumors. There are different types of tumors. Many of them form solid tumors, which contain solid masses of tissue.[1]

Cancer can develop due to external factors, as well as internal factors. Cancers occur due to external factors, such as the usage of tobacco, infectious organisms, as well as exposure to chemicals and radiation, are avoidable. But the development of a cancer due to internal factors, such as inherited mutations, hormones, immune conditions, and mutations that occur due to changes in the metabolism, are unavoidable. These factors can act together or individually to initiate a cancer in a human body.

Cancers can be categorized into different stages. The "stage of cancer" is the stage where the cancer was at when it was first diagnosed. In stage 0, cancer is in the position where it started. Some cancers never go beyond this early stage. At stage 1, which is called localized cancer, cells gain the ability to pass through the "basement membrane" but remain as a single lump. Cancer stays partly in the tissue where it began and partly in a neighboring tissue. In stages 2 and 3, cancer

cells can invade lymph nodes and then divide, forming a lump in the lymph node. This is called "regional spread". There, the cancer has spread within the general region in which it first began but not to other parts of the body. Stage 4 is referred to as the "distant spread". In this stage, cells invade the blood stream, and then can go anywhere in the body to form new colonies and spread further. Identifying the stage of the cancer is very important because it is a critical factor in deciding the best way to treat the cancer.[2]

There are more than 100 types of cancer. Cancers are usually named based on the organs or tissues where the cancers form. There are several ways to treat cancer, such as surgery, radiation, chemotherapy, hormone therapy, biological therapy, and targeted therapy.[3] Regular screening examinations can help detecting cancer at its early stages, as well as removal of precancerous growths. Cancers developing in cervix, colon, and rectum can be prevented by removal of precancerous tissue. Cancers that can be diagnosed early via screening include cancers of the breast, colon, rectum, cervix, prostate, oral cavity, and skin.[3]

Eventhough anyone can develop cancer, the risk of being diagnosed with a cancer increases with age. According to the statistics, about 77% of all cancers are diagnosed in persons 55 years of age and older.[3] According to the statistics, the probability of developing a particular type of cancer and the mortality depends on the gender as well.

**Estimated Deaths**

| Males | | | Females | | |
|---|---|---|---|---|---|
| Lung & bronchus | 85,920 | 27% | Lung & bronchus | 72,160 | 26% |
| Prostate | 26,120 | 8% | Breast | 40,450 | 14% |
| Colon & rectum | 26,020 | 8% | Colon & rectum | 23,170 | 8% |
| Pancreas | 21,450 | 7% | Pancreas | 20,330 | 7% |
| Liver & intrahepatic bile duct | 18,280 | 6% | Ovary | 14,240 | 5% |
| Leukemia | 14,130 | 4% | Uterine corpus | 10,470 | 4% |
| Esophagus | 12,720 | 4% | Leukemia | 10,270 | 4% |
| Urinary bladder | 11,820 | 4% | Liver & intrahepatic bile duct | 8,890 | 3% |
| Non-Hodgkin lymphoma | 11,520 | 4% | Non-Hodgkin lymphoma | 8,630 | 3% |
| Brain & other nervous system | 9,440 | 3% | Brain & other nervous system | 6,610 | 2% |
| **All Sites** | **314,290** | **100%** | **All Sites** | **281,400** | **100%** |

**Figure 1: 2016 Estimated US Cancer Cases** (Taken with permission of Reference [4])

## 1.2 Early cancer detection

In order to treat cancer successfully, it is important to diagnose cancer in early stages. Therefore, it is required to have highly sensitive methods to measure cancer diagnosis markers. Early diagnosis of cancer leads to better treatment methods and thereby reduce the mortality rate by increasing the survival rate.

Most of the cancer related diagnostics have been studied using enzyme-linked immunosorbent assay (ELISA). ELISA is a common laboratory technique which is used to measure the concentration of an analyte (usually antibodies or antigens) in a solution. In cancer diagnostics, ELISA is used to measure the protease/protein concentrations in biological samples.[5] But it is hard to determine the activity of different types of proteases which are associated with cancer by using ELISA. Proteases usually occur as inactive precursors (zymogens), active enzymes or enzyme inhibitor complexes which makes difficult in measuring activity to analyze stages of the cancer.

Apart from ELISA, there are different methods use to diagnose cancer. Electrochemical biosensors[6], immunohistochemical methods[7], chemiluminescence immunosensors[8] and

fluorescence in situ hybridization[9] are few of those widely used methods. Eventhough these methods have been used widely to detect cancer, early detection of cancer has become a challenge due to the lack of sensitivity of the techniques. It is required to have highly sensitive techniques to detect very low molar concentrations of cancer related biomarkers.

The research I have included in my thesis are based on a development of fluorescence based nanobiosensors[10] for the early detection of pancreatic cancer and lung cancer. This is a previously established method and has been used for early detection of breast cancer.[11] In my research, the similar technique is used to detect pancreatic and lung cancer in their early stages. The functionality of the nanobiosensors are based on the Förster resonance energy transfer mechanism.

## 1.3 Förster resonance energy transfer (FRET)

FRET is defined as radiationless energy transfer from an energetically excited fluorophore (donor) to another molecule (acceptor) through dipole-dipole coupling through space. After FRET has completed, the excited acceptor molecule loses its energy via photon emission or internal conversion and returns back to the ground state.[12]

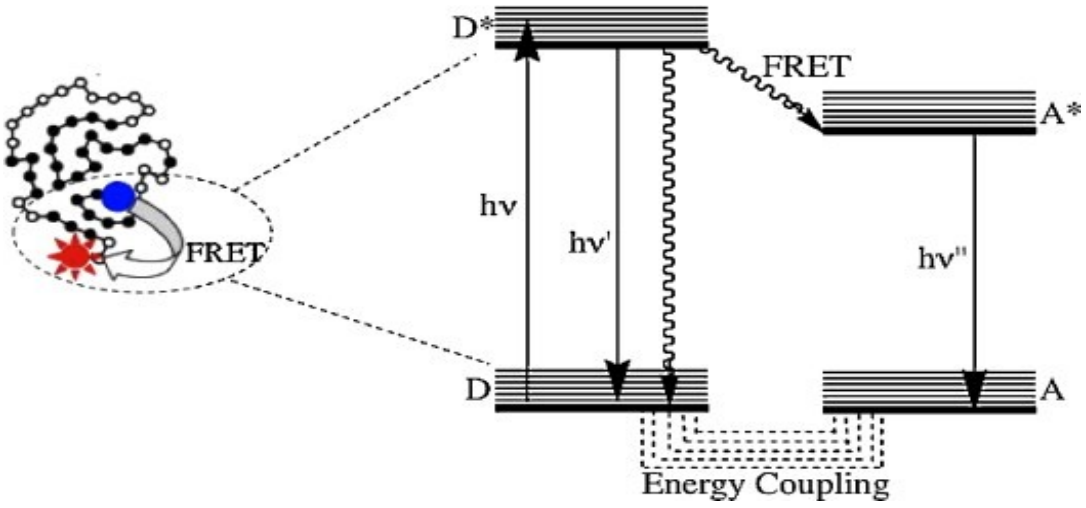


**Figure 2: Schematic representation of FRET demonstrating the energy transfer from excited donor (D*) to acceptor (A) via nonradiative process. Note that external conversion of the acceptor is not shown** (Taken with permission of Reference [12])

FRET efficiency ($E_{FRET}$) varies with the sixth power of the distance between the two molecules and can be expressed by the following equation.[12]

$$E_{FRET} = \frac{R_0^6}{R_0^6 + R^6}$$

$R_0$ is the Förster radius or critical distance, which is the characteristic distance at a FRET efficiency of 50%. This FRET efficiency is varying for different FRET pairs. FRET efficiency is close to maximum at distances less than $R_0$, and minimum for distances greater than $R_0$. *I*n an aqueous solution, $R_0$ is determined by following equation.[12]

$$R_0 = [8.79 \times 10^{-5} (\kappa^2 \eta^{-4} Q_D J(\lambda))]^{1/6} \quad \text{Å}$$

$\kappa^2$ is the angle between the two fluorophore dipole moments, $Q_D$ is the donor quantum yield and $\eta$ is the refractive index of the medium. $J(\lambda)$ is the spectral overlap integral between the normalized donor fluorescence, $F_D(\lambda)$, and the acceptor absorption spectra (which is a direct measure of the molar extinction coefficient, $\varepsilon_A(\lambda)$).[12]

$J(\lambda)$ is determined by the following equation:

$$J(\lambda) = \frac{\int F_D(\lambda)\varepsilon_A(\lambda)\lambda^4 \, d\lambda}{\int F_D(\lambda) \, d\lambda} \quad \text{mol}^{-1}\,\text{cm}^{-1}\,\text{nm}^4$$

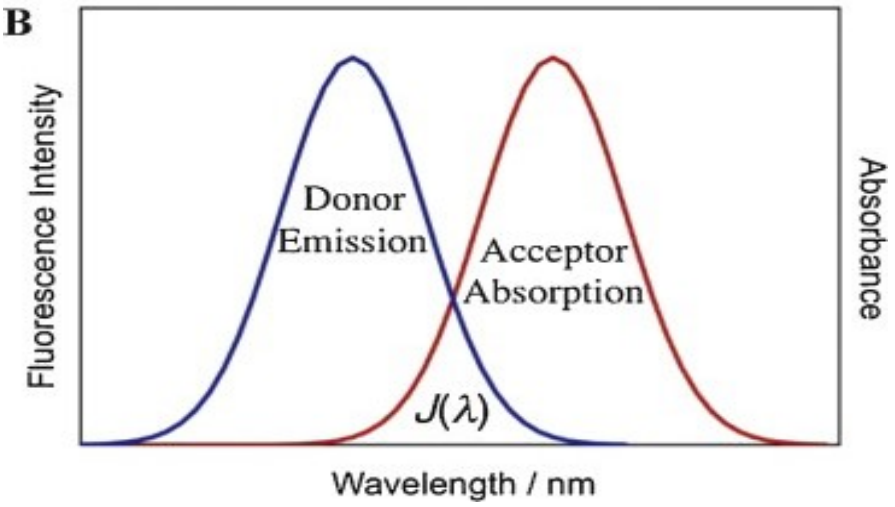


**Figure 3: Graphical representation of spectral overlapping, J(λ), between donor fluorescence/emission spectra and acceptor absorption spectra** (Taken with permission of Reference[12])

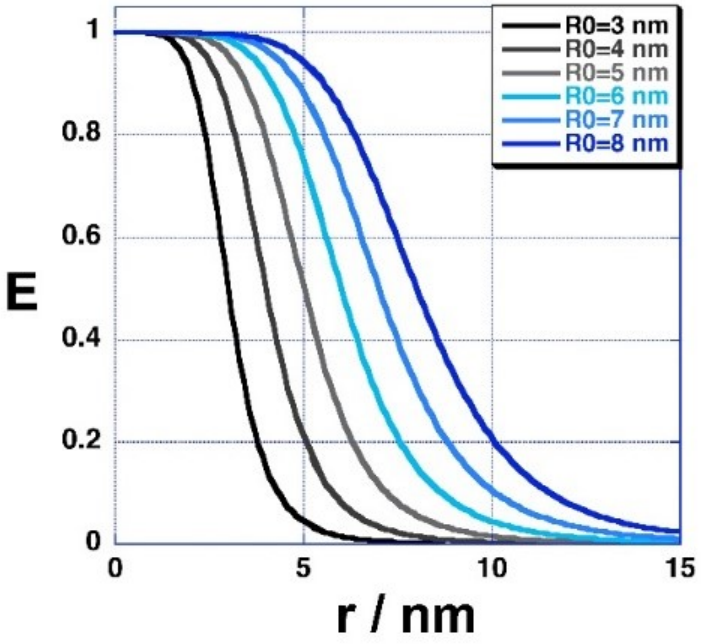


**Figure 4: Energy transfer efficiency E as a function of the distance between donor and acceptor (nm), and the Förster radius $R_0$**

## 1.4 Designs of the Nanobiosensors

These nanobiosensors were developed for the early detection of pancreatic cancer and non-small cell lung cancer. For the early detection of pancreatic cancer, $Fe/Fe_3O_4$-based nanobiosensors for protease[10,11] and arginase[13] were developed and patented in the Bossmann/Troyer groups were used. This technology facilitates the detection of enzymetic activities by measuring the fluorescence increase of a nanoparticle-linked fluorophore upon cleavage or posttranslational modification of an oligopeptide sequence. The synthesis of the nanobiosensors were done according to an established and published procedures.

Nanobiosensors synthesized for proteases contain dopamine coated $Fe/Fe_3O_4$ nanoparticles, TCPP, and cyanine 5.5. Water dispersible, dopamine coated $Fe/Fe_3O_4$ nanoparticles, TCPP, and cyanine 5.5 were synthesized according to established procedures.[11] The consensus peptide sequences were synthesized by solid-supported peptide synthesis.[11] TCPP which is the fluorophore of the nanoplatform was connected to the N-terminal end of the oligopeptides while it is still on the resin.

After the addition of TCPP, the TCPP-oligopeptide is cleaved off the resin and linked to the primary amine groups of $Fe/Fe_3O_4$-bound via an amide bond.[11] Each consensus peptide sequence contains GAG and AG as peptide spacers at the N- and C-terminal ends of the oligopeptide. This facilitates the access by the enzymes to their respective consensus sequence.

The average core diameter of Fe (0) is 13 +/- 0.5 nm and $Fe_3O_4$ shell thickness of 2.0 ± 0.5 nm, respectively. Following a random-deposition, cyanine 5.5 is directly bound to the dopamine coated nanoparticle and the determined optimal density is 50+/-4 per nanoparticle. TCPP is attached to the nanoparticle via oligopeptide and the density is 35+/-3 per nanoparticle. The distribution of ligands per nanoparticle follows a Poisson distribution. Unreacted low molecular

weight components, dyes and oligopeptides will be removed from the nanoplatform via dialysis. Nanoplatform undergoes lyophilisation and dried completely prior to use.

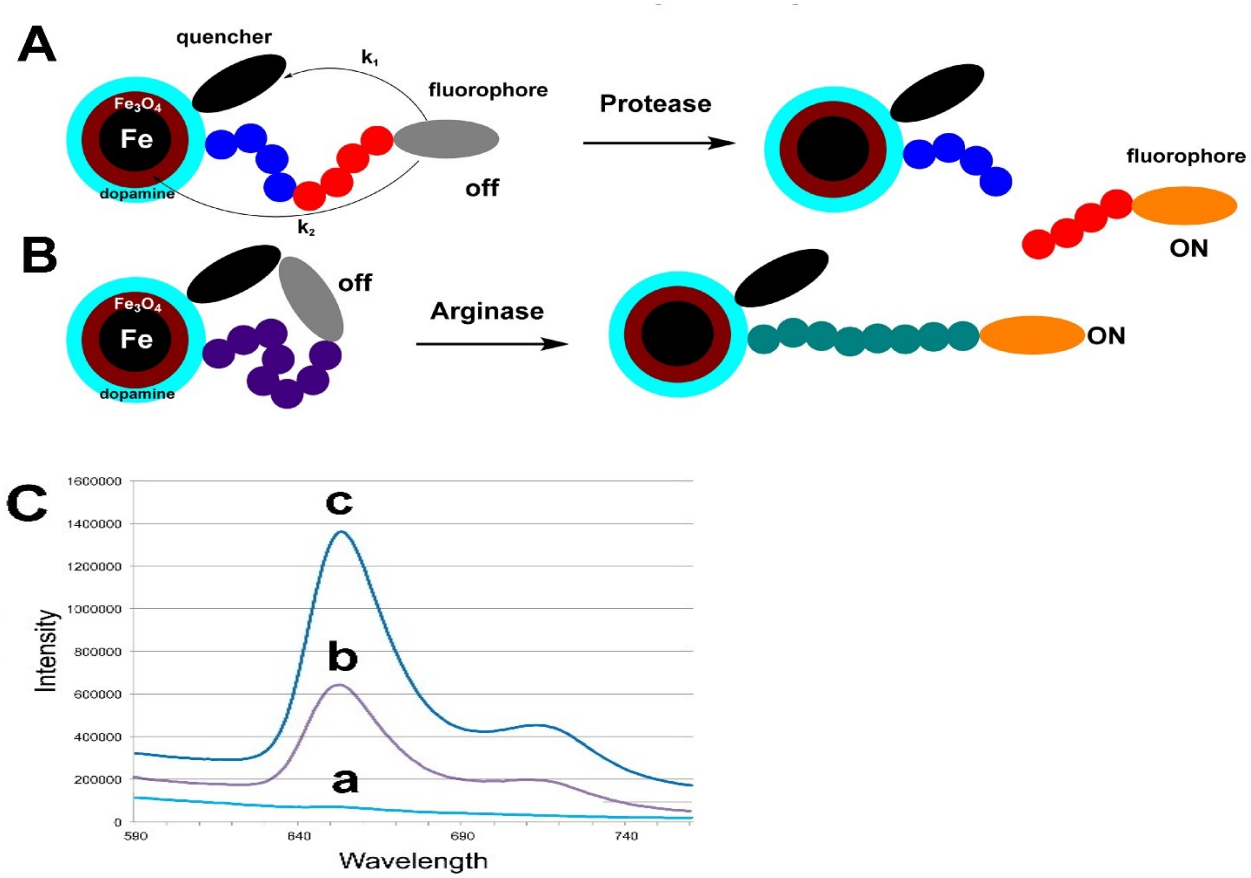


**Figure 5: A: Function principle of nanobiosensors for protease detection: the consensus sequence is cut by the protease; B: Function principle of nanobiosensors for posttranslational modification: the chemical identity of amino acids in the linker is changed via enzymatic reaction; C: Typical emission spectra occurring from the nanosensor for MMP-3 after 1h of incubation at 37°C ($\lambda_{exc}$ = 421nm). a: buffer; b: nanosensor; c: nanobiosensor after incubation with MMP-3**

## 1.5 Proteases

Proteases are a class of enzymes which involve with cleaving peptide bonds in specific peptide chain in a particular protein. There are different types of catalytic classes of proteases such as aspartic, metallo-, cysteine, serine, threonine and glutamic. Depending on the group involving

in nucleophilic attack at the carbonyl group, the proteases have been categorized. Aspartic, metallo- and glutamic proteases have a polarized water molecule as the nucleophile at the active center while serine and threonine proteases have the hydroxyl group and cysteine proteases have the sulfhydryl group at the active center.

There are few proteases which are necessary for cancer development and progression. Those are Matrix Metallo-proteinases (MMPs), urokinase plasminogen activator (uPA) and Cathepsins (CTSs).[14] These proteases are expressed during the tumor progression and metastasis.[15] These proteases incorporate with each other and act in cascade like manner. The cancer related proteases are important and possess reliability as specific biomarkers for the early cancer detection.

Extracellular proteases play a major role in transforming pancreatic cancer into metastatic and invasive phenotype.[16] The expression and the activity of proteases will vary depending on the cell type that express the protease. It has been found that in many cancer types, proteases are produced by the stromal and inflammatory cells.[17] For an example, in pancreatic cancer, there are cancer cells which will induce urokinase (uPA) in stromal cells but will bind to the urokinase receptors on cancer cells.[18]

Three main proteases which are related to cancer are discussed below.

### 1.5.1 Matrix Metalloproteinases

Matrix metalloproteinases (MMPs) is a family of enzymes which has been identified as a major player in tumor progression.[19] MMPs are involved in degradation of the extracellular matrix while wound healing, bone resorption, being a part of pathological conditions such as rheumatoid arthritis, coronary artery disease and cancer.[19] It has been identified that the cancer cells (tumor

cells) use the ability of MMPs to degrade matrix and spread to the sites far away from the tumor environment. MMPs are believed to promote the growth of tumor cells.

There are five subdivisions of MMP family; the collagenases, the stromelysins, the gelatinases, PUMP-1 or matrilysin and membrane type (MT) MMPs.[19] The common characteristics of these metal containing proteases are degrading at least one basement membrane component, active at physiological pH, requires two $Zn^{2+}$ ions to be active, inhibited by metal chelators and tissue inhibitors of metalloproteinases and secreted as zymogens while require activation extracellularly.[20,21] All MMPs have at least three domains; a hydrophobic pre-peptide domain, an amino terminal propeptide domain and a $Zn^{2+}$ catalytic domain.[20,21] There are three levels in MMPs regulations; alteration of gene expression, activation of latent zymogens and inhibition by tissue inhibitors of metalloproteinases. It has been found that the changes in these three levels are associated with tumor progression.[22] Once MMPs are activated, they can be activated by themselves as well. MMP-3 activates MMP-2 while MMP-9 activates MMP-7.[19]

Metastasis is a hallmark of cancer. In metastasis, the cells from primary tumor get colonized in distant sites of the body. There are several major steps involved in metastasis such as tumor cells break from the primary tumor, invasion of cancer cells through the basal membrane into a blood or lymphatic vessel, survival of tumor cells, extravasation from blood or lymphatic circulation and colonization of tumor cells and angiogenesis to form metastatic lesion.[23] Angiogenesis is required for the metastases to grow and includes few steps; the release of angiogenic factors, release of proteolytic enzymes to degrade postcapillary venule basement membrane, endothelial cell migration to the tumor, endothelial cell proliferation and microvessel formation and differentiation.[24]

In order to invade extracellular matrix, malignant cells require proteases. Proteases are used by metastatic cells to invade through the basement membrane and underlying connective tissues, basement membrane of small blood vessels and lynphatics.[19] MMPs play a major role in tumor angiogenesis. According to many studies, endothelial cells can express and activate MMPs and TIMPs differentially. MMP-1 is a main protease in angiogenic cascade.

**Table 1: Matrix Metalloproteinases** (Reproduced with permission of Reference [25])

| Protease | Common/other names |
|---|---|
| MMP-1 | Collagenase-1 / fibroblast collagenase |
| MMP-2 | Gelatinase-A / 72kDa gelatinase |
| MMP-3 | Stomelysin-1 / transin-1 |
| MMP-7 | Matrilysin / PUMP |
| MMP-8 | Collagenase-2 / neutrophil collagenase |
| MMP-9 | Gelatinase-B / 92 kDa gelatinase |
| MMP-10 | Stromelysin-2 / transin-2 |
| MMP-11 | Stromelysin-3 |
| MMP-12 | Macrophage metalloelastase |
| MMP-13 | Collagenase-3 / rat collagenase |
| MMP-14 | MT1-MMP (membrane-type MMP) |
| MMP-15 | MT2-MMP |
| MMP-16 | MT3-MMP |
| MMP-17 | MT4-MMP |
| MMP-18 | Collagenase-4 |
| MMP-19 | - |
| MMP-20 | Enamelysin |
| MMP-21 | - |
| MMP-22 | - |
| MMP-23 | CA-MMP |

| | |
|---|---|
| MMP-24 | MT5-MMP |
| MMP-25 | Leukolysin / MT6-MMP |
| MMP-26 | Endometase / matrilysin-2 |

**Table 2: Key matrix metalloproteinases in relation with the stages of cancer progression and their effect** (Reproduced with permission of Reference [26])

| MMP | Effect |
|---|---|
| Cancer cell invasion | |
| Several MMPs (MT1-MMP, MMP-2 and MMP-9) | Degrade physical barriers |
| Cancer cell proliferation | |
| MMP-1, -2, -3, -7, -9, -11, -19 | Proliferation |
| MMP-3, -7, ADAM17, ADAM10 | Proliferation |
| MMP-9, -2, -14 | Proliferation |
| Cancer cell apoptosis | |
| MMP-7, ADAM10 | Anti-apoptotic |
| Tumor angiogenesis and vasculogenesis | |
| Several MMPs (MMP-2, -9 MMP-3, -10, -11 MMP-1, -8, -13) | Angiogenesis up-regulation/down-regulation |
| Cell adhesion, migration, and epithelial to mesenchymal transition | |
| MMP-2 | Promote migration |
| MMP-2, -3, -9, -13, -14 | Induction of EMT (Epithelial-to-mesenchymal transition); cell migration |
| Immune surveillance | |
| MMP-9 | Decrease T-lymphocyte proliferation |
| MMP-9, -2, -14 | Decrease T-lymphocyte reaction against cancer cells |
| MMP-7, -11, -1, -8, -3 | Decrease cancer cell sensitivity to natural killer cells |

### 1.5.2 Cathepsins

Cathepsins are globular proteases which have intracellular and extracellular functions. In cathepsin family, there are 14 types of cathepsins, cathepsin A, B, C, D, E, F, G, H, L, K, O, S, V and W.[27] In humans, cysteine cathepsin family comprises 11 members. The largest class of cathepsin is represented by cathepsin B, C, F, H, L, K, O, S, V, W and X which are cysteine proteases of the papain family.[28] Initially cathepsins are synthesized as inactive proenzymes. Then they are processed to become mature and active enzymes.

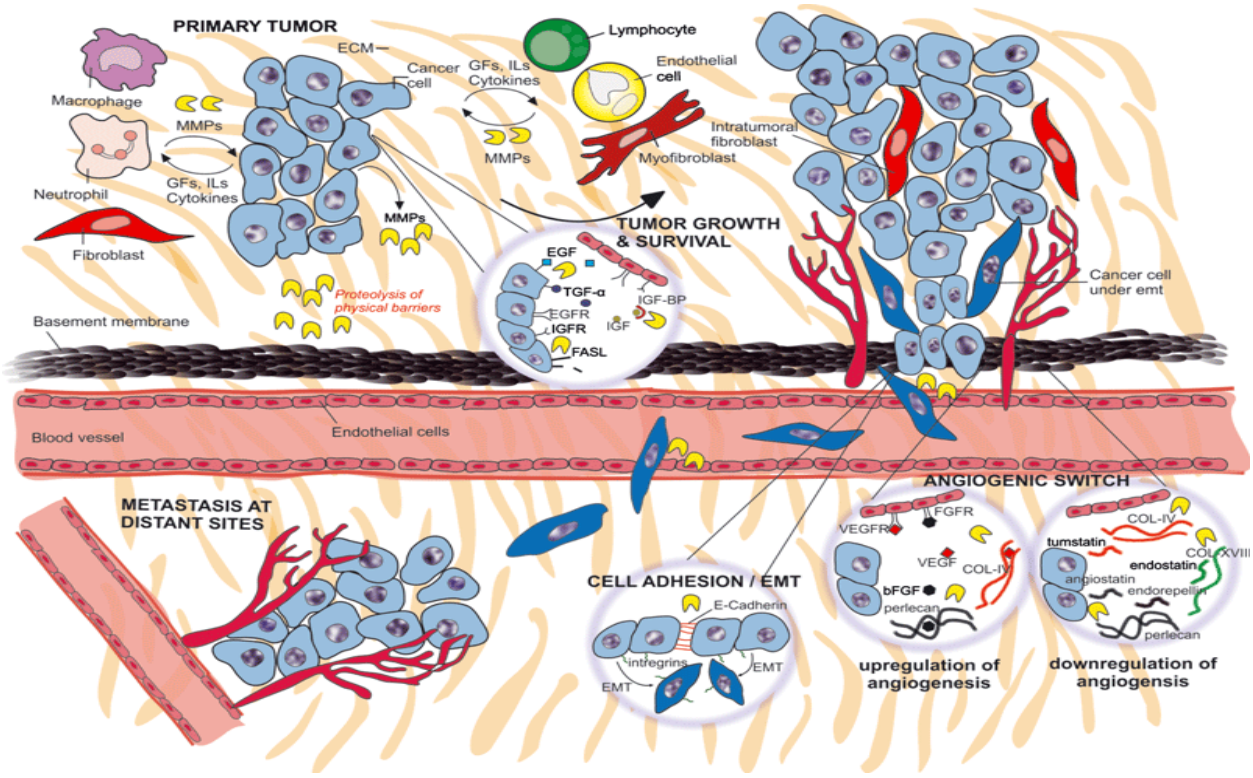


**Figure 6: Cysteine cathepsins expressed in tumor cells and tumor-associated cells which contribute to neoplastic progression** (Taken with permission of Reference [29])

Cystein cathepsins are involved in apoptosis, angiogenesis, cell proliferation and invasion. Protein degradation and processing are the main functions of cysteine cathepsins in normal cells.[30] Studies have found that the activity levels and expression of some cysteine cathepsins are upregulated in human as well as mouse cancers.

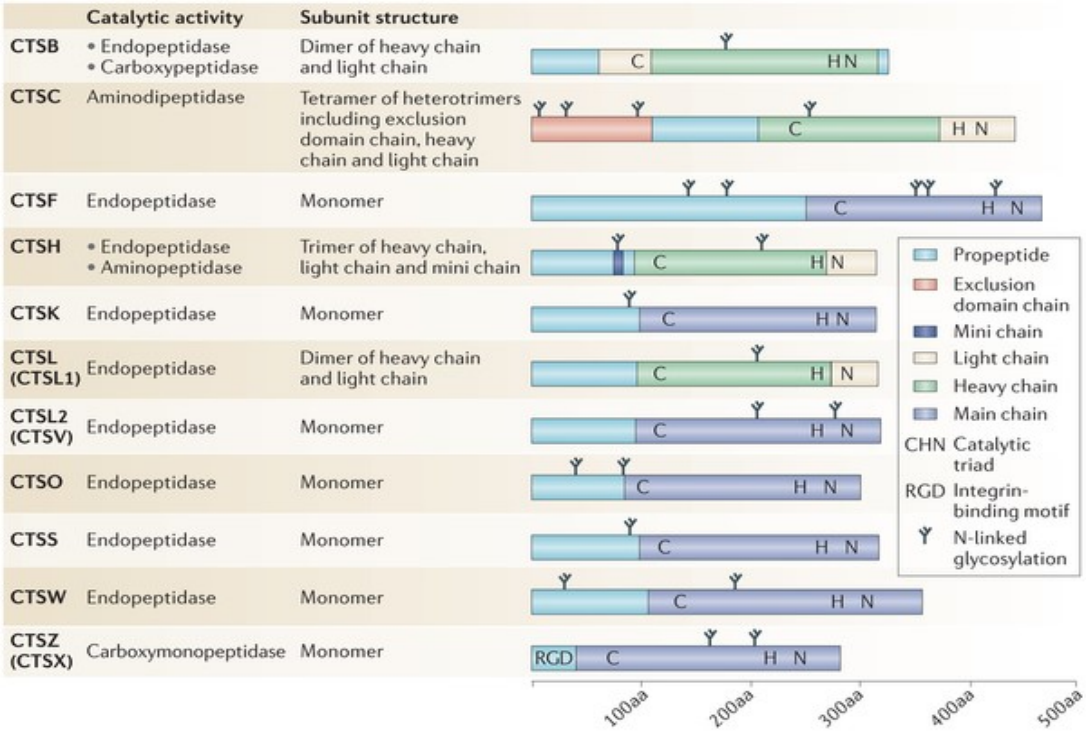


**Figure 7: Cystein Cathepsins** (Taken with permission of Reference [31])

Figure 8 shows the cysteine cathepsin expression of tumor and tumor associated cells in caner progression.

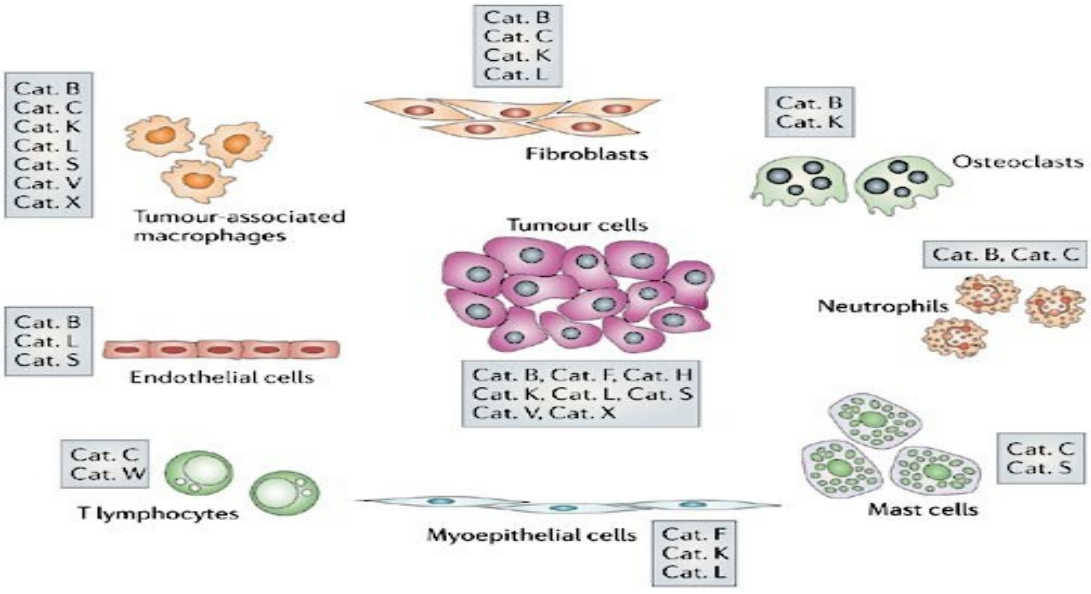


**Figure 8: Cysteine cathepsins expressed in tumor cells and tumor-associated cells which contribute to neoplastic progression** (Taken with permission of Reference [29])

### 1.5.3 Serine Proteases

Serine proteases have a close relationship with cell growth and differentiation. Urokinase is one of the serine proteases which is closely associated with tumor invasion and metastasis.[31] It has been found that the expression and enzyme activity regulation of serine proteases are related to the malignant phenotypes of tumors. Matriptase and trypsin are two other serine proteases involved in cancer.[32] Matriptase is responsible for angiogenesis, extracellular matrix degradation and epithelial cancer progression.[33] In normal cells, matriptase is inhibited by hepatocyte growth factor activator inhibitor-1(HAI-1). The expression of matriptase and loss of HAI-1 can be seen in prostate cancer progression. According to the studies, the ratio between matriptase and HAI-1 act as a very good biomarker for prostate cancer progression.[34]

Trypsin is a well characterized protease among other serine proteases. Trypsin is associated with food digestion, blood coagulation, fibrinolysis, and control of blood pressure. Apart from those, trypsin plays a major role in atherosclerosis, inflammation and cancer.[32] Trypsin is secreted in pancreatic juice as an inactive zymogen (trypsinogen) and activated by enteropeptidase to trypsin.[35] This was done for physiological protection against premature activity. Antiprotease mediator pancreatic secretory trypsin inhibitor (PSTI) also protects from premature activity, but the imbalance between protease and antiprotease system leads to the development of pancreatitis. This makes a risk to develop pancreatic adenocarcinoma.[32] Trypsin also associated with colorectal carcinogenesis while promoting cell proliferation, invasion and metastasis.[36]

Urokinase plasminogen activator (uPA) is also a serine protease which plays a major role in cancer development. It is associated with extracellular matrix degradation as well as basement membrane dissolution.[37]

**Table 3: Serine protease expression in cancer** (Taken with permission of Reference[38])

| | Serine Protease Expression in Cancer | | | | | | | | | | | | | | | |
|---|---|---|---|---|---|---|---|---|---|---|---|---|---|---|---|---|
| Serine Protease | Breast | Cervical | Colon | Endothelia | Endometrial | Gastric | Gastrointestinal | Leukemia | Lung | Renal | Oral | Ovarian | Nasopharyngeal | Pancreatic | Prostate | Salivary gland | Skin |
| Hepsin | ↑ | √ | | | ↑ | | | | √ | ↑ | | ↑ | | | ↑ | | |
| KLK6 | | | | | | | | | | | | √ | | | √ | | |
| KLK7 | ↑↓ | ↑ | ↑ | | | | | | | | ↑ | ↑ | | √ | ↓ | | |
| KLK8 | √ | ↑ | | | ↑ | | | | ↑↓ | | ↑ | ↑ | | | | ↑ | |
| Matriptase | ↑↓ | ↑ | ↑↓ | ↑ | ↑ | ↑ | ↓ | ↑ | ↓ | ↑ | | ↑↓ | | ↑ | ↑ | | ↑ |
| SLPI | √ | ↓ | √ | | | ↑ | | | ↑ | | | ↑↓ | ↓ | | ↓ | | |
| TMPRSS3 | √ | | | | | | | | √ | | | ↑ | | ↑ | √ | | |

## 1.6 Pancreatic Cancer

Pancreatic cancer is one of the deadliest diseases among other various types of cancer.[39] In United States, pancreatic adenocarcinoma is the third leading cause of cancer deaths for both male and female. Since 2003, the death rates due to other cancer types (lung, colorectal, breast, and prostate) were declined while pancreatic adenocarcinoma has increased.[3]

It has been recorded that, since 1998, incidence rates for pancreatic cancer is increasing by 0.8% per year in men and by 1.0% per year in women.[3] The calculated death rate for pancreatic cancer has been increased from 2003 to 2007 by 0.7% and 0.1% for men and women respectively.[3]

### 1.6.1 Early signs and symptoms

It is difficult to identify the early symptoms of pancreatic cancer. Most of the time pancreatic cancers develop without initial stage symptoms. It has been found out that only a small

number of pancreatic cancer patients have showed the early symptoms of the disease. But researchers were unable to find out a specific pattern of early symptoms for the early diagnosis. The signs and symptoms associated with pancreatic cancer are; pain in upper abdomen which can spread over the back, weight loss, loss of appetite, high blood glucose, dark urine, yellow skin and eyes etc.[3] According to the studies, 4% of the pancreatic diagnosed patients had sudden disgust for preferred tastes such as coffee, smoking, wine etc. for more than 6 months prior to the disease diagnosis.[40] Also 5% of the patients had weakness, loss of appetite while 1% of patients had attacks of acute pancreatitis.[4] Due to the vagueness of these early symptoms, it is difficult to use these situations in diagnosis of pancreatic cancer in its early stages.

### 1.6.2 Risk factors

The incident rates of pancreatic cancer are twice higher in smokers than nonsmokers. It has been found that 25%-30% of pancreatic cancer cases were caused by smoking cigarette.[41] This indicates that the risk for pancreatic cancer is increased by tobacco smoking and use of smokeless tobacco. Family history of pancreatic cancer and the personal history of pancreatitis increase the risk for pancreatic cancer. Apart from that, alcohol consumption, diabetes, obesity and consumption of red meat are some of the risk factors associated with pancreatic cancer.[3]

### 1.6.3 Diagnosis

In pancreatic cancer, the symptoms are undetectable until it spreads over to distant organs. That causes the early detection of pancreatic cancer more difficult and challenging. Currently, there is no specific diagnostic method to detect pancreatic cancer in its early stages. Only 8% of

pancreatic cancer cases have been detected at early stages and there are ongoing research developments for early detection of pancreatic cancer.[3]

### 1.6.4 Treatments

There are several different options available for the treatment of pancreatic cancer. Surgery, radiation therapy and chemotherapy options help to increase the survival rate of patients and relieve symptoms. But those methods will not produce cure very often. Most of the time pancreatic cancer is detected after it spreads beyond the pancreas. Therefore, less than 20% of patients undergo surgery for the removal of the cancer.[3] Gemcitabine is a chemotherapy drug used to treat the patients who undergo surgeries. This increases the survival of many patients after going through a surgery. Erlotinib (Tarceva) is another anticancer drug used along with gemcitabine for the improvement of pancreatic cancer survival.[3]

### 1.6.5 Survival and deaths

According to the literature, with all combines stages, 1 and 5 year relative survival rates are 26% and 6% respectively. It has been found that the 5 year survival for pancreatic cancer is very less regardless of stage. During 2001-2007, five-year survival rate for local-staged cancer, regional-staged cancer, and distant-staged cancer are 21.9%, 9.1% and 1.8% respectively. According to the estimated calculations, 37390 deaths were expected to occur in 2012 in both men and women populations.[3]

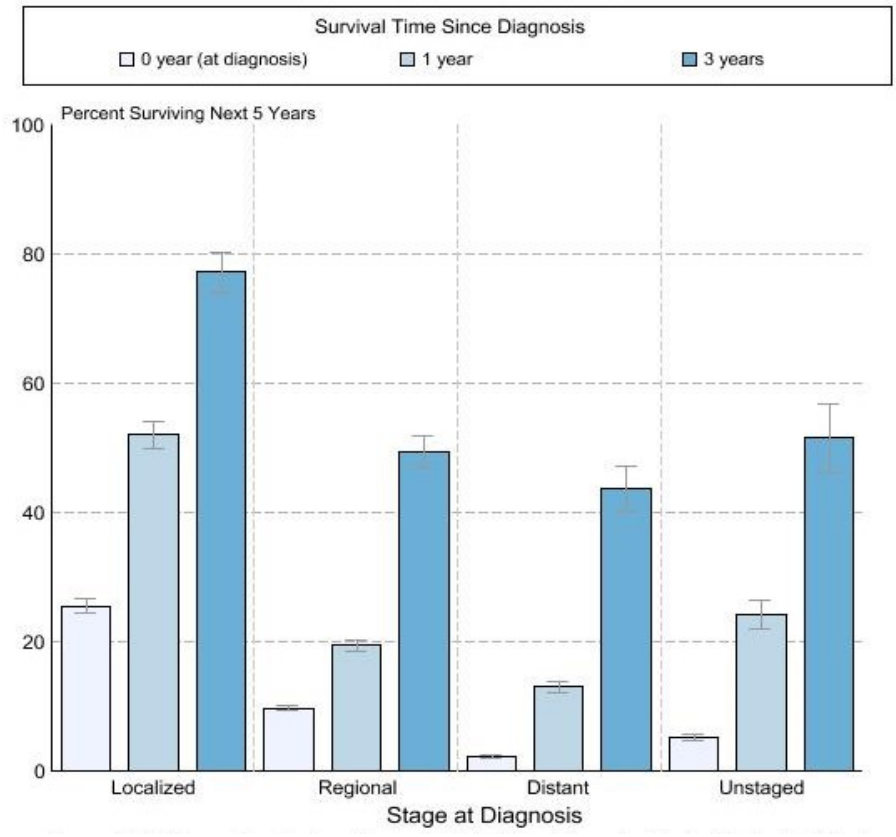


**Figure 9: Pancreatic cancer 5-year relative survival and 95% confidence intervals** (Taken with permission of Reference [42])

### 1.6.6 Pancreatic cancer and Proteases

As discussed earlier, pancreatic cancer is a challenging disease which has 5 years survival rate less than 6%.[43] Therefore, in developed countries, disregarding the advanced medical therapies and surgical techniques available, pancreatic cancer lead to the higher number of deaths compared to the other cancer related deaths.[44] Early dissemination and high local tumor progression are the major hallmarks associated with pancreatic cancer. Due to those factors, ¾ patients diagnosed with this disease will not undergo initial treatments thus leading to a high mortality rate among pancreatic cancer patients.[43] Generally, in cancer, invasion and metastasis taking place at the tumor environment. In tumor environment, tumor cells and stroma can exchange signals in order to increase cell proliferation, cell migration as well as survival.[43]

Several types of proteases play a significant role in the progression and development of pancreatic cancer. According to the previous studies, MMP-2, MMP-9, TIMP-1 and TIMP-2 were found in excess amounts in pancreatic cancer tissue samples with compared to the normal pancreatic tissue samples.[45] While collagens type I and III are localized in spindle shaped stromal cells, MMP-9 was elevated in the tumor cells. MMP-2 elevated amounts also found in stromal cells. More MMP-2, MMP-9, TIMP-1 and TIMP-2 were detected in both tumor cells and stromal cells. Even distribution of TIMP-1 and TIMP-2 were seen in tumor and stromal cells.[45] This study shows a good correlation between MMPs and TIMPs overexpression with collagen protein levels and transcript coding levels for ECM proteins.

In chronic pancreatitis, elevated levels of MMP-2 and TIMP-2 were recorded. But mRNA encoding transcripts for MMP-1, MMP-3 and TIMP-1 were not detected in chronic pancreatitis tissues.[46] Immunohistochemistry has proven that the MMP-2, MMP-3 and TIMP-1 levels are higher in pancreatic and ampullary carcinomas. The studies show that the immunoreactivity in pancreatic and ampullary malignant epithelial cells is greater than in stromal tissues.[47]

Type IV collagen distribution in basement membrane tissues in pancreatic adenocarcinoma was found to be discontinuous and irregular. This may be due to the abnormal degradation and deposition of collagen.[48] In pancreatic ductal adenocarcinoma, tumor extracts show the elevated amounts of collagen I and V.[49]

## 1.7 Lung Cancer

Lung cancer is the most common cancer worldwide. In 2012, we had 1.8 million new cases and caused 1.6 million deaths.[50] It is a leading cancer killer of men and women in the United States and since 1987, lung cancer mortality has surpassed breast cancer mortality among women.[51] In

2016, it has been estimated that 158,080 Americans died from lung cancers. This is approximately 27% all recorded cancer deaths.[4] The lung cancer mortality patterns show differences between men and women, depending whether they are smokers or not.

Lung cancer is predominantly detected in the elderly. The majority of lung cancer patients are diagnosed within the last 5 years of disease progression. According to the statistics, in 2013, 83% of lung cancer patients were 60 years of age or older.[52]

### 1.7.1 Early signs and symptoms

Most lung cancers do not show any symptoms or signs until they become distant. There are common symptoms of lung cancer, such as a cough that does not go away, blood or rust-colored sputum that is coughed-up, chest pain, hoarseness, loss of appetite and weight loss, feeling tired, as well as the occurrence of lung infections and pneumonia.[3] If lung cancer spreads to distant organs, bone pain, headache, dizziness, seizures, yellow skin and eyes and lumps near the surface of the body may occur.[3]

### 1.7.2 Risk factors

The main risk factor for lung cancer is cigarette smoking. Studies show that the cigar and pipe smoking also can increase the risk of getting a lung cancer.[3] The risk of getting a lung cancer increases with the quantity and the duration of smoking. Apart from cigarette smoke, gases released from soil and building materials, environmental exposure to cancer hazardous gases, asbestos, paint, organic chemicals and Cr, As, Cd like metals, air pollution and radiation cause lung cancer among people. Family history and the medical history of tuberculosis may increase the risk factor for lung cancer.[3]

### 1.7.3 Diagnosis

Recent studies prove that the chest x-ray screenings do not reduce the mortality rate of lung cancer patients.[53] Modern tests such as low-dose spiral computed tomography (CT)[3] and molecular markers[53] in sputum are found to be better techniques to detect lung cancer in their early stages. National Lung Screening Trial results show 20% fewer lung cancer deaths among lung cancer patients (heavy smokers) who went through spiral CT screenings compared to normal chest x-ray screenings.[3]

Screening of high risk individuals enhances lung cancer survival rates by diagnosing the disease at an early stage, which makes treatments more successful. It has been estimated that at least 8.6 million Americans, who are considered as high risk lung cancer patients should receive low-dose CT scans annually.[54] It is possible to prevent over 13,000 deaths if the half of these high risk individuals have been tested via low-dose CT scans.[55]

### 1.7.4 Treatments

There are few stages of a lung cancer. Non-small cell lung cancer and small cell lung cancer.[55] Non-small cell lung cancers are diagnosed as 4 different stages from stage I to stage IV, depending on disease progress. Stage I is where the cancer is confined to the lung. In stage II and III, cancer can be seen in lung as well as in lymph nodes. Stage IV is the stage where cancer is spread away from lungs and has moved to other organs of the body (e.g. liver or brain).

Treatments are strictly dependent on the type and the stage of the lung cancer.[3] Surgery, radiation therapy, chemotherapy and some other targeted therapies are the few treatment methods currently used. Surgeries are commonly performed for the localized non-small cell lung cancers. Radiation therapy and chemotherapy will be usually done after a surgery, because it improves the

survival rate. Patients who have advanced (stage III and IV) non-small cell lung cancer are normally treated with targeted drugs and chemotherapy. For small cell lung cancer patients, chemotherapy alone or combination with radiation are the most common treatments available.[3]

### 1.7.5 Survival and Mortalities

Statistical data shows that the 1 year relative survival for lung cancer has increased from 37% in between 1975-1979 to 43% in between 2003-2006.[3] However, the 5 year survival rate for all stages in lung cancer has been estimated to be 15%. For small cell lung cancer, the 5 year survival rate is about 6%, while for non-small cell lung cancer is about 17%.[56]

According to the studies, developing a lung cancer in male smokers is 23 times higher and in female smokers it is about 13 times higher compared to nonsmokers.[56] As mentioned earlier, lung cancer is the main contributor to the cancer related mortalities in the United States and surpassed colon cancer in men and breast cancer in women in the early 1950s and early 1980s, respectively.

According to the statistics, men from age 40 years onward have a high risk of mortality due to lung cancer compared to the other cancer related mortalities. For women lung cancer mortality surpasses breast cancer mortality at age 60 years and older.[57]

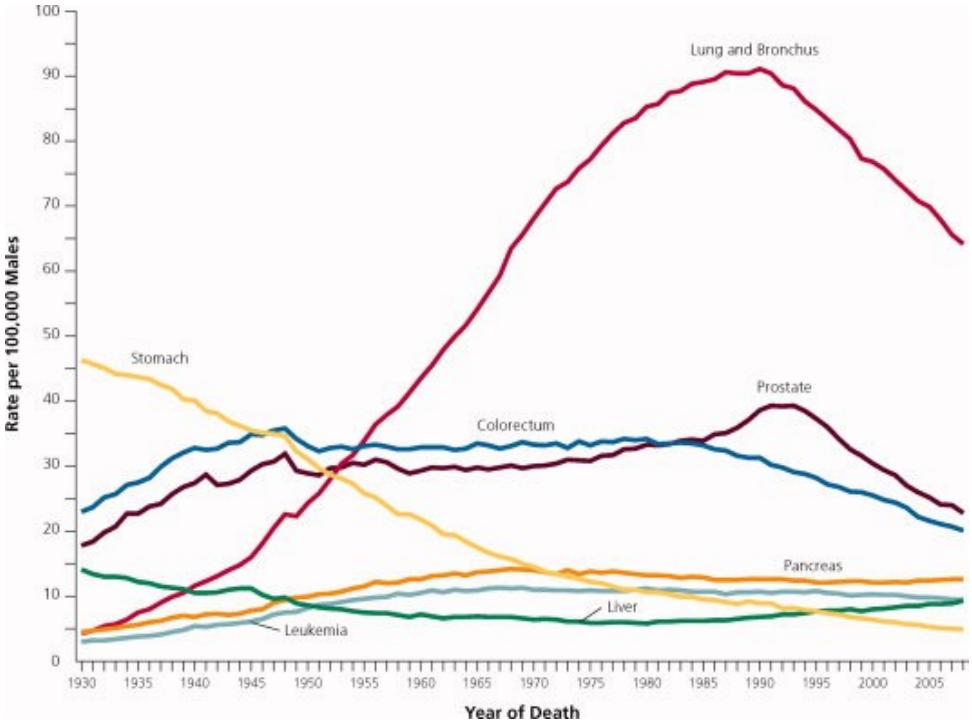


**Figure 10: Trends in Death Rates Among Males for Selected Cancers, United States, 1930 to 2008** (Taken with permission of Reference [57])

### 1.7.6 Lung Cancer and Proteases

There are many proteases involved in lung cancer development and tumor generation. We have discussed three main protease categories in section 1.5. Most of those proteases play major roles in lung cancer development.

Urokinase-type plasminogen activator (uPA) is overexpressed in lung carcinomas in stromal and cancer cells.[58] In non-small-cell, non-NE (neuroendocrine) carcinomas, stromal expression of uPA and MMP-11 was amounting to 80 to 90% of the expression in the whole tumor.[59] Studies showed that uPA overexpression is detected in stromal fibroblasts and in tumor cells in both non-small cell lung carcinomas and neuroendocrine lung tumors.[60] Epithelial expression of uPA in non-small cell lung carcinomas is linked to the presence of node metastasis and expression in fibroblasts was correlated to the tumor size.[60]

In matrix metalloproteinases, MMP-2 (gelatinase A) and MMP-9 (gelatinase B) were expressed in lung cancer tumor cells.[61] Also, in non-small cell lung carcinomas MMP-1, MMP-9 and MMP-11 were found in tumor samples.[62] Tokuraku *et al*. reported a matrix metalloproteinase (MT-MMP or MMP-14) which is expressed on the cell surface. It is capable of activating MMP-2. A correlation between MMP-2 expression in tumor tissue and expression of MT-MMP (MMP-14) was discovered. MMP2 also correlates with lymph node metastases.[63] Analysis of human lung tumor tissues indicated that MMP-1 and MMP-10 are overexpressed in lung tumors, but MMP-7 is detected in lower concentrations.[64]

Cathepsin S has been analyzed in tissue cytosols of lung parenchyma, lung tumors and lymph nodes by using ELISA. The levels of Cathepsin S in lymph nodes were significantly higher compared to lung parenchyma or tumors.[3] Studies on the cysteine proteinases, Cathepsin L and Cathepsin B indicated that they are involved in tumor progression and angiogenesis, because they are able to degrade extracellular matrix proteins.[65]

# Chapter 2 - Early Detection of Pancreatic Cancers in Liquid Biopsies by Ultrasensitive Fluorescence Nanobiosensors

**Acknowledgement**

I would like to acknowledge all the co-authors, who contributed their expertise towards the success of this project. This work was funded by NSF (CBET 1159966) and 1337438, and the Johnson Cancer Center at Kansas State University.

Madumali Kalubowilage[a‡], Aruni Malalasekera, PhD[a‡], Obdulia Covarrubias-Zambrano[a‡], Sebastian O. Wendel, PhD[ab‡], Hongwang Wang, PhD[a‡], Asanka S. Yapa, PhD[a], Lauren Chlebanowski[a], Yubisela Toledo[a], Raquel Ortega[a], Katharine Janik[a], Gary Gadbury, PhD[c], Anup Kasi, MD[d], Stephen Williamson, MD[d], Deryl L. Troyer, PhD, DVM[b], Stefan H. Bossmann, PhD[a*]

[a] *Department of Chemistry, Kansas State University, Manhattan, KS, USA*

[b] *Department of Anatomy & Physiology, Kansas State University, Manhattan, KS, USA*

[c] *Department of Statistics, Kansas State University, Manhattan, KS, USA*

[d] *University of Kansas Medical School, Kansas City, KS, USA*

My research was focused on synthesizing, purifying peptides while assembling, purifying and characterizing functional nanobiosensors. Furthermore, I was engaged with designing fluorescence plate reader experiments and carried out sample analysis reported in this chapter and contributed to the data analysis in this project.

**Abbreviations**

MMP: matrix metalloproteinase, CTS: cathepsin, uPA: urokinase-type plasminogen activator, PBS: phosphate-buffered saline, HEPES: (4-(2-hydroxyethyl)-1-piperazineethanesulfonic acid), FRET: Förster Resonance Energy Transfer, SET: dipole-surface energy transfer

NSCLC: non-small-cell lung cancer

## 2.1 Abstract

Numerous proteases, such as matrix metalloproteinases (MMP's), cathepsins (CTS), and urokinase plasminogen activator (uPA), are either dysfunctional, over- or under-expressed in solid tumors, when compared to healthy human subjects. This offers the opportunity to detect early tumors in liquid biopsies, such as serum. This approach is of particular advantage for the early detection of pancreatic cancer, which is a “silent killer”, because it shows only distinct symptoms at the distant stage when the survival rates are especially low.

We have developed fluorescence nanobiosensors for ultrasensitive (sub-femtomolar) protease detection, consisting of water-dispersible $Fe/Fe_3O_4$ core/shell nanoparticles and two tethered fluorescent dyes: tetrakis(4-carboxyphenyl)porphyrin (TCPP) and cyanine 5.5. These nanobiosensors exhibit both, dipole-surface energy transfer (SET) quenching and Förster Resonance Energy Transfer (FRET) of tethered TCPP. Upon enzymatic cleavage, the fluorescence of TCPP increases, which enables the detection of numerous proteases at sub-femtomolar activities.

Additionally, we have tested a recently tested arginase sensor as well. The major difference in design is that the tether between $Fe/Fe_3O_4$ and TCPP is not cleaved, but biochemically altered by arginases I + II. The change in tether dynamics then leads to an increase of TCPP fluorescence, thus permitting the detection of arginase activity.

We have identified a protease/arginase signature for the detection of pancreatic adenocarcinomas in serum, consisting of arginase, MMPs -1, - 3, and -9, cathepsins -B, and -E, urokinase plasminogen activator and neutrophil elastase. This is a potential game-changer in pancreatic cancer detection.

## 2.2 Introduction

Pancreatic Cancer is the third leading cancer in the United States, with a 5-year survival rate of less than 6%. In 2016, in the U.S. alone there were an estimated 53,070 new cases of pancreatic cancer and 41,780 deaths.[66] Pancreatic cancers are markedly on the increase over the past three decades. Despite the high mortality rate associated with pancreatic cancer, its etiology is poorly understood.[67] Pancreatic cancer has one of the worst prognoses of all gastrointestinal malignancies.

The symptoms are not easily detectable (only 7% of cases are detected at stage I, virtually no cases are detected at stage 0), and there is to date no reliable screening test for pancreatic cancer. Detection is usually accomplished in an advanced-stage, leading to a very poor prognosis. The development of a feasible early warning test for pancreatic cancer would not only save lives, it would also have a positive impact on the projected health care costs in the US.[68]

Many cases are already in well-advanced stages of metastases and dissemination with peripheral invasion of the retroperitoneum, vascular system, or nerves when pancreatic cancer is diagnosed. The rate of resection is <15% and the 5-year survival rate is 7–25% in the curative resected cases.[69,70] In the majority of cases, recurrences from pancreatic cancer are liver metastases and peritoneum dissemination.[70,71] It is well established that surgical treatment for liver metastases from pancreatic cancer cannot offer long-term survival for the vast majority of patients. Additionally, the outcomes of radiotherapy and chemotherapy are equally unfavorable.[72] Pancreatic ductal adenocarcinoma (DAC, 85-90% of all cases) is characterized by desmoplasia, which is the abundance of extracellular matrix (ECM) containing collagen, fibronectin, proteoglycans, and hyaluronic acid, as well as catalytically active enzymes and proteinases.[70] The accumulation of ECM components alters the architecture of pancreatic tissue causing abnormal

configurations of blood and lymphatic vessels leading to poor perfusion.[70] This effect is ultimately responsible for the inefficacy of classic chemotherapy against DAC.[70] Based on data from the National Cancer Data Base (1992-2004, statistics last revised on 09/15/2016), the 5-year observed survival for exocrine pancreatic cancer is 14% when the cancer was discovered at stage IA, 12% at IB, 7% at IIA, 5% at IIB, 3% at III, and 1% at stage IV. Endocrine pancreatic cancers show higher survival rates: 61% at stage I, 52% at II, 41% at III, and 15% at stage IV.[73] Note that this data is for patients who have received surgery. All stages used here were defined in accordance with the American Joint Committee on Cancer (AJCC) TNM staging system.[74]

Approximately 96% of all pancreatic cancers are exocrine. They comprise of adenocarcinomas (more than 90% of all pancreatic cancers), adenosquamous carcinomas, squamous cell carcinomas, signet ring cell carcinomas, undifferentiated carcinomas, undifferentiated carcinomas with giant cells, and solid pseudopapillary neoplasms of the pancreas.[75] The only viable strategy to distinguish between these cancer types to date is their position within the pancreas and the histological identification of the cell type. Pancreatic neuroendocrine tumors/carcinomas, or islet cell tumors, are uncommon (approx. 4% of pancreatic tumors). Among them are insulinomas, gastrinomas, glucagonomas, somatostatinomas, VIPomas (VIP: vasoactive intestinal peptide), PPomas (PP: pancreatic polypeptide) and carcinoid tumors. Insulinomas and gastrinomas are the most common. Although pancreatic neuroendocrine tumors/carcinomas are less aggressive than exocrine pancreatic cancers, the differentiation between benign neuroendocrine tumors (50%) and aggressive neuroendocrine cancers (50%) solely based on histological results is challenging.[76]

### 2.2.1 Liquid Biopsies

Detecting cancer and other diseases by means of a simple blood test has become a realistic possibility. Virtually all competing companies, among them Personal Genome Diagnostics[77], Genomic Health[78], Myriad Genetics[79], Guardant Health[79] and Pathway Genomics[79] rely on PCR to detect genetic mutations, and various RNA's that are overexpressed in tumors. In sharp contrast, the approach discussed here focuses on detecting the protease/arginase[80-82] signature of various solid tumors (breast[81], non-small lung[82] and pancreatic cancers (reported here)). Including blood tests for the estimated 14.5 million cancer survivors in the United States, the market potential for liquid biopsies is currently estimated to more than $20 billion a year. The average genomic test is currently between $5,000 and $6,000, which may prove prohibitively expensive for many patients. Compared to the state-of-the-art in liquid biopsies, protease profiling using the proposed approach will result in significantly reduced costs: $100 to $200 per protease/arginase profile for the end-user appears to be realistic. It should also be noted that there is a high potential for synergy between genomic and proteomic tests: genetic tests often show the potential for disease development, but not exactly when the transition to a tumor actually occurs. Protease/arginase assays can do exactly that.

### 2.2.2 Standard of care in detecting pancreatic cancer

The standard of care is based on symptoms, which are developed only when pancreatic cancer has progressed.[83] Nonspecific symptoms of exocrine pancreatic cancer are jaundice or diabetes. Pancreatic neuroendocrine tumors can have a variety of symptoms, among them stomach ulcers, diabetes, hypoglycemia, glossitis, diarrhea, and gallbladder problems. If unspecific symptoms exist or any masses or fluid buildup have been detected, state-of-the-art imaging

methods, such as Computed Tomography (CT scans), Magnetic Resonance Imaging (MRI), Positron emission tomography (PET), Ultrasonography (ultrasound or US) or more specialized methods (e.g. Somatostatin receptor scintigraphy (SRS) and Endoscopic retrograde cholangiopancreatography (ERCP)) will be used. Although the information that is obtainable by using these different methods is important with regard to therapy decisions, none of these methods is capable of routinely detecting *in-situ* pancreatic cancers, because the pancreas is obscured by other organs, making the detection of tumors with volumes of 1-5 $mm^3$ difficult.[84]

There are three types of common pre-cancerous lesions for pancreatic cancer, "Pancreatic Intraepithelial Neoplasia" or PanINs, Intraductal Papillary Mucinous Neoplasms (IPMNs) and "Mucinous Cystic Neoplasms" or MCNs.[85]

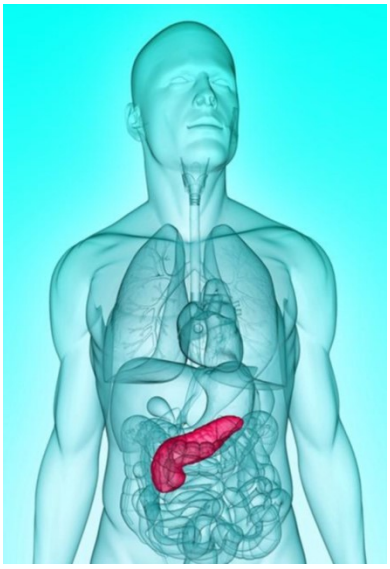

**Figure 11: The location of the pancreas obstructs early in-vivo diagnostics**

Blood tests for pancreatic cancer have been focusing on CA19-9 (carbohydrate antigen 19-9)[86], CEA (carcinoembryonic antigen)[87] and recently K-ras gene mutations.[88] These tests are not suitable for the detection of *in-situ* pancreatic cancers. CA19-9 is overexpressed in many types of gastrointestinal cancer (e.g. colorectal cancer, esophageal cancer, and hepatocellular carcinoma),

but it is also elevated during pancreatitis, cirrhosis, and other diseases in which inflammation occurs, resulting in numerous false positives. [86] False negatives also arise frequently due to genetic factors, especially in the Caucasian population. Therefore, the American Society of Clinical Oncology discourages the use of CA19-9 in screening for tumors.[89] Besides tumors, CEA (carcinoembryonic antigen) concentrations in the blood of adults are known to be influenced by numerous factors, many of them unrelated to cancer. Although the genetic landscape of pancreatic cancer shows nearly ubiquitous mutations of K-ras, the detection of oncogenic K-ras mutations alone is not sufficient to lead to pancreatic ductal adenocarcinoma (PDAC) in either human or in genetically modified adult mouse models.[90]

### 2.2.3 The Protease Web in Healthy and Cancer Patients

**Matrix metalloproteinases** (MMPs), **serine proteases** and **cysteine proteases** have well-documented roles in malignant progression, including angiogenesis, invasion, and metastasis.[91] It is of importance that tumor-promoting proteases act as a part of an extensive multidirectional network of proteolytic interactions. There are 570 known human proteases, coupled with a smaller group of endogenous protease inhibitors that tightly regulate their activity.[92] In general, cathepsin B, urokinase plasminogen activator (uPA), metallo-proteinases (MMP), occupy central nodes for amplifying proteolytic signals passing through the network. Recent research has shown that this proteolytic signaling network interacts with other important signaling networks, such as chemokines, cytokines, and kinases.[91] Understanding this extensive network of proteolytic interactions as a system of activating and inhibiting reactions may prove to be an important key to unlock tumor biology.

**Urokinase plasminogen activator** (uPA) is a very specific protease that binds to its

receptor, uPAR, and cleaves the inactive plasminogen to the active plasmin. This is the first step in a well-known protease cascade that causes angiogenesis. Therefore, uPA is associated with angiogenesis in tumors. It is also very active in tumor metastasis. Plasmin is a somewhat non-specific protease that goes on to cleave many targets including activating pro-collagenases, degrading the extracellular matrix (ECM), and releasing/activating growth factors. uPA has been identified as a target in clinical trials for advanced breast and pancreatic cancer.[93]

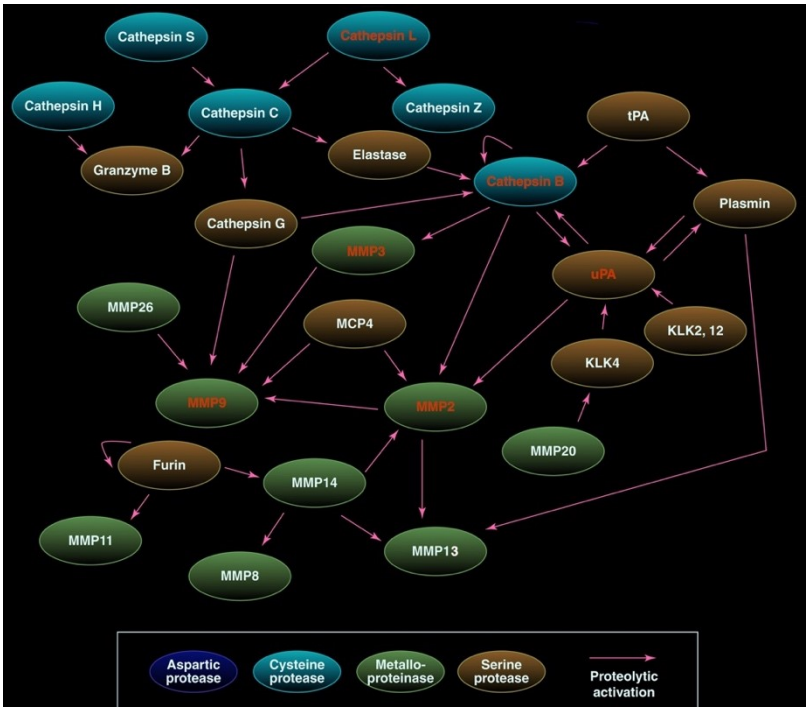


**Figure 12: Dysfunctional proteolytic networks in cancer[91]**

Figure 12 emphasizes the principles of protease biochemistry, but it is by no means comprehensive. Further interlinked protease networks exist. Proteases in red have been used successfully for the detection of early solid tumors (Tables 4 and 5).

**Cathepsins**, with a few exceptions, are cysteine proteases.[94] Often found in the lysosomal/endosomal pathway, cathepsins usually operate at low pH values, but many are able to retain some activity at neutral pH. Cathepsins are either largely overexpressed or misexpressed by

cancerous cells, causing activation outside of the cells. This activation outside of the cell can cause ECM degradation and initiate known ECM degradation cascades. For instance, cathepsin B is known to activate uPA.[91] Cathepsins are highly up-regulated in pancreatic cancer and contribute to the development and progression of the cancer phenotype.[73,94-96]

### 2.2.4 Diagnostic Strategy in Liquid Biopsies

Our diagnostic strategy is based on the paradigm that protease networks in pancreatic cancer are dysfunctional. However, some proteases are known to be context-specific, which adds to the complexity. For instance, down-regulation of cathepsin L is known to inhibit pancreatic islet cell carcinogenesis[97], but enhances epidermal tumor progression.[98] Several MMPs (-3, -9, -11) are known to either impair[99] or promote[100] tumor progression, depending on cell type and tumor microenvironment.

## 2.3 Gene Expression Analysis

Gene Expression Analysis[101] is straightforward approach to determine the proteases that are overexpressed in solid tumors, such as pancreatic cancer. A wealth of data is available from databases, such as NCBI GEO, Entrez Gene ID, Unigene ID and Gene Symbol.[101] This strategy is able to select protease candidates that have a high probability of being proximal biomarkers for pancreatic cancer from the total of 570 proteases that are known from the human genome.[92] This makes the selection process far less arbitrary that it would have to be based on protease-related cancer literature alone.

The relevant datasets for this study were obtained from the publicly accessible NCBI GEO database.[102] Criteria for datasets included in the analysis were that the investigated species is homo

sapiens and that the dataset contains samples from both primary tumor samples and healthy human tissue. The fold change of gene expression is taken as an indicator of the up- or downregulation of the genes of interest and R was used to extract the relevant raw data, calculate p-values and generate boxplots to illustrate data-ranges.[103,104]

Arginase is found in mammalian bodies in two isoforms: arginase I (L-arginase ureahydrolase, AI, UniProt P05089) and arginase II (AII, UniProt P78540). Arginase I and II share 61% amino acid sequence identity.[105] Arginase I is a liver enzyme[106], whereas arginase II is found in tissue.[107] From the data summarized in Figure 13, arginase II is a more suitable candidate for pancreatic cancer detection, if this tissue enzyme is able to find its way into the bloodstream in sufficient concentrations. Unfortunately, the sensor for arginase activity developed in the Bossmann group won't be able to differentiate between arginase I and II.[80]

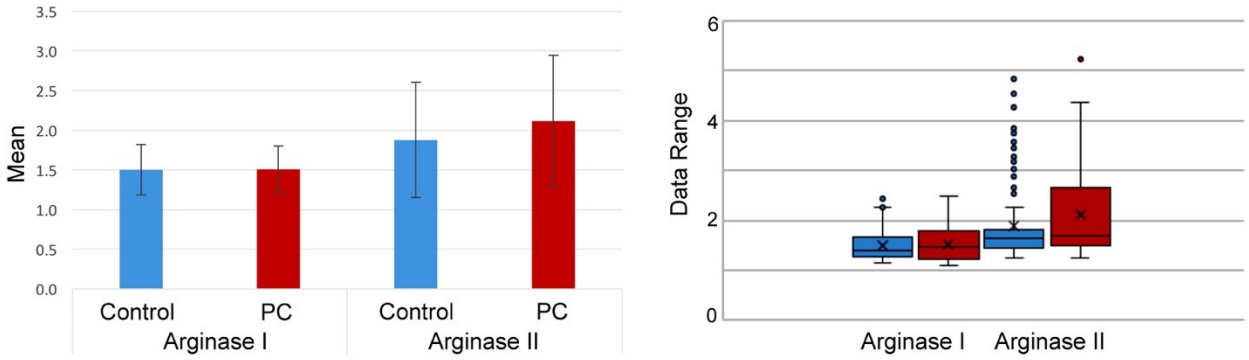


**Figure 13: Statistical genetic expression analysis of Arginases I and II in primary tumor samples and healthy human tissue (group sizes: n(ARG I) = 117, n(ARG 2) =117). All data were obtained from the NCBI GEO database.[102] Bar graph (left, showing means and standard deviations) and box plot (right, indicating the observed data range). PC: primary pancreatic cancer tissue. Control: apparently non-cancerous tissue from the same patient.**

From the data shown in Figure 14, cathepsin B appears to be an excellent candidate, which is in agreement with numerous reports in the literature.[73,94,95,97,108-111] Cathepsin B won't be

specific for pancreatic cancer, because it is also enhanced in breast and lung cancer. However, it can be an important component of a panel of enzymes for early cancer detection.

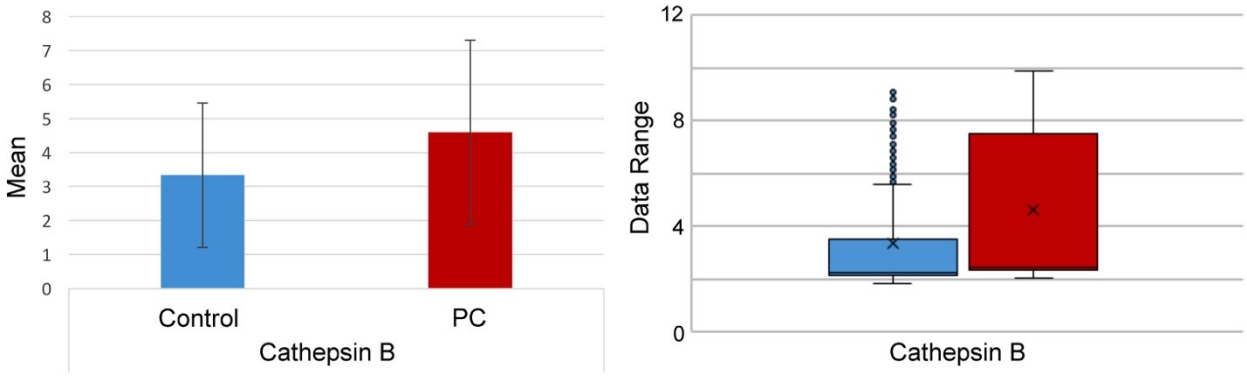


**Figure 14: Statistical genetic expression analysis of Cathepsin B in primary tumor samples and healthy human tissue (group sizes: n(CTS B) = 117). All data were obtained from the NCBI GEO database.[102] Bar graph (left, showing means and standard deviations) and box plot (right, indicating the observed data range). PC: primary pancreatic cancer tissue. Control: apparently non-cancerous tissue from the same patient.**

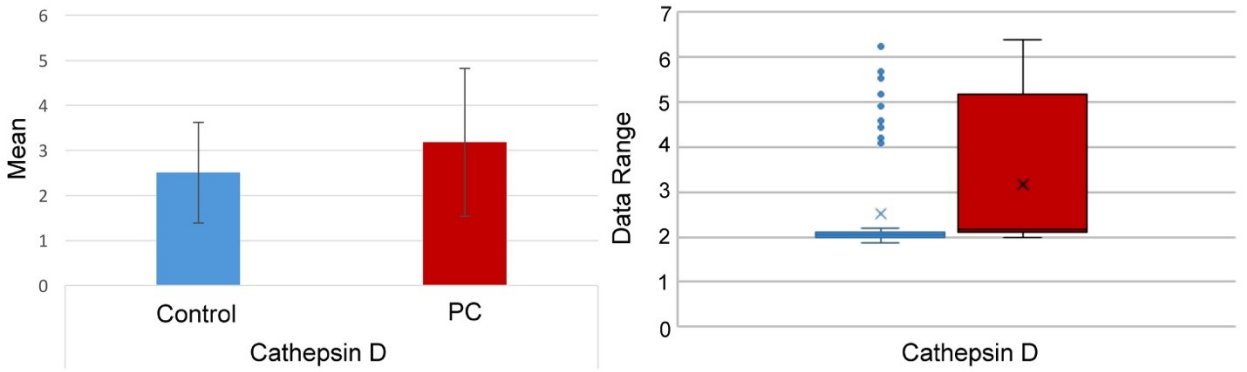


**Figure 15: Statistical genetic expression analysis of Cathepsin D in primary tumor samples and healthy human tissue (group sizes: n(CTS D) = 117. All data were obtained from the NCBI GEO database.[102] Bar graph (left, showing means and standard deviations) and box plot (right, indicating the observed data range). PC: primary pancreatic cancer tissue. Control: apparently non-cancerous tissue from the same patient.**

According to the data summarized in Figure 15, cathepsin D appears to be a slightly better candidate for detecting pancreatic cancer than cathepsin B. However, since this data is obtained

from primary cancerous tissue and apparently healthy tissue from the same patient, it does not exactly reflect the different expression pattern in truly healthy and pancreatic cancer patients.

The gene expression analysis performed here (Figure 16) clearly identified cathepsin E as the best candidate for pancreatic cancer detection.

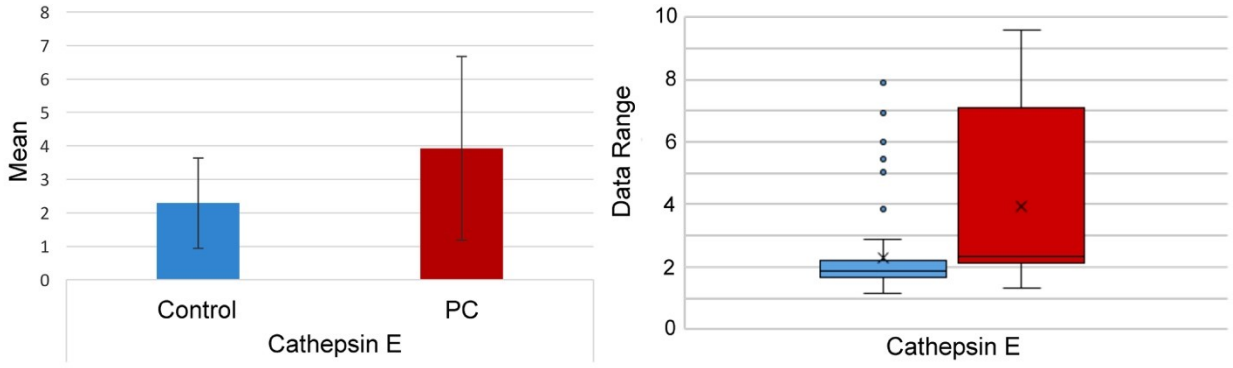


**Figure 16: Statistical genetic expression analysis of Cathepsin E in primary tumor samples and healthy human tissue (group sizes: n(CTS E) = 117). All data were obtained from the NCBI GEO database.[102] Bar graph (left, showing means and standard deviations) and box plot (right, indicating the observed data range). PC: primary pancreatic cancer tissue. Control: apparently non-cancerous tissue from the same patient.**

Both, urokinase-plasminogen-type activator (uPA)[112] and urokinase-plasminogen receptor[113] exist in multiple isoforms. Depending on the location where uPA is active, we decide between uPA (all isoforms which can be found in blood) and uPA-tissue type, which comprises all isoforms found in tissue. As shown in Figure 17, uPA-tissue type is most promising as biomarker for pancreatic cancer. However, the nanobiosensors in the Bossmann group are not yet able to differentiate between the uPA isotypes. Furthermore, uPA-tissue type has to migrate into the bloodstream before it can be detected besides uPA in liquid biopsies based on serum. During the recent years, the uPA-Receptor isoforms in blood and tissue have become the target of great interest[113], because they appear to be proximal biomarkers for metastases in numerous solid

tumors.[114] The Bossmann group is currently working on supramolecular detectors, which will be able to detect the uPA receptor in the future.

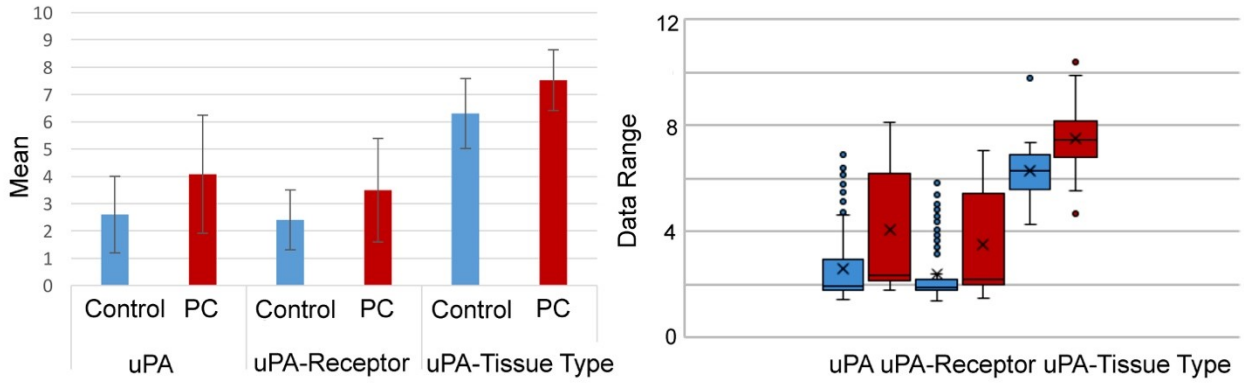


**Figure 17: Statistical genetic expression analysis of urokinase-plasminogen activators (uPA's), urokinase-plasminogen activators receptor and uPA – tissue type in primary tumor samples and healthy human tissue (group sizes: n(uPA) = 117, n(uPA tissue) = 117, n(uPA receptor = 117). All data were obtained from the NCBI GEO database.[102] Bar graph (left, showing means and standard deviations) and box plot (right, indicating the observed data range). PC: primary pancreatic cancer tissue. Control: apparently non-cancerous tissue from the same patient.**

MMP-1 is a marker for tissue remodeling and, therefore, overexpressed in numerous solid tumors.[115] It has been found to be a proximal marker for non-small-cell-lung cancer as well.[82]

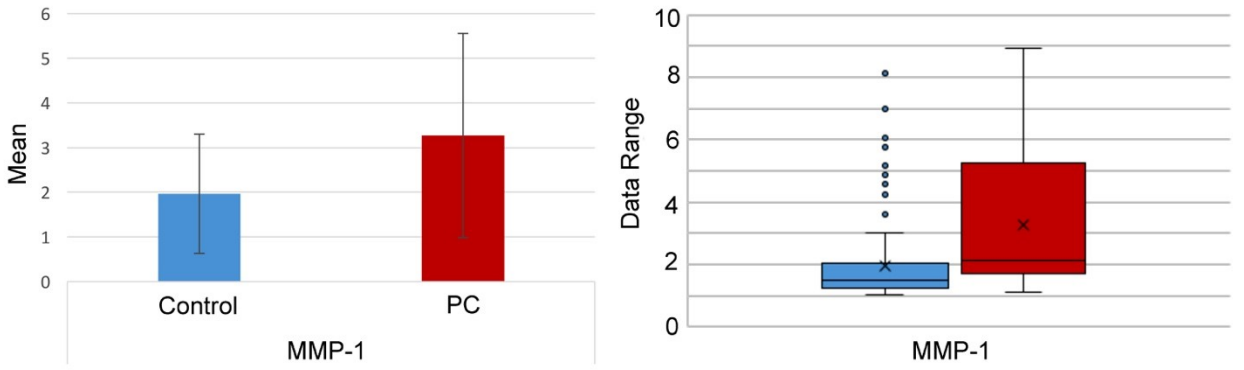


**Figure 18: Statistical genetic expression analysis of Matrix Metalloproteinase 1 (MMP-1) in primary tumor samples and healthy human tissue (group sizes: n(MMP-1) = 117. All data were obtained from the NCBI GEO database.[102] Bar graph (left, showing means and standard deviations) and box plot (right, indicating the observed data range). PC: primary pancreatic cancer tissue. Control: apparently non-cancerous tissue from the same patient.**

MMP-3 has been recently proposed as a prognostic factor for poor survival in pancreatic, pulmonary, and mammary carcinoma.[116] Furthermore, MMP-1, -2, -3, -7. -11 (not tested here), and MMP-13 (not tested here) are implicated in inflammation-induced epithelial-to-mesenchymal transitions (EMT).[117]

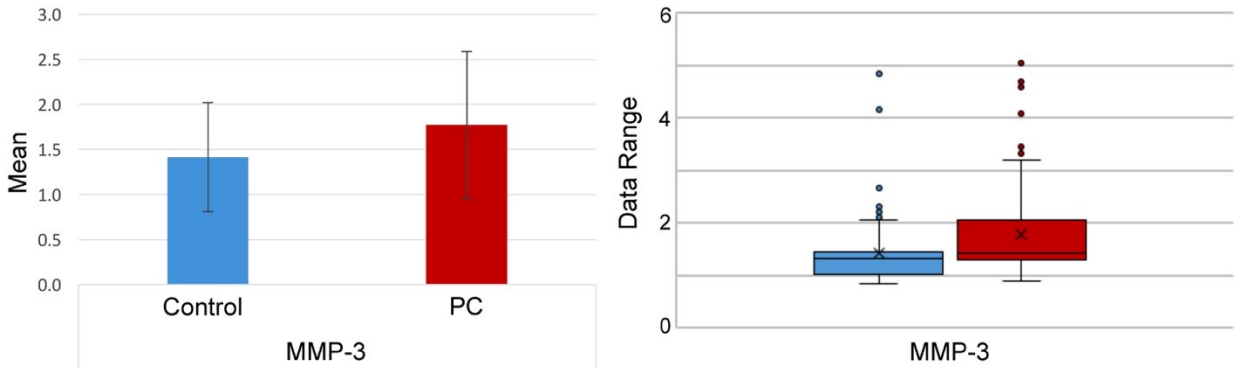


**Figure 19: Statistical genetic expression analysis of MMP-3 in primary tumor samples and healthy human tissue (group sizes: n(MMP-3) = 117). All data were obtained from the NCBI GEO database.[102] Bar graph (left, showing means and standard deviations) and box plot (right, indicating the observed data range). PC: primary pancreatic cancer tissue. Control: apparently non-cancerous tissue from the same patient.**

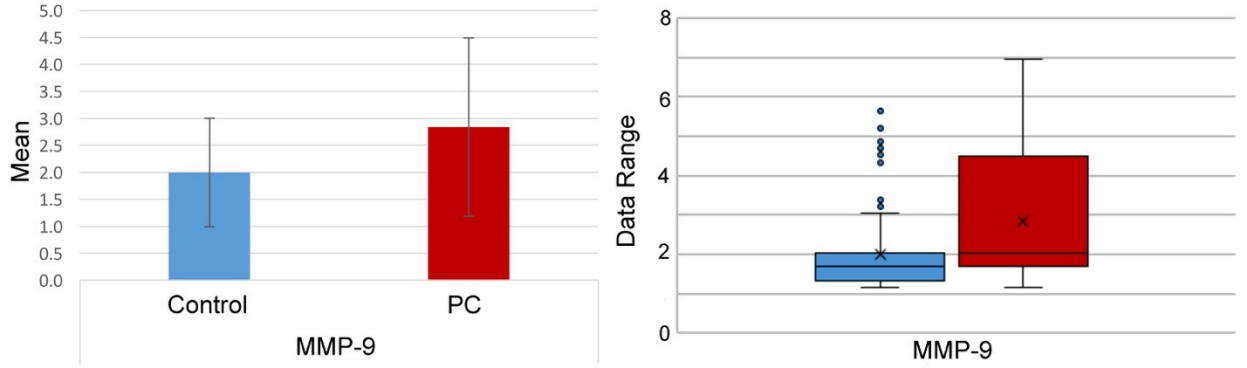


**Figure 20: Statistical genetic expression analysis of MMP-9 in primary tumor samples and healthy human tissue (group sizes: n(MMP-9) = 117). All data were obtained from the NCBI GEO database.[102] Bar graph (left, showing means and standard deviations) and box plot (right, indicating the observed data range). PC: primary pancreatic cancer tissue. Control: apparently non-cancerous tissue from the same patient.**

In previous studies, MMP-9 was found in excess amounts in pancreatic cancer tissue samples with compared to the normal pancreatic tissue samples.[45]

Neutrophil elastase has been included into this panel, because it was predicted that it will be less active in tumor tissue than in presumably healthy tissue of the same patient. This offers the opportunity to further experimentally test the predictions of statistical genomic expression analysis. Neutrophil elastase is produced by active neutrophils and a mediator of the innate immune system.[118] However, tumor tissue is highly immune-depressed, as characterized by high arginase activity.[80] Therefore, it can be expected that neutrophil elastase activity is low in pancreatic tumor tissue.

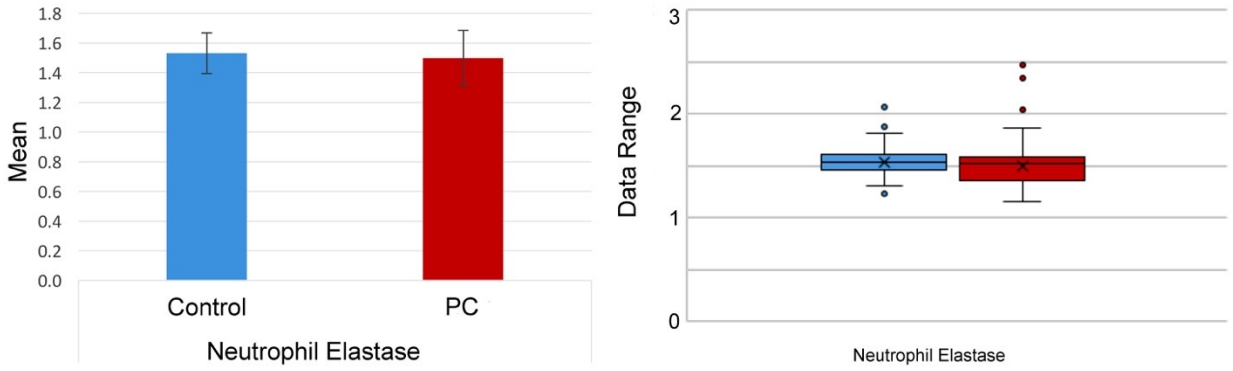


**Figure 21: Statistical genetic expression analysis of neutrophil elastase (NE) in primary tumor samples and healthy human tissue (group sizes: n(NE) = 117). All data were obtained from the NCBI GEO database.[102] Bar graph (left, showing means and standard deviations) and box plot (right, indicating the observed data range). PC: primary pancreatic cancer tissue. Control: apparently non-cancerous tissue from the same patient.**

In Table 4, the ID's, p-values[119] and logFC (down- or up-regulation of genes) for the group of target proteases in pancreatic cancer tissue samples are summarized.[103,104] It should be noted again that this data is obtained from comparing the protease expression levels in primary pancreatic tumors and apparently healthy tissue samples from the same patients. Since cancer is a systemic disease, it cannot be expected that all of these correlations can be verified by measuring the activity

(not the concentration) of proteases in a group of pancreatic cancer patients and a group of age-matched healthy volunteers. Much more likely, also noncancerous tissue will be affected by a tumor somewhere in the patient's body, because this tumor is connected to the blood supply starting from stage I. [91,120,121]

**Table 4: NCBI GEO ID's, p-values[119] and logFC (down- or up-regulation of genes) for the group of target proteases in pancreatic cancer tissue samples.[103,104]**

| ID | P-Value | logFC | Gene symbol | Gene title |
|---|---|---|---|---|
| Arginase 2 | | | | |
| 7975268 | 4.20E-02 | 0.17303 | ARG2 | Arginase 2 |
| Cathepsin B | | | | |
| 8149330 | 3.18E-07 | 0.848623 | CTSB | Cathepsin B |
| Cathepsin D | | | | |
| 7945666 | 5.64E-07 | 0.534505 | CTSD | Cathepsin D |
| Cathepsin E | | | | |
| 7909164 | 6.00E-15 | 2.684101 | CTSE | Cathepsin E |
| uPA | | | | |
| 7928429 | 2.54E-10 | 1.374367 | PLAU | Plasminogen activator, urokinase |
| 8037374 | 7.25E-07 | 0.843846 | PLAUR | Plasminogen activator, urokinase receptor |
| MMP1 | | | | |
| 7951271 | 1.96E-04 | 1.225159 | MMP1 | Matrix metallopeptidase 1 |
| MMP3 | | | | |

| | | | | |
|---|---|---|---|---|
| 7951284 | 1.93E-05 | 0.66726 | MMP3 | Matrix metallopeptidase 3 |
| MMP9 | | | | |
| 8063115 | 5.12E-09 | 1.116676 | MMP9 | Matrix metallopeptidase 9 |
| Neutrophil Elastase | | | | |
| 8024056 | 8.87E-02 | -0.09965 | ELANE | Elastase, neutrophil expressed |

## 2.4 Synthesis and Validation of Ultrasensitive Nanobiosensors for Protease and Arginase

A detailed account of the Bossmann group's recent development of $Fe/Fe_3O_4$ nanoparticle based diagnostic nanobiosensors is given in references.[80,81,122,123] $Fe/Fe_3O_4$ nanoparticles are synthesized by thermal decomposition of $Fe(CO)_5$.[122,124,125] The nanoparticles have a well-defined core/shell structure, with the average Fe(0) core diameter of 13 +/- 0.5 nm and the $Fe_3O_4$ shell thickness of 2.0 ± 0.5 nm, respectively.[122] Dopamine forms robust organic coatings with binding constants of the order of $10^{15}$ l $mol^{-1}$.[126] It also increases the water-solubility of the resulting nanoplatforms to > 5g $L^{-1}$.[126] Porphyrins have been used as cleavable fluorescent dyes, because their photophysical properties are well characterized.[127] Cyanine 5.5 has been co-attached as FRET quencher due to its large molar extinction coefficient.[128] Figure 22 shows the structure of the nanoplatform comprised of dopamine-coated $Fe/Fe_3O_4$, consensus sequence, TCPP, and Cy 5.5. In Table 5, the consensus sequences that will be employed for detecting the selected proteases[129], as well as the peptide tether for measuring arginase[80], are summarized. Cyanine 5.5 is permanently linked to dopamine without using an enzyme-cleavable tether. The optimal average density of cyanine 5.5, which is directly bound to the dopamine units, and TCPP, which is tethered via oligopeptide, was determined to 50+/-4 (Cy 5.5) and 35+/-3 (TCPP) per nanoparticle, following a

random-deposition based modelling approach[130], assuming a core/shell structure, with average Fe(0) core diameter of 13 +/- 0.5 nm and $Fe_3O_4$ shell thickness of 2.0 +/- 0.5 nm, respectively.To date, the Bossmann group has scaled up the synthesis of the nanobiosensors to the 5g stage.

The nanoplatforms are activated via enzymatic cleavage or posttranslational modification of the tether between central nanoparticle and dye, which leads to increased TCPP-fluorescence (*light switch effect, see* Figure 23).[122]

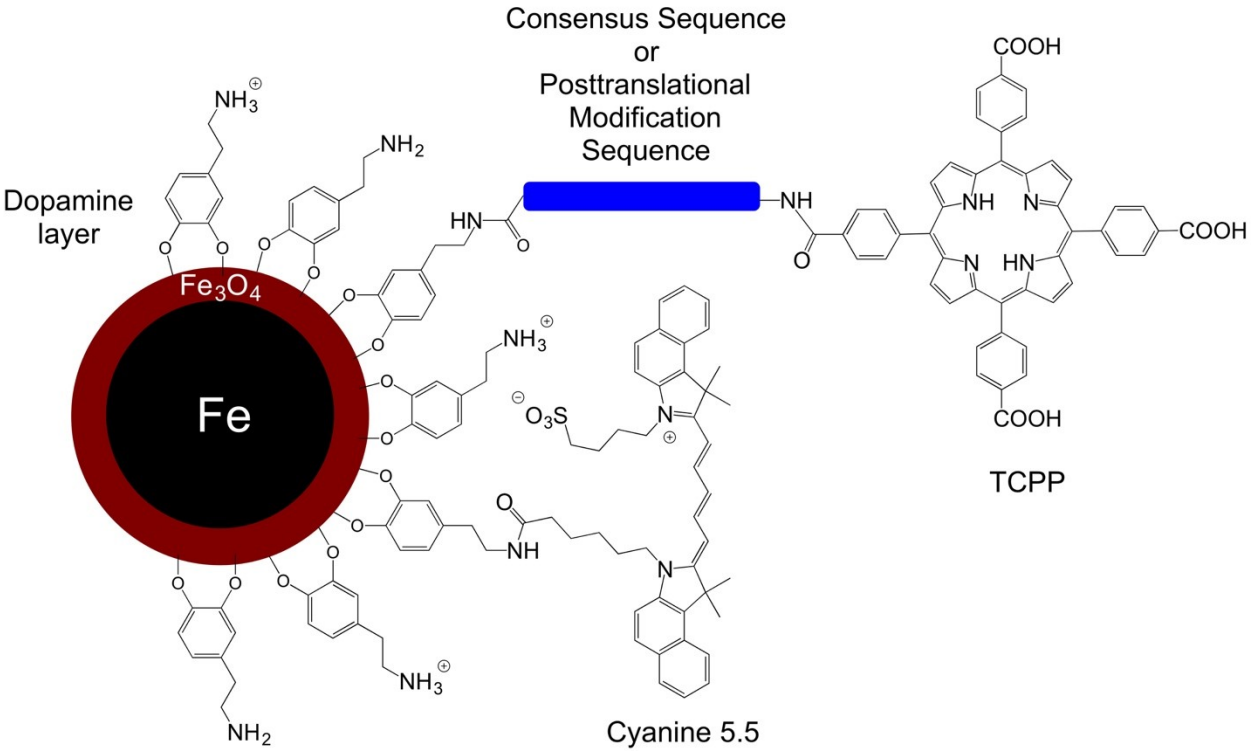


**Figure 22: Chemical structure of the nanobiosensors for protease and arginase detection**

Figure 22 shows the core of the nanobiosensor consists of dopamine-coated a $Fe/Fe_3O_4$ core to which 50+/-4 cyanine 5.5 and 35+/-3 TCPP molecules are bound, following a random-deposition based modelling approach.[130] The consensus sequences experience proteolytic cleavage by their respective proteases, whereas the chemical constitution of the posttranslational

modification sequence is changed. For instance, arginases I + II convert arginine to ornithine without proteolytic cleavage of the oligopeptide.[80]

Due to the inferior scattering properties of Fe(0)-nano-particles (compared to Ag and Au)[131], the limits of detection (LOD) when using central $Fe/Fe_3O_4$-nano-particles in optical nanobiosensors are significantly lower. For all MMPs and cathepsins use here, **sub-femtomolar** limits of detection (LOD) have been realized.[122,132] After optimization, ten repetitions of the calibration procedure established a relative error under 2%, which is sufficient for clinical applications.

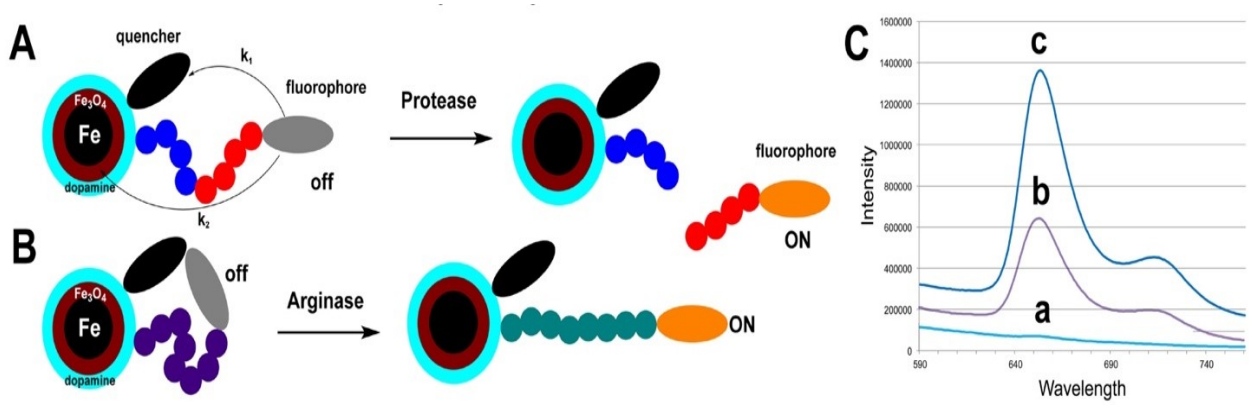


**Figure 23: A: Function principle of nanobiosensors for protease detection: the consensus sequence is cut by the protease; B: Function principle of nanobiosensors for posttranslational modification: the chemical identity of amino acids in the linker is changed via enzymatic reaction;** C**: Typical emission spectra occurring from the nanosensor for MMP-3 after 1h of incubation at 37°C ($\lambda_{exc}$ = 421nm).** a**: buffer;** b**: nanosensor in HEPES buffer after 1h of incubation at 37°C;** c**: nanosensor after 1h of incubation with MMP-3 at 37°C.**

## 2.5 Methods

### 2.5.1 Nanobiosensor Synthesis

The synthesis of the nanobiosensors has been performed according to established and published procedures.[80,122,125,132] In short, water-dispersible $Fe/Fe_3O_4$ nanoparticles featuring dopamine ligands[126], TCPP[122], and cyanine 5.5[122] were synthesized according to established procedures.

Oligopeptides were synthesized by means of solid phase peptide synthesis on 2-chlorotrityl resin.[125,133] Three equivalents of $F_{moc}$ (N-(9-fluorenyl)methoxycarbonyl) protected amino acid and HBTU were dissolved in a DIEA/DMF solution, and added to the 2-chlorotrityl resin preloaded with 0.20 mmol of amino acid per g. The solution was drained from the resin after 30 minutes of reaction. This process was repeated one more time. Then, the $F_{moc}$ group of the newly introduced amino acid was removed by using 20% (v/v) piperidine in DMF. Following this procedure, stepwise addition of $F_{moc}$-protected amino acids resulted in the desired peptides. The consensus sequences used are summarized in Table 5. TCPP has been connected to the N-terminal end of the oligopeptides while it was still on the resin. The TCPP-oligopeptide was then cleaved off the resin and linked to the primary amine groups of $Fe/Fe_3O_4$-bound via an amide bond.[122] Note that these sequences also contain GAG and AG as peptide spacers at the N- and C-terminal ends of the oligopeptides to facilitate easier access by the enzymes to their respective consensus sequence. The oligopeptides have been purified by quantitative HPLC if their purity did not exceed 90%, as determined by analytical HPLC.[80,81,122] Their chemical identity has been confirmed by MALDI-TOF.[1-3] Nanobiosensors were assembled according to the published procedures[80,122,125,132] and the separation of the nanobiosensors from unreacted low molecular weight components, dyes, and oligopeptides, will be achieved via dialysis (cut-off: 5,000 Da). After subsequent lyophilisation,

the resulting nanobiosensors have a shelf-life of at least 2 years when stored under argon between + 4 and – 80ºC.

**Table 5: Peptide Sequences for Nanobiosensors**[129]

| Nanobiosensor | Oligopeptide Tether |
|---|---|
| **MMP 1** | GAG**VPMS-MRGG**AG |
| **MMP 3** | GAG**RPFS-MIMG**AG |
| **MMP 9** | GAG**VPLS-LYSG**AG |
| **uPA** | GAG**SGR-SA**G |
| **Cathepsin B (CTS B)** | GAG**SLLKSR-MVPNFN**AG |
| **Cathepsin D** | GA**GDSG-LGRA**G |
| **Cathepsin E** | GAG**EVAL-VALK**AG |
| **Neutrophil Elastase** | GAG**GEPV-SGLP**AG |
| **Arginase** | GAG **RRRRRRR**AG |

Peptide sequences are written in single-letter code.

### 2.5.2 Fluorescent Plate Reader Measurements: Calibration and Validation

A BioTek Synergy 2 plate reader (tungsten halogen lamp, excitation bandpass filter: 421 ± 10 nm, analysis bandpass filter: 650 ± 25 nm) with 96-well plates was used. Solution (1) HEPES buffer (25 µmol) (2-[4-(2-hydroxyethyl) piperazin-1-yl]ethanesulfonic acid) was prepared enriched with Ca(II), Mg(II), and Zn(II) (10 µmol each) at 298 K (pH=7.2) to ensure full enzymatic activities. Solution (2) containing the $Fe/Fe_3O_4$ based nanobiosensor was prepared by dissolving 0.30 mg of the selected nanobiosensor in 1.0 mL of HEPES buffer by sonication for 10 min at 298 K. The following samples were prepared and plated by adding solution (1) or solution (2) to 5 µL of serum/protease sample; A: Sample Control (125 µL of solution (1) + 5 µL serum/protease sample); B: Assay (125 µL of solution (2) + 5 µL of serum/calibration solution containing known

concentrations of commercially available proteases; C: Assay Control (125 µL of solution (2) + 5 µL of solution (1)); and D: Blank (130 µL of solution (1)). Each sample (total 130 µL) was loaded into one well of 96 wells plates, having at least three replicates of each assay per serum/protease sample. Solutions were incubated at 310 K for 60 min, followed by detection of nanoplatform fluorescence at 298 K utilizing a 96-well fluorescence plate reader. Matrix effects have been previously evaluated by using heat-inactivated combined sera from the control group of healthy volunteers. The results were previously published.[81] Heat inactivation of serum was performed according to established procedures.[134] Whereas in previous analyses of the protease activities in serum, we have calculated the protease activity for each measured protease, the main focus of this study was on developing a quick fluorescence plate-reader method for pancreatic cancer detection, which will work reliable in a clinical setting. Therefore, the actual fluorescence signals measured by the plate reader were used to calculate the results discussed below.

## 2.6 Results and Discussion

Arginase activity appears to be higher in patients with pancreatic ductal adenocarcinomas (DAC) and metastatic pancreatic adenocarcinoma (MAC) than in the control group (Figure 24). However, the observed variations are much higher in both groups of pancreatic cancer patients than in the apparently healthy control groups. It is noteworthy that arginase activity is about the same in healthy and patients having pancreatic neuroendocrine tumors (NET), whereas the arginase activity is actually lower in patients with metastatic pancreatic neuroendocrine tumors than in the control group. As summarized in Table 6, there are statistically significant differences for ductal adenocarcinomas, which have the highest incidence and mortality of all pancreatic cancers, and for metastatic neuroendocrine tumors.[66]

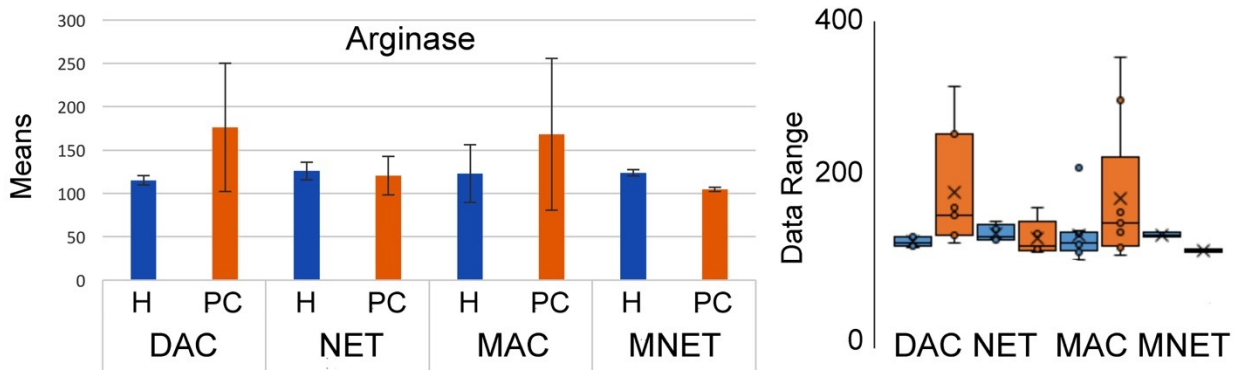


**Figure 24: Bar graph (left, showing means and standard deviations of fluorescence intensities) and box plot (right, indicating the observed data range) for Arginase. Group sizes: apparently healthy volunteers: n=48, pancreatic ductal adenocarcinoma (DAC): n=7, metastatic adenocarcinoma (MAC): n=9, pancreatic neuroendocrine tumors (NET): n=5, metastatic NET (MNET): n=2, all pancreatic cancers (ALL): n = 35. All samples were obtained from the Biospecimen Repository Facility of the University of Kansas Cancer Center.[135] H=age-matched healthy volunteers; PC=pancreatic cancer patients**

The variations that are observed in the control groups arise from the age-matching process. The same numbers of age-matched healthy volunteers than in the respective cancer groups were selected from the control group to avoid an age-bias in the analysis of this data, except for MNET, which was too small. Gene expression analysis predicted upregulation of arginase expression in tumors tissue. For two sub-groups, DAC and MAC, we did observe higher arginase activities.

Cathepsin B expression was lower in all investigated sub-groups of pancreatic cancer, with the exception of pancreatic neuroendocrine tumors (NET), where it was slightly higher (Figure 25). Although the expression patterns were not consistent, the data for both, ductal adenocarcinomas (DAC) and neuroendocrine tumors (NET) were statistically significant, whereas no significance was calculated for both groups of metastasizing pancreatic cancer. Gene expression analysis predicted upregulation of cathepsin B expression. Higher cathepsin B activity was only observed in NET, all other groups were lower in activity.

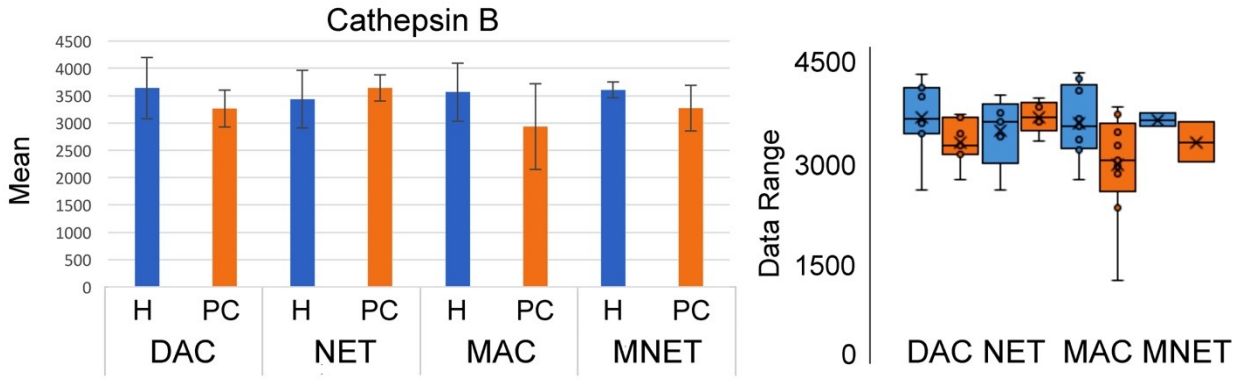


**Figure 25: Bar graph (left, showing means and standard deviations of fluorescence intensities) and box plot (right, indicating the observed data range) for Cathepsin B. Group sizes: apparently healthy volunteers: n=48, pancreatic ductal adenocarcinoma (DAC): n=9, metastatic adenocarcinoma (MAC): n=9, pancreatic neuroendocrine tumors (NET): n=5, metastatic NET (MNET): n=2, all pancreatic cancers (ALL): n = 35. All samples were obtained from the Biospecimen Repository Facility of the University of Kansas Cancer Center.[135] H=age-matched healthy volunteers; PC=pancreatic cancer patients**

Although some patients in the sub-groups of ductal adenocarcinoma (DAC), neuroendocrine tumors (NET) and metastasizing adenocarcinomas (MAC) were characterized by high cathepsin D activities in serum, no statistically significant differences between all four pancreatic cancer sub-groups and their respective control groups have been detected. This is surprising, because gene expression analysis predicted significant over-expression of cathepsin D in pancreatic tumor tissue. This may be an indication that for cathepsin D, there is no good correlation between activity in tumor tissue and in blood, or this may have been caused by the relatively small group sizes of this study. Another reason for the observed discrepancy is that all proteases are being biosynthesized as zymogens (inactive enzymes). They require enzymatic activation, usually by another protease. Therefore, cathepsin D, as well as some of the other proteases, which do not fit the predicted pattern, may be synthesized in high concentration, but not activated.[91,95,136]

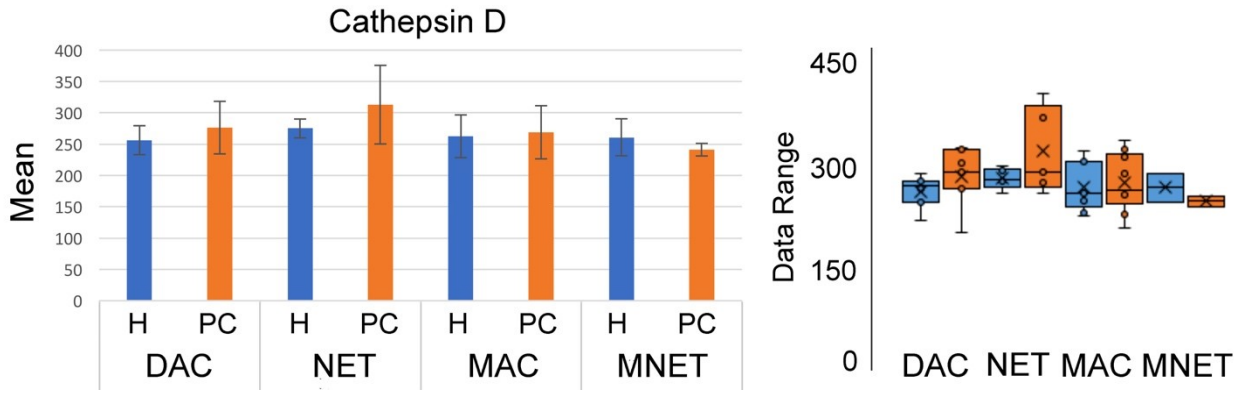


**Figure 26: Bar graph (left, showing means and standard deviations of fluorescence intensities) and box plot (right, indicating the observed data range) for Cathepsin D. Group sizes: apparently healthy volunteers: n=48, pancreatic ductal adenocarcinoma (DAC): n=7, metastatic adenocarcinoma (MAC): n=9, pancreatic neuroendocrine tumors (NET): n=5, metastatic NET (MNET): n=2, all pancreatic cancers (ALL): n = 35. All samples were obtained from the Biospecimen Repository Facility of the University of Kansas Cancer Center.[135] H=age-matched healthy volunteers; PC=pancreatic cancer patients**

Genetic expression analysis also predicted that cathepsin E will be an excellent marker for pancreatic cancers and over-expressed in tumor tissue. Elevated activity of cathepsin E was found in the sera of patients with neuroendocrine tumors (Fiigure 27), whereas in all other three pancreatic cancer sub-groups cathepsin E activity was lower than in the respective control groups. The data distributions yielded statistically significant differences for pancreatic ductal adenocarcinomas (DAC) and neuroendocrine tumors (NET), but not for both groups of metastasizing pancreatic cancer. Cathepsin E will be a valuable member of the panel of proteases designed for early diagnosis of pancreatic cancer.

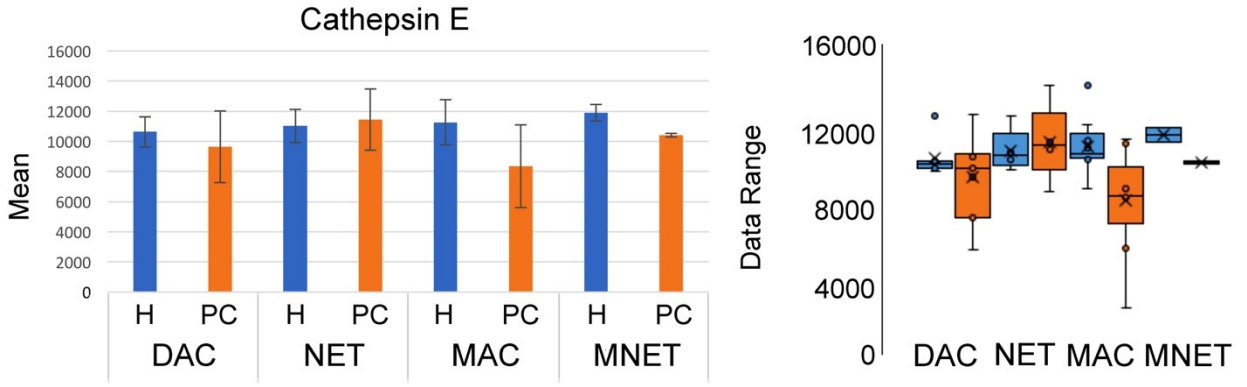


**Figure 27: Bar graph (left, showing means and standard deviations of fluorescence intensities) and box plot (right, indicating the observed data range) for Cathepsin E. Group sizes: apparently healthy volunteers: n=48, pancreatic ductal adenocarcinoma (DAC): n=7, metastatic adenocarcinoma (MAC): n=9, pancreatic neuroendocrine tumors (NET): n=5, metastatic NET (MNET): n=2, all pancreatic cancers (ALL): n = 35. All samples were obtained from the Biospecimen Repository Facility of the University of Kansas Cancer Center.[135] H=age-matched healthy volunteers; PC=pancreatic cancer patients**

Gene expression analysis correctly predicted the upregulation of urokinase plasminogen activator (uPA). UPA's activity is enhanced in all four patient sub-groups, compared to their respective control groups (Figure 28). However, there is a considerable variability of uPA activity within the sub-groups of cancer patients, as well as the apparently healthy volunteers. Therefore, only neuroendocrine tumors could be detected with statistical significance. Since uPA has numerous functions within the human body[91], it is not surprising that its expression pattern varies, to a degree, between different human subjects. However, uPA may play a more important role with regard to early pancreatic cancer detection when data obtained from larger patient groups can be analyzed in the near future.

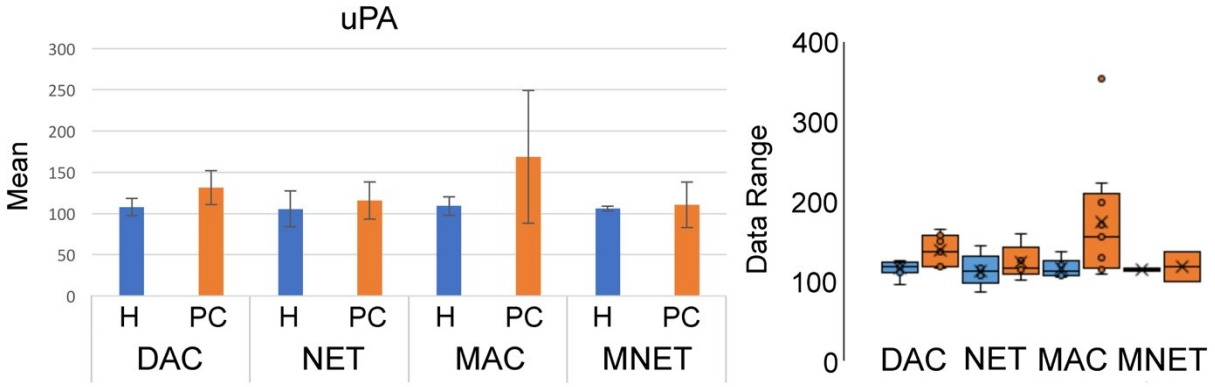


**Figure 28: Bar graph (left, showing means and standard deviations of fluorescence intensities) and box plot (right, indicating the observed data range) for urokinase plasminogen activator. Group sizes: apparently healthy volunteers: n=48, pancreatic ductal adenocarcinoma (DAC): n=7, metastatic adenocarcinoma (MAC): n=9, pancreatic neuroendocrine tumors (NET): n=5, metastatic NET (MNET): n=2, all pancreatic cancers (ALL): n = 35. All samples were obtained from the Biospecimen Repository Facility of the University of Kansas Cancer Center.[135] H=age-matched healthy volunteers; PC=pancreatic cancer patients**

Genetic expression analysis also predicted overexpression of MMP-1 in pancreatic tissue. In this case, we were able to find enhanced MMP-1 activity in virtually all sera from pancreatic cancer patients. For the group of early pancreatic cancers (ductal adenocarcinomas and neuroendocrine tumors), MMP-1 is a proximal biomarker. For the group of metastasizing pancreatic cancers, detecting MMP-1 leads to less significant data. Again, the calculation of the p-values is affected by the relatively small numbers[119]: metastatic adenocarcinoma (MAC): n=9, and metastatic neuroendocrine tumors (MNET): n=2. It is our expectation that statistically significant differences between MAC and MNET and their control groups can be seen when larger patient cohorts become available.

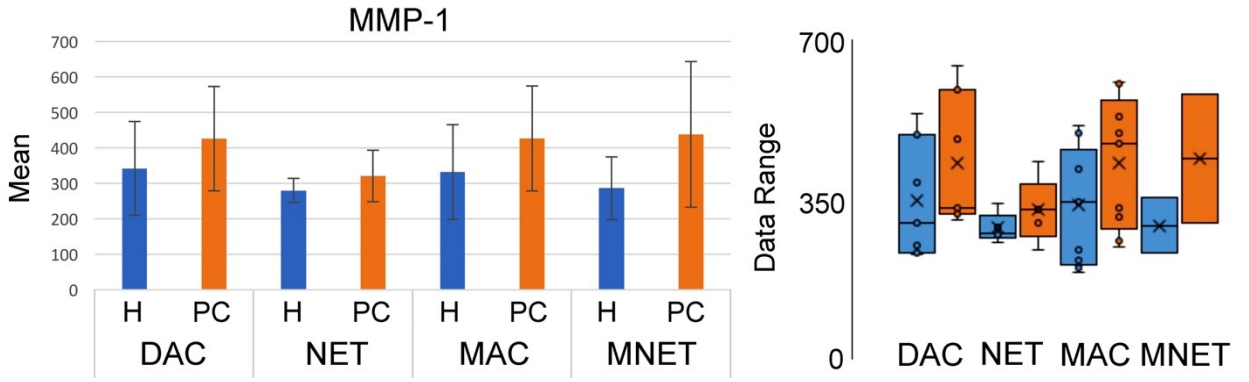


**Figure 29: Bar graph (left, showing means and standard deviations of fluorescence intensities) and box plot (right, indicating the observed data range) for Matrix Metalloproteinase 1 (MMP-1). Group sizes: apparently healthy volunteers: n=48, pancreatic ductal adenocarcinoma (DAC): n=7, metastatic adenocarcinoma (MAC): n=9, pancreatic neuroendocrine tumors (NET): n=5, metastatic NET (MNET): n=2, all pancreatic cancers (ALL): n = 35. All samples were obtained from the Biospecimen Repository Facility of the University of Kansas Cancer Center.[135] H=age-matched healthy volunteers; PC=pancreatic cancer patients**

In agreement with gene expression analysis, MMP-3 activities are enhanced in all four sub-groups of pancreatic cancer patients (Figure 30). However, only for ductal adenocarcinomas (DAC), a statistically significant difference between the cancer and the control group was observed. In the other three groups, the differences were systematic, but too small, considering the small number of patients in each group (NET, MNET), or the experimental variance was too high (MAC). For detecting DAC, MMP-3 was the best biomarker in this study (see Table 6).

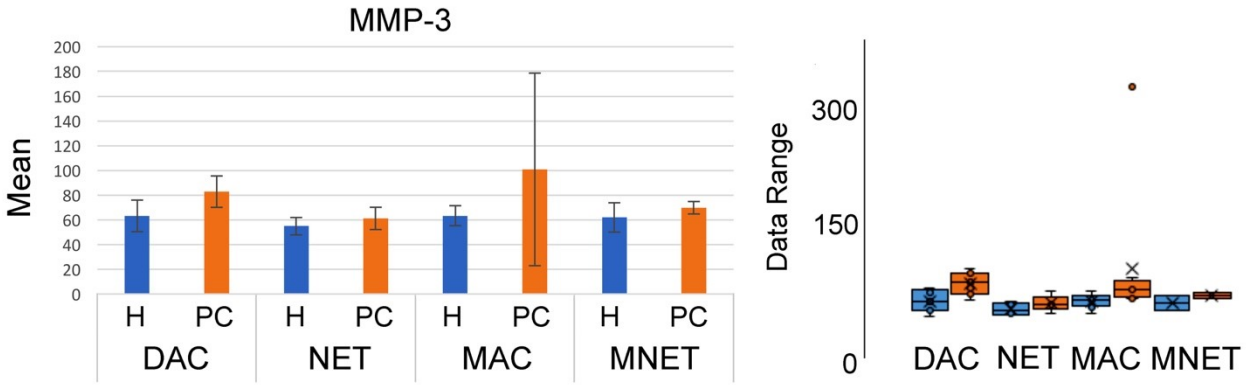


**Figure 30: Bar graph (left, showing means and standard deviations of fluorescence intensities) and box plot (right, indicating the observed data range) for Matrix Metalloproteinase 3 (MMP-3). Group sizes: apparently healthy volunteers: n=48, pancreatic ductal adenocarcinoma (DAC): n=7, metastatic adenocarcinoma (MAC): n=9, pancreatic neuroendocrine tumors (NET): n=5, metastatic NET (MNET): n=2, all pancreatic cancers (ALL): n = 35. All samples were obtained from the Biospecimen Repository Facility of the University of Kansas Cancer Center.[135] H=age-matched healthy volunteers; PC=pancreatic cancer patients**

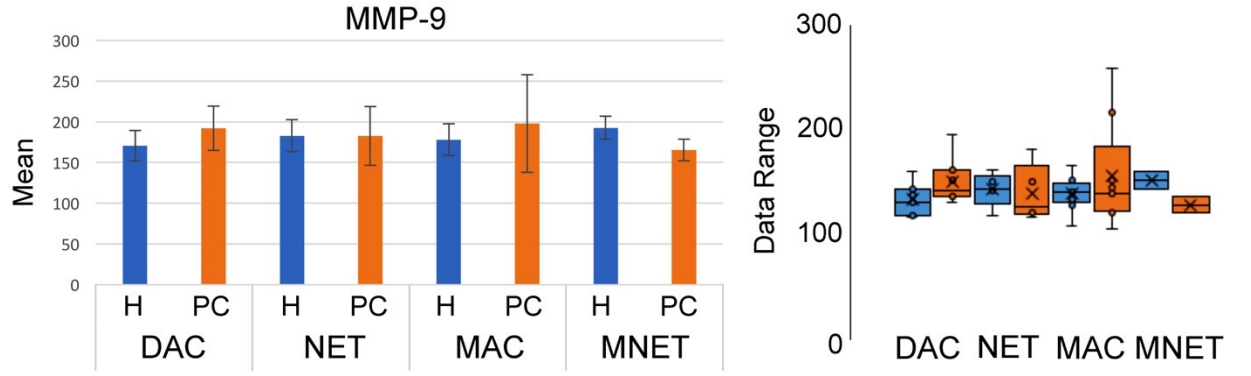


**Figure 31: Bar graph (left, showing means and standard deviations of fluorescence intensities) and box plot (right, indicating the observed data range) for Matrix Metalloproteinase 9 (MMP-9). Group sizes: apparently healthy volunteers: n=48, pancreatic ductal adenocarcinoma (DAC): n=7, metastatic adenocarcinoma (MAC): n=9, pancreatic neuroendocrine tumors (NET): n=5, metastatic NET (MNET): n=2, all pancreatic cancers (ALL): n = 35. All samples were obtained from the Biospecimen Repository Facility of the University of Kansas Cancer Center.[135] H=age-matched healthy volunteers; PC=pancreatic cancer patients**

MMP-9 activity was enhanced in ductal adenocarcinomas, neuroendocrine tumors and metastasizing adenocarcinomas, which is in agreement with the prediction from gene expression

analysis (Figure 31). However, for all three sub-groups, the differences in MMP-9 activities detected in the sera of cancer patients and healthy volunteers were not statistically significant.

Only for the group of metastasizing neuroendocrine tumors, for which MMP-9 activity was decreased, a potential significance could be discerned, as indicated by $p = 0.0715$ for $n=2$. However, further analyses with larger patient numbers have to be performed to either verify or falsify this result. This will depend on the availability of de-identified quality serum samples.

Genetic expression analysis predicted a decreased activity of neutrophil elastase (NE) in tumor tissue. Interestingly and quite contrary to this prediction, NE activity was increased in all four sub-groups, compared to their respective control groups (Figure 32). Due to the large variations found in both, patient and control groups, statistically significant differences were found in none of the sub-groups. Without further experimental data, it is not possible for us to speculate about the observed discrepancy between gene expression analysis and protease activity measurements.

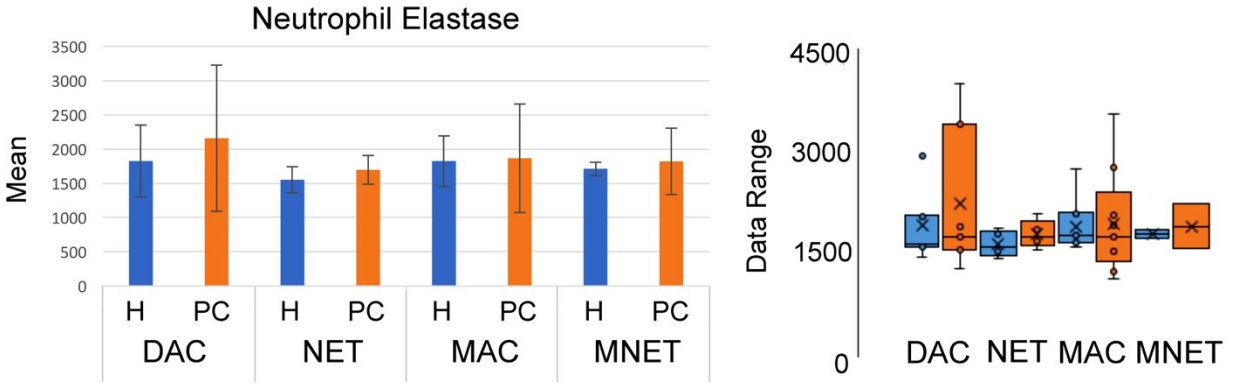


**Figure 32: Bar graph (left, showing means and standard deviations of fluorescence intensities) and box plot (right, indicating the observed data range) for Neutrophil Elastase (NE). Group sizes: apparently healthy volunteers: n=48, pancreatic ductal adenocarcinoma (DAC): n=7, metastatic adenocarcinoma (MAC): n=9, pancreatic neuroendocrine tumors (NET): n=5, metastatic NET (MNET): n=2, all pancreatic cancers (ALL): n = 35. All samples were obtained from the Biospecimen Repository Facility of the University of Kansas Cancer Center.[135] H=age-matched healthy volunteers; PC=pancreatic cancer patients**

The results of all protease/arginase activity measurements are summarized in Table 6, which is called **"Significance Table",** because it contains the calculated p-values for each comparison between the pancreatic cancer sub-groups and their age-matched control groups, as well as for the comparison between the groups of all pancreatic cancer patients and all apparently healthy volunteers. All pairings of pancreatic cancer (sub-)groups and enzymes, for which a significant difference in activity is found ($p < 0.05$) are shown in green, all pairings for which this is not the case, are shown in red. They may become significant when more human subjects become available. One combination (MNET/MMP-9) is shown in light green, because it is almost significant.

**Table 6: Significance Table Pancreatic Cancers:**

**DAC:** Pancreatic Ductal Adenocarcinoma; **NET:** Pancreatic Neuroendocrine Tumors;

**MAC:** Metastatic Pancreatic Adenocarcinoma; **MNET:** Metastatic Pancreatic Neuroendocrine Tumors

| | ARG | CTS B | CTS D | CTS E | MMP-1 | MMP-3 | MMP-9 | uPA | NE |
|---|---|---|---|---|---|---|---|---|---|
| **DAC** | 0.0227 | 0.0384 | 0.3742 | 0.0229 | 0.0049 | 0.0041 | 0.1370 | 0.1043 | 0.3084 |
| **NET** | 0.1234 | 0.0266 | 0.7318 | 0.0156 | 0.0426 | 0.1446 | 0.1889 | 0.0472 | 0.1385 |
| **MAC** | 0.8583 | 0.8063 | 0.3206 | 0.5352 | 0.3093 | 0.2129 | 0.9322 | 0.6045 | 0.4473 |
| **MNET** | 0.0172 | 0.3467 | 0.5111 | 0.1484 | 0.4022 | 0.2053 | 0.0715 | 0.3359 | 0.5391 |
| **ALL** | 0.0011 | 0.0003 | 0.2785 | 0.0296 | 0.0018 | 0.0061 | 0.0328 | 1.1E-06 | 0.0091 |

**In Table 6, the p-values[119] obtained for comparisons of the protease/arginase expression pattern in each cancer sub-group with those of the healthy control group are tabulated. The color green denotes measured fluorescence signals that are different from the control group with high significance ($p < 0.05$). Red denotes all cases where there is no statistically significant difference between the cancer (sub)group and the control group can be found. Group sizes: apparently healthy volunteers: n=48, pancreatic ductal adenocarcinoma**

**(DAC): n=7, metastatic adenocarcinoma (MAC): n=9, pancreatic neuroendocrine tumors (NET): n=5, metastatic NET (MNET): n=2, all pancreatic cancers (ALL): n = 35. All samples were obtained from the Biospecimen Repository Facility of the University of Kansas Cancer Center.[135] ARG: arginase, CTS: cathepsin, MMP: matrix metalloproteinase, uPA: urokinase plasminogen activator, NE: neutrophil elastase**

## 2.7 Conclusions

**All pancreatic cancer patients vs. all volunteers:** Owing to the larger groups of human subjects, compared to the sub-groups (pancreatic cancer patients: n=35, healthy volunteers: n=48), the p-values are generally lower. The result from this study is that arginase, cathepsins B and E, MMP-1, -3, -9, urokinase plasminogen activator and neutrophil elastase are capable of detecting pancreatic adenocarcinomas and neutroendocrine tumors at early and distant stages. In the clinical practice, this means that this panel of enzymes will be able to detect that a patient has potentially pancreatic cancer. Further methods of clinical diagnostics, for instance a CT scanner of high-field MRI will then follow to ascertain the patient's clinical condition.

**Pancreatic Ductal Adenocarcinoma (DAC): n=7:** As already discussed in detail above, pancreatic ductal adenocarcinomas comprise more than 90 percent of all pancreatic cancers.[76] They also possess the lowest survival rate among pancreatic cancers.[76] Therefore, detecting them early by means of a simple blood test (liquid biopsy) is most desirable. This study has identified a panel of five enzymes: arginase, cathepsins B, E, and MMP-1, and -3 that can detect DAC with high significance. Detecting pancreatic ductal adenocarcinomas at the earliest possible time has the potential to safe numerous patients' lives.

**Metastatic Adenocarcinoma (MAC): n=9:** For other solid tumors, such as breast[81]- and non-small-cell lung tumors[82], protease expression increases steadily with tumor stage. Therefore, higher stages are easier detectable by means of protease activity measurements. This is not the case for metastatic adenocarcinoma. The major reason for this difference is the great variance that is observed in this sub-group.

**Pancreatic Neuroendocrine Tumors (NET): n=5:** Cathepsin B and E, MMP-1 and uPA are suitable biomarkers for neuroendocrine tumors. Because this class of pancreatic tumors is much less aggressive than pancreatic ductal adenocarcinomas, early detection offers a greater potential of saving patents' lives.

**Metastatic Pancreatic Neuroendocrine Tumors (MNET): n=2:** Arginase and, potentially, MMP-9 are, to date, suitable biomarkers for metastatic neuroendocrine pancreatic tumors. Because of the very small group size, conclusions are very limited.

# Chapter 3 - Early Detection of Non-Small-Lung Cancer in Liquid Biopsies by Means of Ultrasensitive Protease-Activity Analysis

**Acknowledgement**

I would like to acknowledge all the co-authors, who contributed their expertise towards the success of this project. This work was funded by NSF (CBET 1159966) and 1337438, and the Johnson Cancer Center at Kansas State University.

Dinusha Udukala, PhD[a‡], Sebastian O. Wendel, PhD[ab‡], Madumali Kalubowilage[a‡], Hongwang Wang, PhD[a‡], Aruni Malalasekera, PhD[a‡] Asanka S. Yapa[a], Yubisela Toledo[a], Raquel Ortega[a], Pamela Maynez[a], Leonie Bossmann[a], Katharine Janik[a], Gary Gadbury, PhD[c], Deryl L. Troyer, PhD, DVM[b], Stefan H. Bossmann, PhD[a]

[‡]These authors have contributed equally

[a] *Department of Chemistry, Kansas State University, Manhattan, KS, USA*

[b] *Department of Anatomy & Physiology, Kansas State University, Manhattan, KS, USA*

[c] *Department of Statistics, Kansas State University, Manhattan, KS, USA*

My research was focused on synthesizing peptides, assembling, purifying and characterizing functional nanobiosensors. Furthermore, I have contributed to the data analysis in this project.

**Abbreviations**

MMP: matrix metalloproteinase, CTS: cathepsin, uPA: urokinase-type plasminogen activator, PBS: phosphate-buffered saline, HEPES: (4-(2-hydroxyethyl)-1-piperazineethanesulfonic acid), FRET: Förster Resonance Energy Transfer, SET: dipole-surface energy transfer

NSCLC: non-small-cell lung cancer

## 3.1 Abstract

Solid tumors are characterized by dysfunctional protease expression pattern. Consequently, numerous proteases, such as matrix metalloproteinases (MMP's), cathepsins (CTS), and urokinase plasminogen activator (uPA) are either over- or under-expressed, when compared to the proteasome of healthy human subjects. This enables the detection of solid tumors in liquid biopsies. We have developed nanobiosensors for ultrasensitive (sub-femtomolar) protease detection, consisting of a water-dispersible $Fe/Fe_3O_4$ core/shell nanoparticle and attached fluorescent dyes tetrakis(4-carboxyphenyl)porphyrin (TCPP) and a cyanine 5.5. Both, the central nanoparticle and cyanine 5.5 can quench photoexcited TCPP, which is attached via a protease-cleavable consensus sequence. The specificity and sensitivity of the nanobiosensors permit the accurate measurements of the activities of nine signature proteases in serum samples as small as 5 μL. This technology can detect non-small-cell lung-cancer at stage 1, which has the potential of significantly reducing lung-cancer-mortality because of earlier detection. Principally, this technology is working for the detection of virtually all solid tumors, of which many feature distinct protease signatures.

## 3.2 Background

Despite the tremendous efforts dedicated to cancer prevention, diagnosis and treatment, mortality remains unacceptably high. Specifically, lung cancer is the most commonly diagnosed deadly cancer worldwide with a disappointing 15% overall 5-year survival rate. This high mortality rate is mainly due to the absence of clinical symptoms early in the disease, lack of methods for effective screening, the molecular heterogeneity of lung cancer and the lack of techniques that can be used to select the optimum therapeutic intervention for the treatment of lung

cancer. [137,138] Non-small cell lung cancer (NSCLC) is the most common histological type of lung cancer, representing 80% of all lung cancers diagnosed and accounting for over one million deaths world-wide each year.[139] NSCLC is strongly etiologically linked to smoking/smoke exposure, an association that has been well established in large-scale epidemiological studies. These prior studies have clearly demonstrated that cigarettes are the greatest risk factor, accounting for 87% of lung cancers.[139] In addition, environmental or second-hand tobacco smoke is also linked to lung cancer.[139] Currently more than one billion people around the world are smokers. It is expected that more than eight million people will die annually from tobacco-related diseases by 2030 unless current trend is reversed.[140]

The clinical outcome of treatment for NSCLC is highly dependent on the stage of disease at the time of diagnosis. Unfortunately, the vast majority of NSCLC (70%) are diagnosed at advanced disease stages with very poor prognosis.[3] Typically, 5-year survival rates for NSCLC drop from 49% (stage IA) and 45% (IB) to 30% (II), and then rapidly to 14% (IIIA), 5% (IIIB) and less than 1% (IV).[3] Based on this data, there is a critical need for the development of analysis methods that are capable of detecting NSCLC (and other lung cancers) at its earliest stages.

Since the 1970s, researchers have investigated whether chest radiography can be used for screening and early detection of lung cancer. Later in the 1990s, high resolution CT scans produced significant improvement in the outcome for thoracic resection for lung cancer. However, similar to chest x-rays, the use of CT imaging has not been widely adopted. Reasons for this include 1) the high cost of CT scans, 2) the clinical expertise needed for their interpretation, 3) the safety concerns that the high prevalence of false positives result in surgical interventions in patients who do not actually suffer from lung cancer and 4) the lack of availability of this technique in

resource-limited environments.[141] Consequently low-dose CT is only used as a screening tool in very high-risk populations.

Thus, it is well-accepted by the medical community that new screening tools that will allow for non-invasive, cost effective and reliable screening of NSCLC need to be developed and translated to the clinic for earlier detection and improved treatment of lung cancer.[142]

### 3.2.1 Competing Technologies

The recognition of the need for the development of molecular-based screening techniques and liquid-based biopsy approaches that can be used to detect and quantify early changes that are known to accompany the onset of lung cancer before malignant changes has resulted in the development of promising techniques for non-invasive detection and staging of lung cancer.[143] While significant progress has been made for the diagnosis of intermediate and late stage lung cancer[144] in the field of liquid biopsy and the use of markers of cancer that can be detected based on the analysis of blood borne analytes (e.g. circulating proteins[145], autoantibodies[146], circulating tumor cells (CTCs)[147], circulating tumor microemboli (CTM)[148], and CTC-derived nucleic acid signatures[147]) , these techniques have failed to detect NSCLC at early stage of development mainly due to their failure to detect molecular markers of NSCLC and particularly those of EMT associated with the onset of NSCLC.[149] Although molecular-based diagnostics can, principally, help distinguish early stage lung cancer from benign nodules that are incidentally detected by a CT scan, the impact has been incremental reducing the number of false positives by 32%.[150]

### 3.2.2 Protease Activity and Cancer

Extracellular proteases are associated with a variety of disease processes.[110,136,151] In particular increased activity of matrix metalloproteinases[136] and cathepsins[110] have been reported for a variety of diseases and that makes them potential biomarker candidates. The activities of these enzymes, however, are regulated through a complex network of proteases[91] and, therefore, their activities are highly context dependent. This hampers their potential use as clinical biomarkers of disease states. Following the pioneering research of Weissleder *et al.*[108], molecular[152], macromolecular[153] and nanoparticle-based[154] protease sensors have been reported for *in-vivo* imaging and *in-vitro* diagnostics of proteases and posttranslational modification enzymes (e.g. arginase[80]) that make use of fluorescence and magnetic principles.[155] However, the limits of protease detection (LOD's) of the state-of-the-art technology are sub-picomolar (sub-ng/mg)[108,152-155], which is sufficient for *in-vivo* imaging of tumors[108,152-155], but not for the *in-vitro* detection of human cancers[156] in their earliest stages. Competing technologies for quantitative protease detection, such as immunosorbent assays[157], quantum dot barcode technology[158], and immunobeads[159] have similar LOD's.

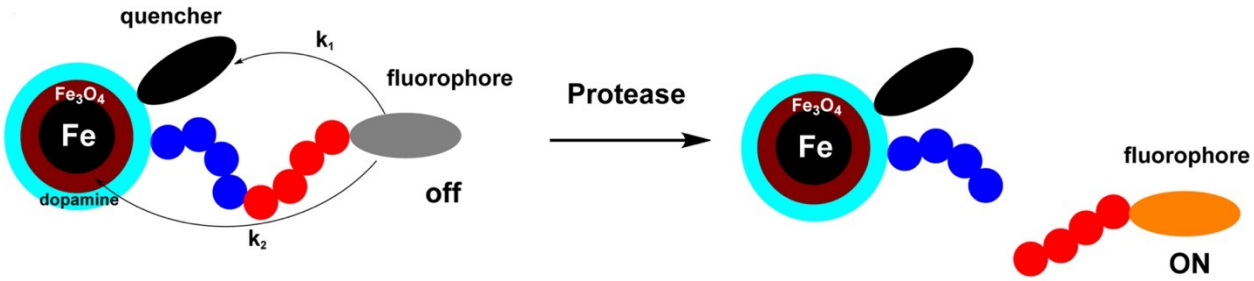


**Figure 33: Mechanistic scheme of the "light switch effect" upon proteolytic cleavage. The fluorophore is switched on due to the increase in distance between the Fe/$Fe_3O_4$ core/shell nanoparticle, leading to decreased Förster Resonance Energy Transfer (FRET), $k_1$, and dipole-surface energy transfer (SET), $k_2$.**

### 3.2.3 $Fe/Fe_3O_4$ core/shell Nanoparticle-based Nanobiosensors

The Bossmann and Troyer groups have developed nanobiosensors for protease detection[122,160] that are capable of detecting protease[122] and arginase[80] activities over a wide activity range down to sub-femtomolar LOD's. These nanoplatforms consist of dopamine-covered, water-dispersible iron/iron oxide core/shell nanoparticles, to which one fluorescent dye (TCPP, tetrakis-carboxyphenyl porphyrin) is tethered via a protease-specific or highly selective consensus sequence.[129] A second dye (Cyanine 5.5) is permanently linked to the dopamine coating. This design enables both, plasmon-resonance quenching (SET)[161] and Förster Resonance Energy Transfer (FRET) quenching[162] of the tethered TCPP units. Once TCPP is released via proteolytic cleavage of the consensus sequence, its fluorescence will increase. This "light switch effect"[122] enables highly sensitive detection of protease activity by quantitative fluorescence measurements. By using a mathematical model describing the quenching occurring between donor-acceptor pairs on a spherical surface[130,163], we have determined that 35 TCPP and 50 cyanine 5.5 dyes result in optimal quenching at the surface of dopamine-coated $Fe/Fe_3O_4$ nanoparticles (Fe(0) core: d = 13 ± 0.5 nm, $Fe_3O_4$ shell: d = 2 ± 0.5 nm, dopamine: 1 ± 0.2 nm, surface: $1.13 \times 10^{-15}$ $m^2$). Therefore, for most proteases, a substantial fluorescence increase is observed when the consensus sequence between the nanoparticle and TCPP is cleaved. However, for uPA and MMP-9, a decrease in fluorescence intensity was detected. In an earlier report, we have discussed possible reasons for this anomaly. In short, the $Fe/Fe_3O_4$ core/shell nanoparticles feature a Fe plasmon that is distinctly weaker than an Au plasmon.[122,164] The Fe-core is able to quench TCPP fluorescence very efficiently, if TCPP is sufficiently close. However, for the consensus sequences for uPA (GAGSGR-SAG) and MMP9 (GAGVPLS-LYSGAG) the distance between $Fe/Fe_3O_4$ and tethered

TCPP is optimal with regard to fluorescence enhancement (between 5 and 7 nm). Therefore, TCPP fluorescence is enhanced while TCPP is bound and it decreases after enzymatic cleavage.

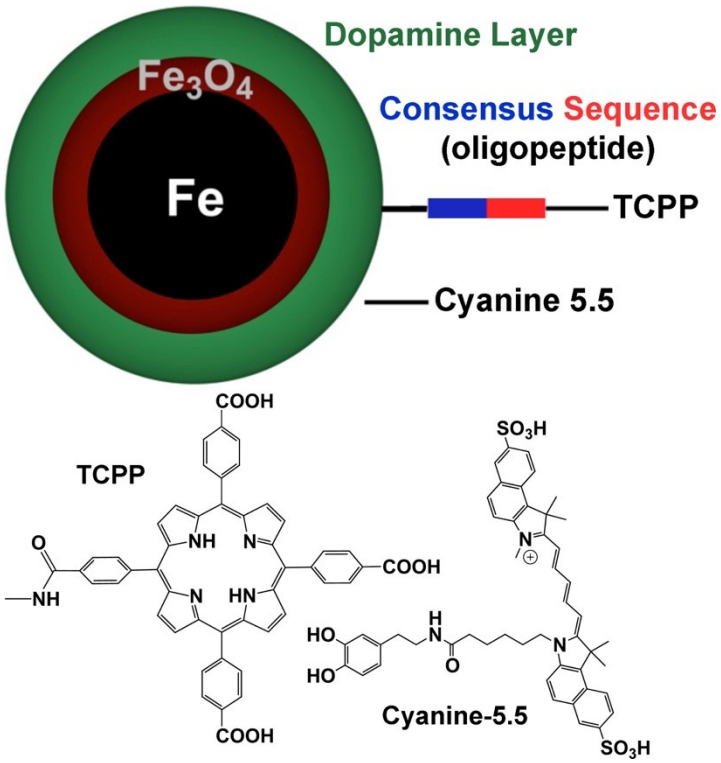


**Figure 34: Nanobiosensor for in-vitro protease detection. For each protease, a highly selective consensus sequence is employed as a tether between nanoparticle and TCPP (tetrakis-4-carboxyphenyl-porphyrin). Cyanine 5.5 is linked permanently to the Fe/$Fe_3O_4$ nanoparticles. Cited from reference [122] with permission from the Beilstein Journal of Nanotechnology.**

In 2014, we have published detailed synthetic procedures of the Fe/$Fe_3O_4$-based nanobiosensors, as well as their calibration for 12 commercially available proteases.[122] In 2016, we have reported the matrix effects of serum for the protease detection by the nanobiosensors.[81] We utilized this data for developing a liquid biopsy for the staging of breast cancer. It is noteworthy that recognition of breast cancer at stage 1 can be routinely achieved and that stage 0 detection of breast cancer is possible. In this report, we would like to extend this methodology to the detection

of non-small-cell lung cancer. As noted earlier, this cancer is characterized by the rapid decrease of survival rates with increasing stage. Therefore, the opportunity to save lives by detecting cancer at the earliest possible stage during routine blood tests is even higher. Furthermore, the liquid biopsy developed here is, principally, also capable of detecting the recurrence of (lung) cancer earlier than any other known method.

## 3.3 Serum Samples from the Southeastern Nebraska Cancer Center

We have obtained serum samples that were stored at -80°C from 33 non-small-cell lung cancer patients (20 males, 13 females, ages 42 to 70 years; 9 stage I, 12 stage II, 12 stage III), as well as 20 healthy human subjects (10 males and 10 females, ages 36 to 80 years) from the Southeast Nebraska Cancer Center, Lincoln, NE. Serum is especially suitable for liquid biopsies, because it retains its proteasome for 10h when frozen at -80°C. All patients were Caucasian. No significant statistical differences in the protease expression pattern between the females and males of the control group were found.

## 3.4 Selection of the Proteases of Interest

Due to the fact that about two percent of the human genome encode for proteases, every selection of target proteases is somewhat arbitrary. Based on literature evidence[95,111,165-167], we have selected the matrix metalloproteinases MMP 1, 2, 3, 7, 9, 13, uPA, the cathepsins CTS B and L. This panel of proteases has the additional advantage that the results can be directly compared with those from the breast cancer detection study reported earlier.[81] We hypothesize that due to dysfunctional protease expression by tumor and stroma cells, the whole web of proteases is out of equilibrium in cancer. This leads to enhanced activity of some proteases and decreased activity of

other. By observing the activity of multiple proteases in a liquid biopsy "barcodes for tumor detection" can be established, which are either "up" or "down" compared to normal protease activities. This will enable the detection of both, the types and stages of numerous solid tumors.

**Table 7: Peptide Sequences for Nanobiosensors**[129]

The consensus sequences are written in single-letter code.

| Nanobiosensor | Oligopeptide Used as Cleavable Tether |
|---|---|
| **MMP 1** | GAG**VPMS-MRGG**AG |
| **MMP 2** | GAG**IPVS-LRSG**AG |
| **MMP 3** | GAG**RPFS-MIMG**AG |
| **MMP 7** | GAG**VPLS-LTMG**AG |
| **MMP 9** | GAG**VPLS-LYSG**AG |
| **MMP 13** | GAG**PQGLA-GQRGI**VAG |
| **uPA** | GAG**SGR-SA**G |
| **Cathepsin B (CTS B)** | GAG**SLLKSR-MVPNFN**AG |
| **Cathepsin L (CTS L)** | GAG**SGVVIA-TVIVIT**AG |

**Consensus Sequences,** Peptide Spacers

## 3.5 Methods

### 3.5.1 Synthesis, Characterization and Validation of the Nanobiosensors

The synthesis and characterization of all components for the nanobiosensors and their final assembly and characterization is described in detail in reference [122] and in chapter 4. The effects of the serum matrix on the nanobiosensors are discussed in reference[81], as well as cross-sensitivity of the nine proteases used for this study.

### 3.5.2 Standard Procedure of Preparing Protease Assays (with thermally inactivated serum[134])

"3.0 mg of nanoplatform were dissolved in 3.0 mL of PBS. The dispersion was sonicated for 10 min. The resulting dispersion is chemically stable for 14 days at 4 °C. 900 mg of dextran was dissolved in 90.0 mL of PBS. Stock solutions of all 9 enzymes were prepared by consecutive dilution of commercially available proteases (Enzo Lifesciences). 3.0 mL of PBS–dextran (10 mg dextran in 1.0 mL of PBS) are mixed with 75 μL of the nanoplatform dispersion (3.0 mg in 3.0 mL of PBS, see above) and 30 μL of each of the proteases at every concentration level in PBS. The dispersions were incubated at 25 °C for 60 min, followed by the recording of a fluorescence spectrum at 25 °C using a Fluoromax2 spectrometer (λem = 421 nm, λex = 620–680 nm)" (Quoted from reference [81] with permission from the Beilstein Journal of Nanotechnology.).

### 3.5.3 Standard Procedure of Preparing Protease Assays (with proteolytically active serum)

Exactly the same procedure as describe above was followed, with the exception that 5 μL of serum were added instead of 30 μL of commercially available proteases in PBS.

## 3.6 Results and Discussion

### 3.6.1 Diagnosis of Non-Small-Cell Lung Cancer in Serum

The activities of MMP-1,-2,-3,-7,-9,-13, uPA, and CTS -B and -L in the sera of 33 non-small-cell lung cancer patients and 20 healthy volunteers were determined by following the procedures described in the section 3.5. Calibration curves obtained with commercially available proteases in heat-deactivated serum were used for determining the protease activities. All

Fe/$Fe_3O_4$- based nanobiosensors utilized possess (sub) femtomolar Limits of Detection (LOD) and an extensive, but non-linear range from $10^{-16}$ to $10^{-6}$ moles $L^{-1}$ of protease activity. The results were statistically analyzed and displayed in a series of boxplots and bar graphs. Our conclusions are based on the data range that correlates with each cancer stage in comparison with the range of presumably healthy persons.[119,168]

The activities of Cathepsin-B in the apparently healthy control group and the groups at NSCLC stages 1, 2, and 3 are shown in Figure 35. A significant increase from state 1 to stage 2 is clearly discernible. This protease is suitable to detect when NSCLC cancer is becoming distant. This is in agreement with the literature, in which cathepsin B is established as a valuable prognostic factor for non-small-cell lung cancer.[109]

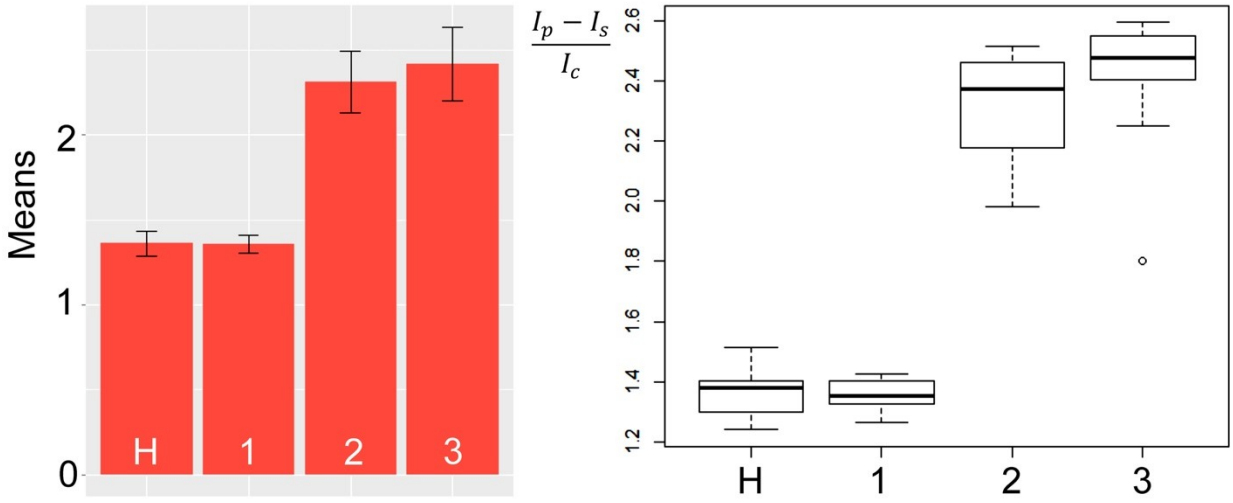


**Figure 35: Bar graph (left, showing means and standard deviations) and box plot (right, indicating the observed data range) for cathepsin B. The group sizes are H (apparently healthy control group, n = 20), 1: NSCLC cancer stage 1 (n = 9), 2: NSCLC cancer stage 2 (n = 12), 3: NSCLC cancer stage 3 (n = 12). All biospecimens were obtained from the Southeastern Nebraska Cancer Center (SNCC). $I_p$: fluorescence intensity of the measured protease, $I_s$: fluorescence intensity of the solvent, $I_c$: fluorescence intensity of the nanobiosensor in the absence of the respective protease.**

Contrary to cathepsin B, the activity of cathepsin L increases stepwise from the group of healthy volunteers to the patient group at stage 3 (Figure 36). One possible reason for the observed stepwise increase is that cathepsin L is involved in angiogenesis.[111,169] The connection of tumors and metastases to blood supply has to increase steadily with tumor growth to fulfill the nutritional needs of the tumor and permit the required access to the body's oxygen supply. Cathepsin L is a very suitable protease to monitor the general process of NSCLC cancer.

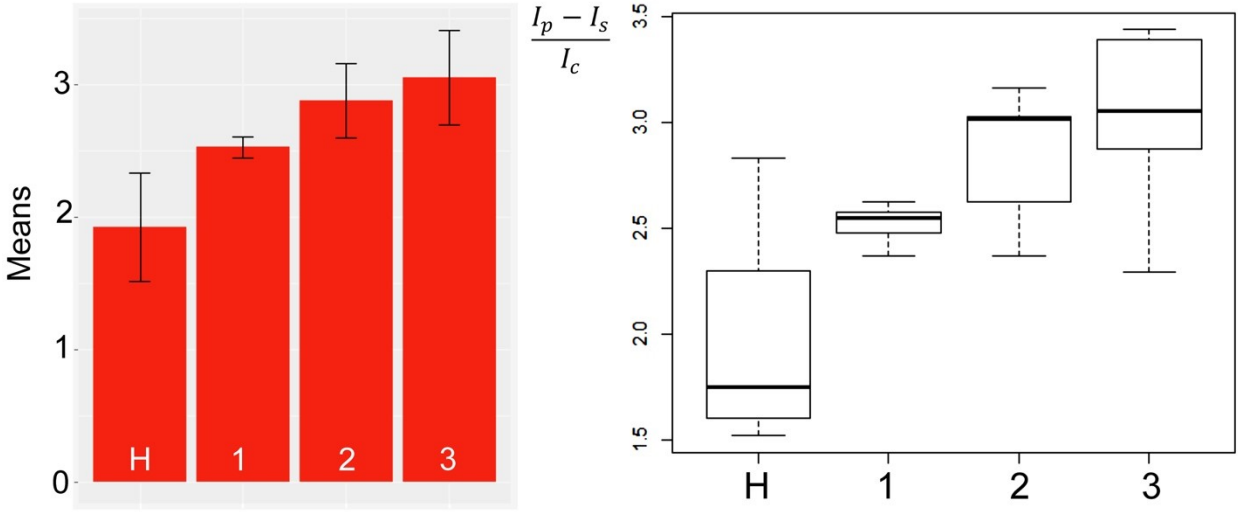


**Figure 36: Bar graph (left, showing means and standard deviations) and box plot (right, indicating the observed data range) for cathepsin L. The group sizes are H (apparently healthy control group, n = 20), 1: NSCLC cancer stage 1 (n = 9), 2: NSCLC cancer stage 2 (n = 12), 3: NSCLC cancer stage 3 (n = 12). All biospecimens were obtained from the Southeastern Nebraska Cancer Center (SNCC). $I_p$: fluorescence intensity of the measured protease, $I_s$: fluorescence intensity of the solvent, $I_c$: fluorescence intensity of the nanobiosensor in the absence of the respective protease.**

Urokinase plasminogen activator (uPA) is, such as cathepsin B, a good indicator for non-small-cell-lung cancer becoming distant (Figure 37). For the selection of a panel of proteases that permits the best "barcode detection", cathepsin B and uPA are probably redundant. However, since the nanobiosensor for uPA is one of the two (to date) that decrease in fluorescence intensity upon enzymatic cleavage of the consensus sequence between dopamine-coated $Fe/Fe_3O_4$ nanoparticles

and TCPP, cathepsin B (which increases in fluorescence when cleaved) is better suited for detection purposes. Monitoring the increase of a fluorescence signal is a better approach than a decrease, which would also be caused by photobleaching of TCPP.[170]

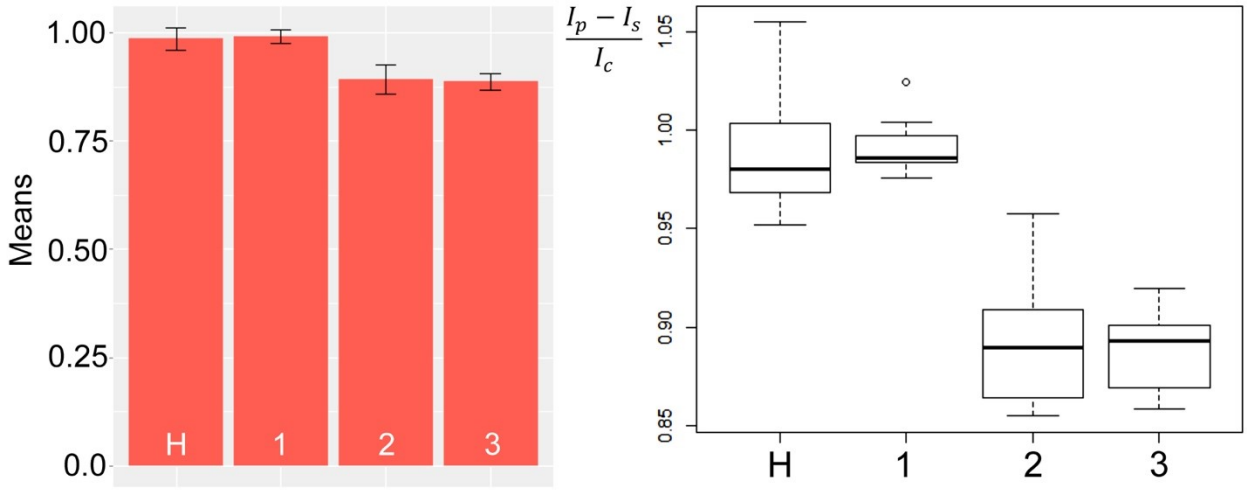


**Figure 37: Bar graph (left, showing means and standard deviations) and box plot (right, indicating the observed data range) for uPA. The group sizes are H (apparently healthy control group, n = 20), 1: NSCLC cancer stage 1 (n = 9), 2: NSCLC cancer stage 2 (n = 12), 3: NSCLC cancer stage 3 (n = 12). All biospecimens were obtained from the Southeastern Nebraska Cancer Center (SNCC). $I_p$: fluorescence intensity of the measured protease, $I_s$: fluorescence intensity of the solvent, $I_c$: fluorescence intensity of the nanobiosensor in the absence of the respective protease.**

Matrix-metalloproteinase 1 (MMP-1) is an excellent enzyme for monitoring the occurrence (or recurrence) of non-small-cell lung cancer, because it is significantly elevated in stage 1, compared to the apparently healthy control group (Figure 38). Therefore, it is especially suited for very early detection of NSCLC.

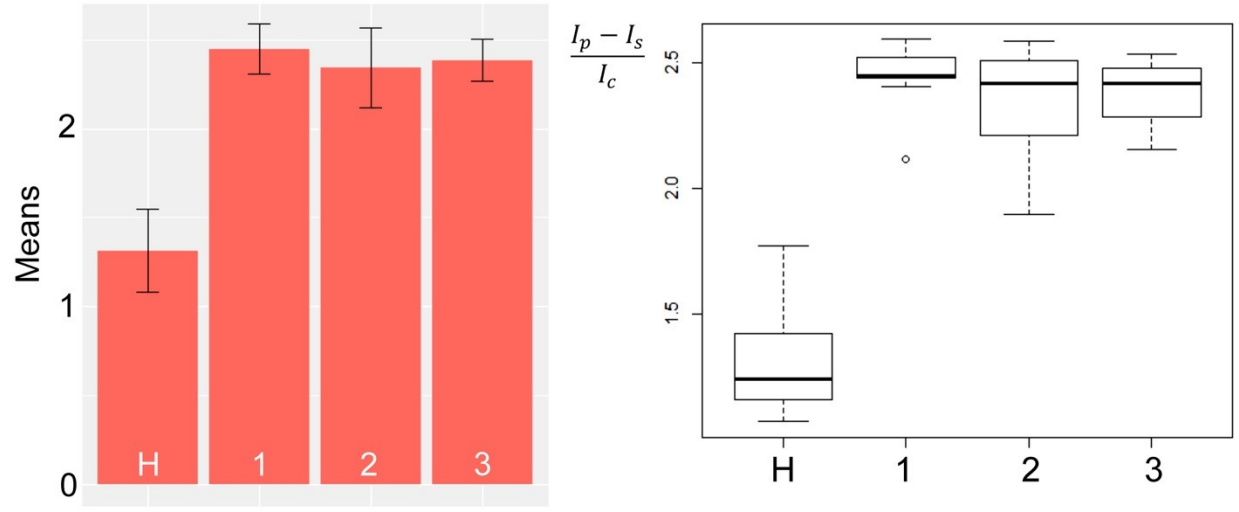


**Figure 38: Bar graph (left, showing means and standard deviations) and box plot (right, indicating the observed data range) for MMP-1. The group sizes are H (apparently healthy control group, n = 20), 1: NSCLC cancer stage 1 (n = 9), 2: NSCLC cancer stage 2 (n = 12), 3: NSCLC cancer stage 3 (n = 12). All biospecimens were obtained from the Southeastern Nebraska Cancer Center (SNCC). $I_p$: fluorescence intensity of the measured protease, $I_s$: fluorescence intensity of the solvent, $I_c$: fluorescence intensity of the nanobiosensor in the absence of the respective protease.**

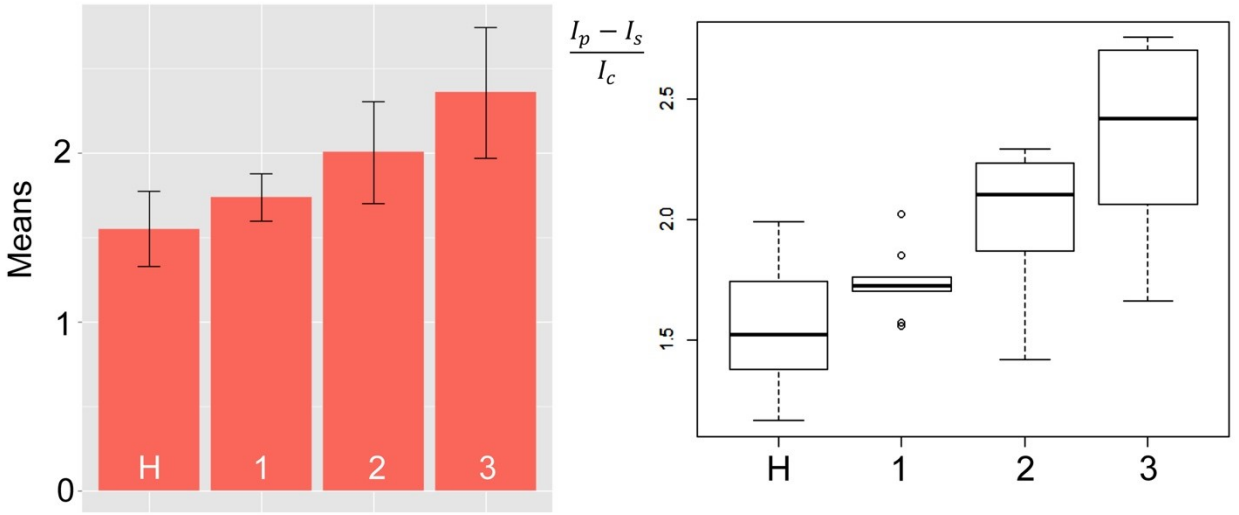


**Figure 39: Bar graph (left, showing means and standard deviations) and box plot (right, indicating the observed data range) for MMP-2. The group sizes are H (apparently healthy control group, n = 20), 1: NSCLC cancer stage 1 (n = 9), 2: NSCLC cancer stage 2 (n = 12), 3: NSCLC cancer stage 3 (n = 12). All biospecimens were obtained from the Southeastern Nebraska Cancer Center (SNCC). $I_p$: fluorescence intensity of the measured protease, $I_s$: fluorescence intensity of the solvent, $I_c$: fluorescence intensity of the nanobiosensor in the absence of the respective protease.**

Contrary to MMP-1, which is a good marker for tissue alveolar remodeling processes[115], the activity of MMP-2 increases again stepwise with increasing cancer stage of non-small-cell lung cancer (Figure 39). MMP-2 is associated in the literature with TMN stage, pathological differentiation and lymph node metastasis in NSCLC. [171] The steady increase in fluorescence signal and, at the same time, low signal-to-noise, makes MMP-2 a very suited biomarker for non-small-cell lung cancer.

MMP-3 is a similar biomarker as MMP-2, since it also shows a stepwise increase in nanobiosensor fluorescence as a function of non-small-cell lung cancer staging (Figure 40). MMP-3 has been identified as a major player in matrix-metalloproteinase-induced lung fibrosis and other malignancies, among them lung cancer.[172] MMP-3 has been recently proposed as a prognostic factor for poor survival in pancreatic, pulmonary, and mammary carcinoma.[116] In this study, we were able to corroborate this finding while, at the same time, the sensitivity of detection of the nanobiosensors used is 100-1000 times for sensitive than conventionally used immunoassay technologies.

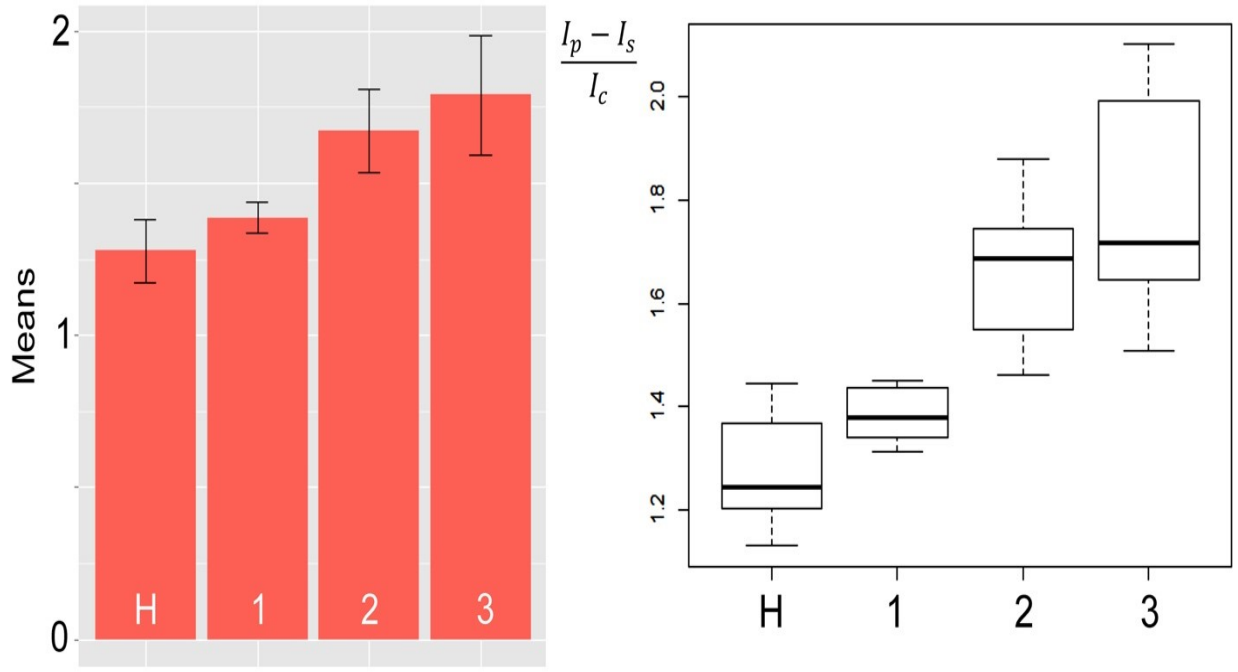


**Figure 40: Bar graph (left, showing means and standard deviations) and box plot (right, indicating the observed data range) for MMP-3. The group sizes are H (apparently healthy control group, n = 20), 1: NSCLC cancer stage 1 (n = 9), 2: NSCLC cancer stage 2 (n = 12), 3: NSCLC cancer stage 3 (n = 12). All biospecimens were obtained from the Southeastern Nebraska Cancer Center (SNCC). $I_p$: fluorescence intensity of the measured protease, $I_s$: fluorescence intensity of the solvent, $I_c$: fluorescence intensity of the nanobiosensor in the absence of the respective protease.**

Contrary to the results obtained when detecting MMP-7 in the serum of breast cancer patients vs. healthy volunteers[81], MMP-7 is statistically significant when diagnosing non-small-cell lung cancer, albeit less significant than most other proteases (See Table 8). The fact that in NSCLC, MMP-7 slightly increases with increased cancer stage (Figure 41), but not in breast cancer, is an indication that the protease expression pattern of solid tumors differs according to tumor origin and stage. This can be explained by small differences in the biochemistry of the various cell types from which these solid tumors originate. These differences are partially retained in the developing tumors. However, major changes in protease expression occur during later stages.

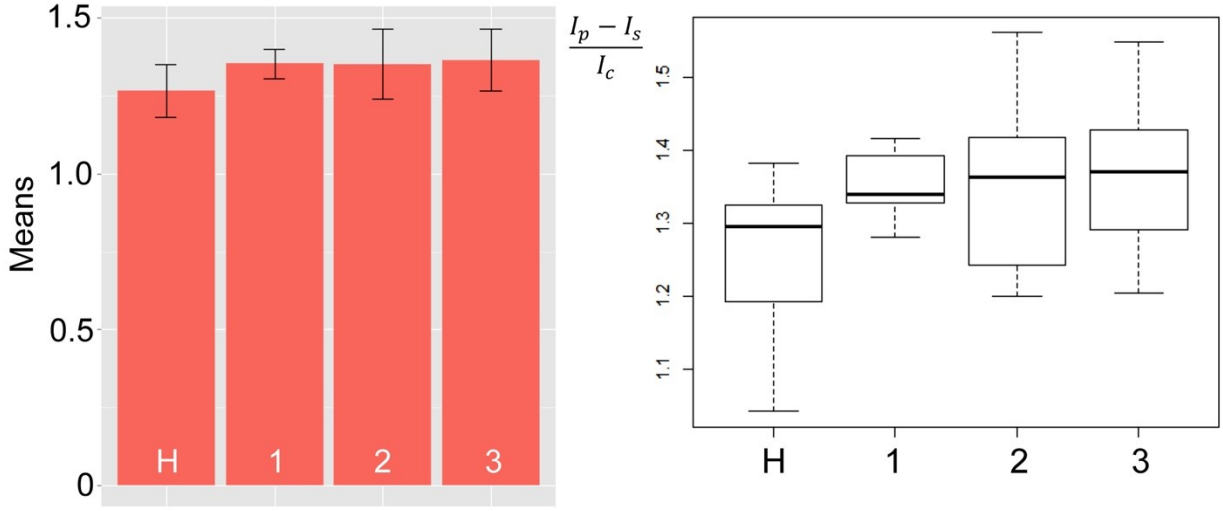


**Figure 41: Bar graph (left, showing means and standard deviations) and box plot (right, indicating the observed data range) for MMP-7. The group sizes are H (apparently healthy control group, n = 20), 1: NSCLC cancer stage 1 (n = 9), 2: NSCLC cancer stage 2 (n = 12), 3: NSCLC cancer stage 3 (n = 12). All biospecimens were obtained from the Southeastern Nebraska Cancer Center (SNCC). $I_p$: fluorescence intensity of the measured protease, $I_s$: fluorescence intensity of the solvent, $I_c$: fluorescence intensity of the nanobiosensor in the absence of the respective protease.**

As already discussed, the nanobiosensor for detecting MMP-9 in serum shows a decrease of TCPP fluorescence upon proteolytic cleavage (Figure 42). Therefore, the actual changes in fluorescence intensity as a factor of stage are small. However, since the experimental error is smaller than 2%, we can detect MMP-9 changes with very good accuracy. As shown in Table 8, MMP-9 is a viable biomarker for NSCLC. However, MMP-9 has been implicated in numerous inflammatory diseases, such as cardiovascular disorders, cancer, and even neuropsychiatric disorders.[173] Therefore, it is not suited to be a "stand-alone biomarker". However, it adds value to a panel of proteases for non-small-cell cancer detection, because this disease is inflammatory.

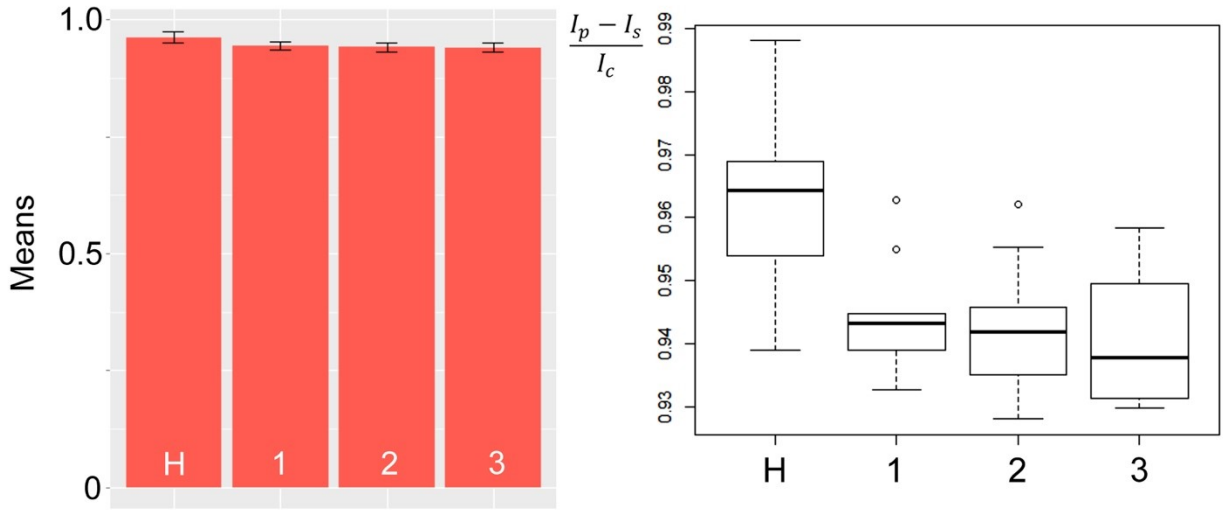


**Figure 42: Bar graph (left, showing means and standard deviations) and box plot (right, indicating the observed data range) for MMP-9. The group sizes are H (apparently healthy control group, n = 20), 1: NSCLC cancer stage 1 (n = 9), 2: NSCLC cancer stage 2 (n = 12), 3: NSCLC cancer stage 3 (n = 12). All biospecimens were obtained from the Southeastern Nebraska Cancer Center (SNCC). $I_p$: fluorescence intensity of the measured protease, $I_s$: fluorescence intensity of the solvent, $I_c$: fluorescence intensity of the nanobiosensor in the absence of the respective protease.**

Together with MMP-1, -2, -3, -7. -11 (not tested here), MMP-13 (Collaginase-3) is implicated in inflammation-induced epithelial-to-mesenchymal transitions (EMT).[117] However, MMP-13 does not correlate with NSCLC staging. One possible explanation for the observed behavior is that EMT occurs very early in the cancerogenesis.[174] Therefore, significant changes in MMP-13 expression may occur before stage 1 is reached.

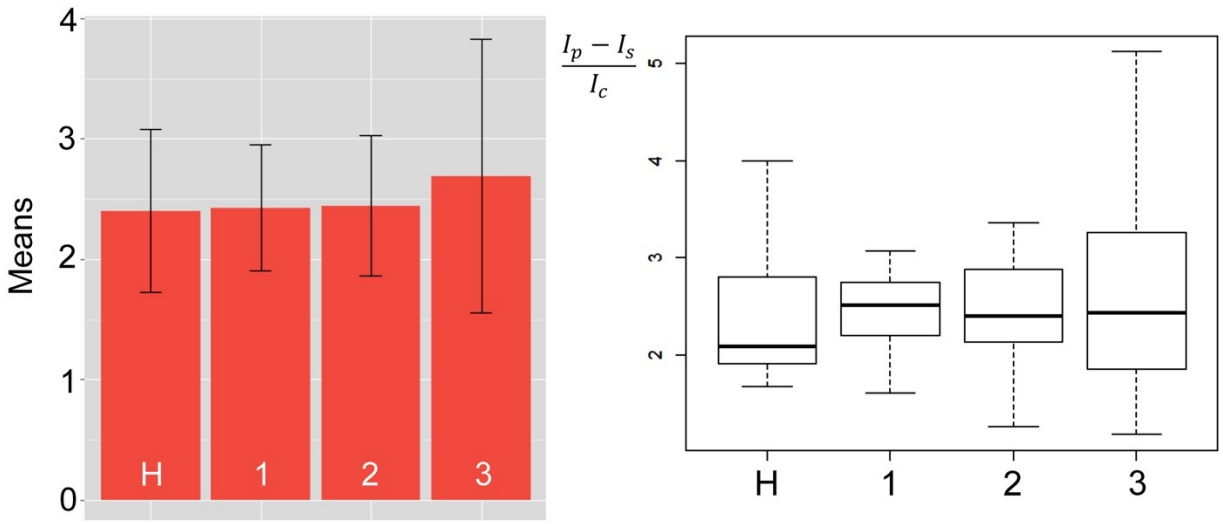


**Figure 43: Bar graph (left, showing means and standard deviations) and box plot (right, indicating the observed data range) for MMP-13. The group sizes are H (apparently healthy control group, n = 20), 1: NSCLC cancer stage 1 (n = 9), 2: NSCLC cancer stage 2 (n = 12), 3: NSCLC cancer stage 3 (n = 12). All biospecimens were obtained from the Southeastern Nebraska Cancer Center (SNCC). $I_p$: fluorescence intensity of the measured protease, $I_s$: fluorescence intensity of the solvent, $I_c$: fluorescence intensity of the nanobiosensor in the absence of the respective protease.**

From the bar graphs, box plots and especially the significance table (Table 8), it is apparent that the signal quality of Cathepsin B and L, as well as MMP-1, -2 and -3 is superior to the signal quality of MMP-7 and -13. Highly significant differences are achieved with Cathepsin B and L, MMP- 1, -2 and -3.

**Table 8: Significance Table: plot of the calculated p-values of each protease vs. cancer stage.**

Green: p-value significant ($p < 0.05$), nanobiosensor fluorescence in the disease group is higher than in the control group. Yellow: p-value significant ($p < 0.05$), nanobiosensor fluorescence in the disease group is lower than in the control group. Red: protease activity does not differ significantly in both, the cancer and the control groups.

| NSC Lung Cancer | | | | | | | | | |
|---|---|---|---|---|---|---|---|---|---|
| | Cathepsin B | Cathepsin L | uPA | MMP1 | MMP2 | MMP3 | MMP7 | MMP9 | MMP13 |
| Stage 1 | 0.4318 | 1.08E-06 | 0.2097 | 7.15E-15 | 5.91E-03 | 0.000379 | 0.000741 | 0.00015 | 0.4591 |
| Stage 2 | 1.37E-09 | 6.17E-09 | 3.81E-08 | 3.00E-12 | 1.23E-04 | 3.71E-08 | 0.01586 | 8.93E-06 | 0.43 |
| Stage 3 | 9.09E-11 | 5.85E-09 | 3.95E-13 | 2.20E-16 | 3.51E-06 | 2.61E-07 | 0.004205 | 4.43E-06 | 0.2194 |

As summarized in the **Significance Table** (Table 8), Cathepsin-L and MMP-1, -2, -3, -7, and -9 are capable of detecting a statistically significant difference in nanobiosensor fluorescence between the group of patients with non-small-cell-lung cancer at stage 1 and the apparently healthy and age-matched control group. As already discussed in the introduction section, all patients were Caucasian. The nanobiosensors for eight proteases (Cathepsin-L, -B, uPA, MMP-1, -2, -3, -7 and -9) were able to differentiate between stage 2 and stage 3 NSCLC patients and the control group.

The results presented in the **Significance Table** clearly indicate that the detection of stage I non-small-cell lung cancer and beyond is clearly possible by means of a liquid biopsy using either fresh serum or serum that has been stored for several years (up to five) at – 80°C. The $Fe/Fe_3O_4$ core/shell nanoparticle-based nanobiosensors have been synthesized on the gram scale and can be stored (frozen) for up to four years under nitrogen/argon without losing activity. In aqueous buffers, they are stable for up to 7 days. Therefore, the technology that is described in this report is, principally, available for use in clinical laboratories. Conservatively estimated, the mortality of

non-small-cell lung cancer could be decreased by more than 30% if these tests would be routinely performed during yearly health check-ups.

## 3.7 Application of a Multivariate Model

A combination of MMP 1 and Cathepsin B was chosen for the multivariate model. MMP-1 achieves a good separation between the healthy group and stage 1, while Cathepsin B increases the separation between the later stages, a quality that MMP-1 lacks. The parameter's values were linearized (log). This model's coefficients are highly significant. The $R^2$-value reaches 0.91. The cubic graph (Figure 44) shows how the data groupings shift to the right (MMP-1 influence) and back (Cathepsin B influence) with increasing cancer stages. This permits the precise detection of stage 1 NSC lung cancer by looking at only two variables. This approach can be, principally, enhanced by including more than two proteases.

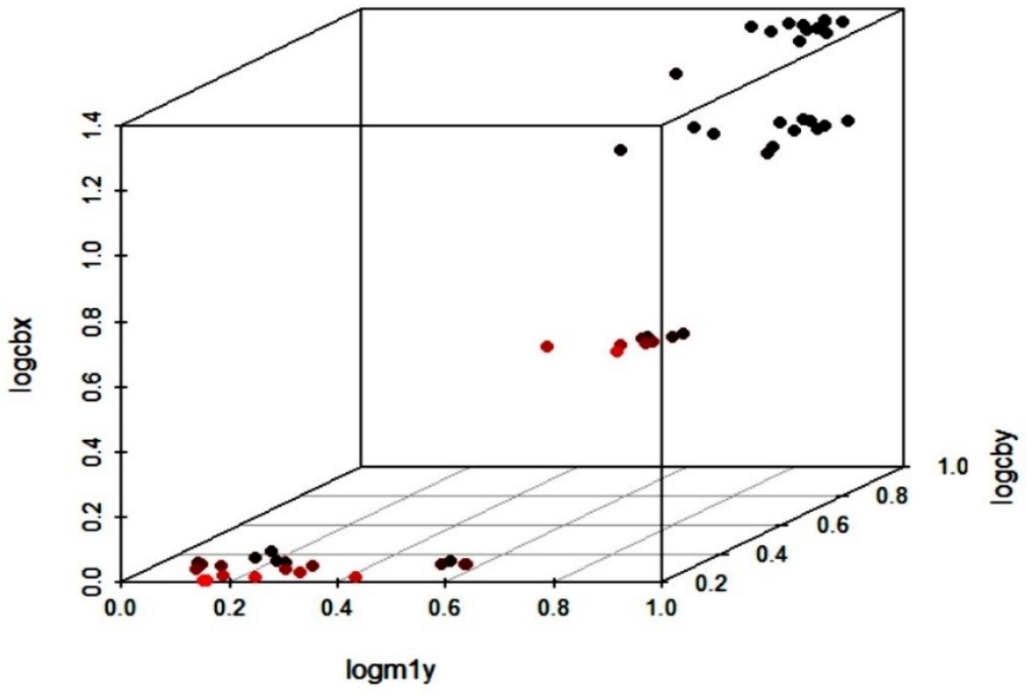


**Figure 44: Multivariate Model: Cancer State over MMP-1 (1y) and Cathepsin-B (y)**

**Table 9: Multivariate Model: Cancer State over MMP-1 (1y) and Cathepsin-B (y) readings:**

| Coefficients: | Estimate | Standard Error | t-value | Pr(>\|t\|) |
|---|---|---|---|---|
| **z-axis Intercept** | -0.52849 | 0.05615 | -9.413 | $1.18 \times 10^{-12}$ |
| **MMP1 slope** | 0.90623 | 0.09336 | 9.707 | $4.34 \times 10^{-13}$ |
| **Cathepsin B slope** | 1.13514 | 0.10446 | 10.867 | $9.11 \times 10^{-15}$ |
| | | | | |
| Signif. codes: | 0'***' | 0.001 '**' | 0.01 '*' | 0.05 '.' 0.1 '' 1 |
| Residual standard error: 0.1686 on 50 degrees of freedom<br>Multiple **R-squared: 0.9181**, Adjusted R-squared: 0.9148<br>F-statistic: 280.1 on 2 and 50 DF, p-value: $< 2.2 \times 10^{-16}$ | | | | |

## 3.8 Summary

Non-small-cell lung cancer (NSCLC) can be reliably detected in a liquid biopsy measuring the protease activity of eight proteases (Cathepsin B, L, MMP-1, -2, -3, -7, -9), and uPA) utilizing Fluoromax2 spectrometer ($\lambda$em = 421 nm, $\lambda$ex = 620–680 nm). MMP-13 proved to be an unreliable marker. Based on the fluorescence readings obtained from the groups of NSCLC patients and healthy volunteers (Figures 35-43), we have calculated the average protease concentrations for each NSCLC-stage and the age-matched control group. The results are summarized in Figure 45. From the real protease activities, not the integrated nanobiosensor fluorescence signals, it can be discerned that MMP-1 and MMP-9 exhibit the highest activities in the serum of non-small-cell lung cancer patients. It is reasonably well established that the activities of numerous proteases in cancer tissue and stroma correlate with their activities in blood, because virtually all proteases are involved in angiogenesis and ECM (extracellular matrix) degradation.[121] Beginning with from stage 1, virtually all solid tumors are well connected to the blood supply. MMP-1 activity is related to tissue remodeling processes in the lung[115], whereas MMP-9 is an inflammation marker, which

is involved in numerous processes in the human body and is not necessarily related to a disease.[173] This may explain the relatively high average activity of MMP-9 ($8.60 \times 10^{-13}$ M) in the apparently healthy control group.

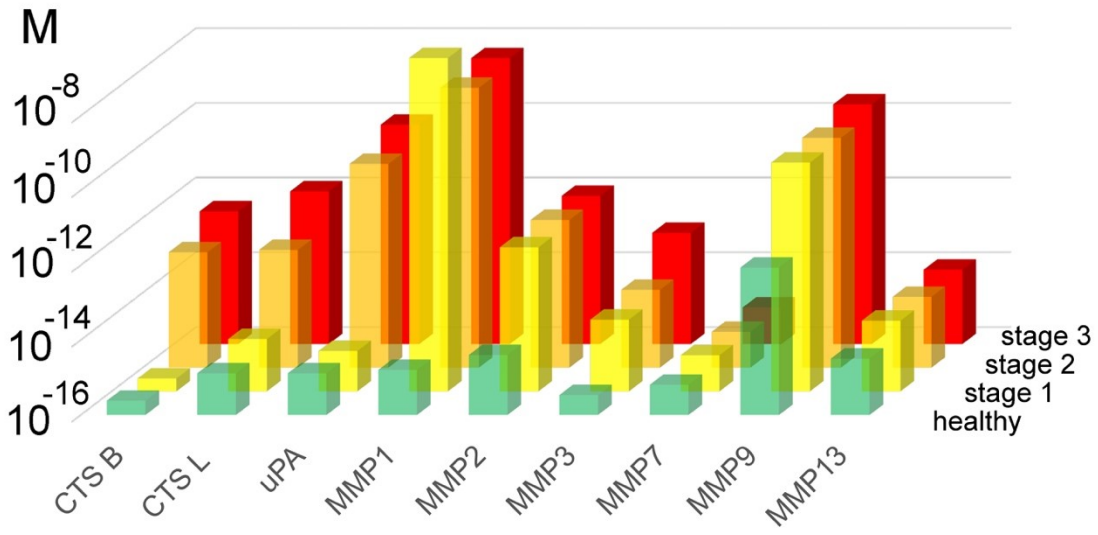


**Figure 45: Average protease activity as a function of NSCL cancer stage/healthy control group for all nine proteases monitored in this study.**

The calibration curves reported in reference [81] were used for calculating the protease activities measured in serum. Note that the activity is shown on a logarithmic scale ($\log_{10}$ (protease activity)). The data summarized in this figure is also reported in Chapter 4, Section 4.4.

# Chapter 4 - Experimental Section and Additional Procedures

## 4.1 Determination of Matrix Effects on the Observed Fluorescence Intensities of the Nanoplatforms

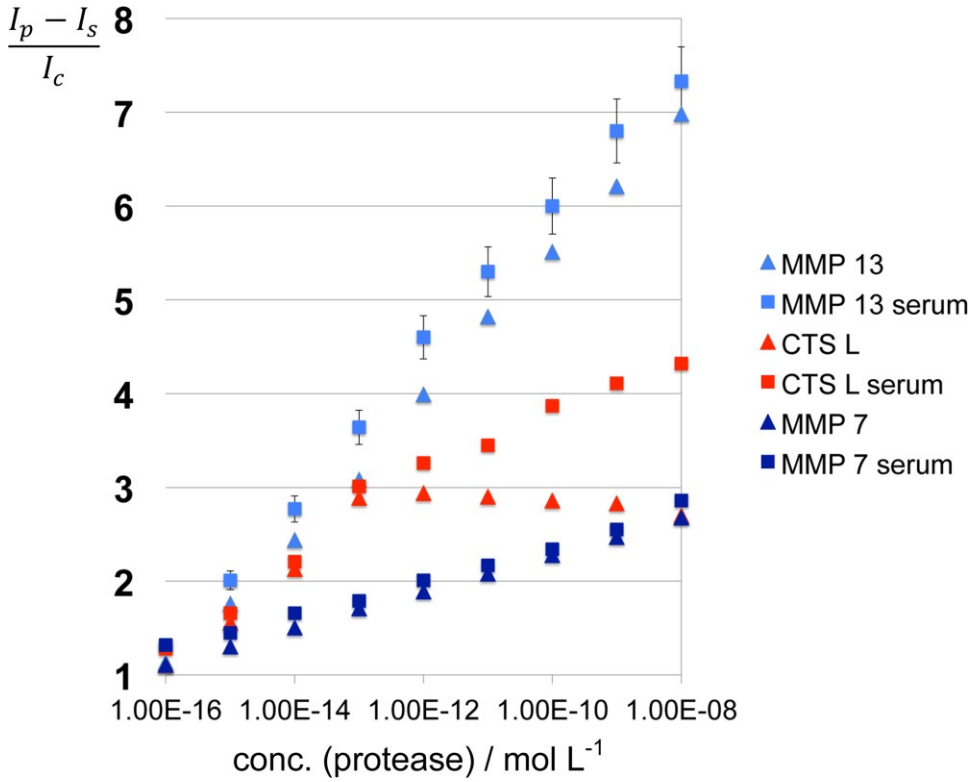


**Figure 46: "Matrix effects for MMP7, MMP13, and cathepsin L after 60 min of incubation at 25 °C under standard conditions** (Taken with permission of Reference[81])

$I_p$: fluorescence signal after 60 min. of incubation; $I_c$: fluorescence signal in the absence of protease after 60 min. incubation; $I_s$: fluorescence signal of serum/PBS-dextran alone. Experimental errors are indicated."[81]

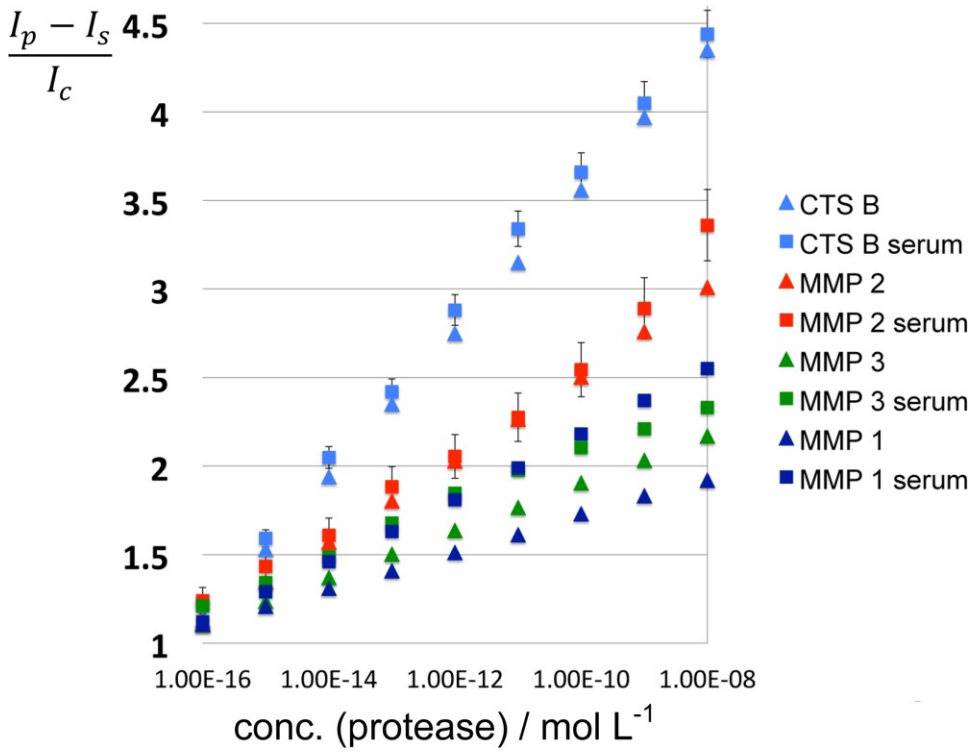


**Figure 47: "Matrix effects for MMP1, MMP 2, MMP 3, and cathepsin B after 60 min of incubation at 25 °C under standard conditions** (Taken with permission of Reference[81])

Triangles: fluorescence readings in PBS; Squares: fluorescence readings in PBS containing inactivated serum. $I_p$: fluorescence signal after 60 min. of incubation; $I_c$: fluorescence signal in the absence of protease after 60 min. incubation; $I_s$: fluorescence signal of serum/PBS-dextran alone. Experimental errors are indicated."[81]

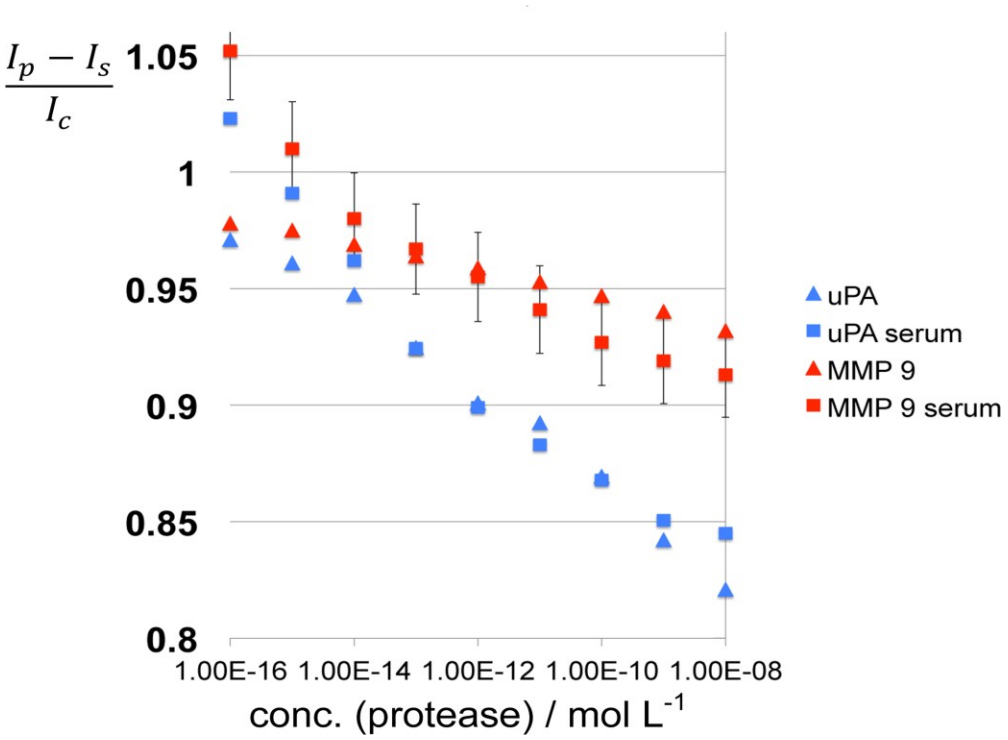


**Figure 48: "Matrix effects for MMP9 and uPA after 60 min of incubation at 25 °C under standard conditions** (Taken with permission of Reference[81])

Triangles: fluorescence readings in PBS; Squares: fluorescence readings in PBS containing inactivated serum. $I_p$: fluorescence signal after 60 min. of incubation; $I_c$: fluorescence signal in the absence of protease after 60 min. incubation; $I_s$: fluorescence signal of serum/PBS-dextran alone. Experimental errors are indicated."[81]

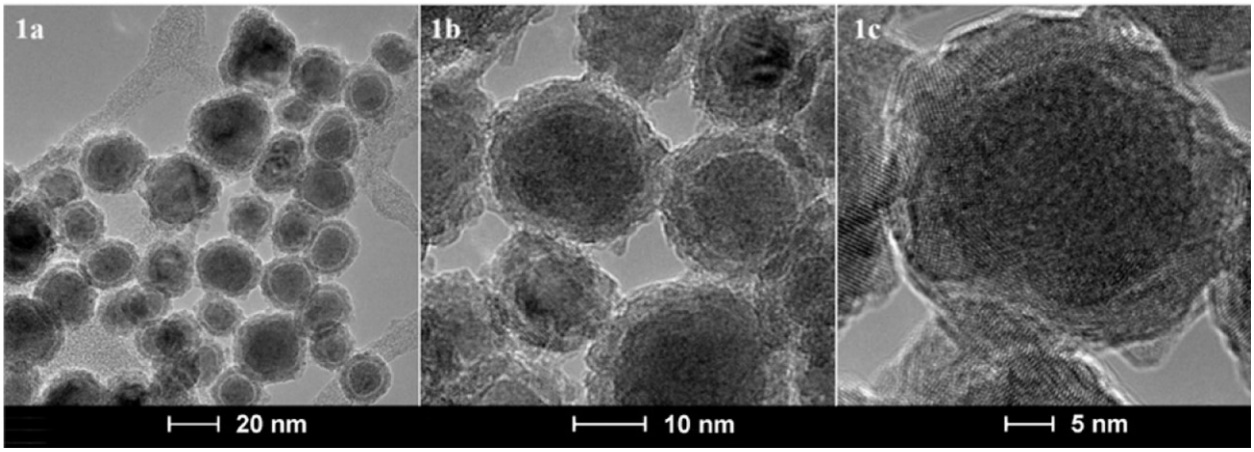


**Figure 49: "TEM (1a,1b) and HRTEM (1c) images of Fe/Fe3O4-core/shell nanoparticles that are forming the inorganic core of the nanoplatforms for protease detection, HRTEM images revealed that the Fe(0) centers are mostly crystalline (BCC)."[122]** (Taken with permission of the Royal Society of Chemistry[122])

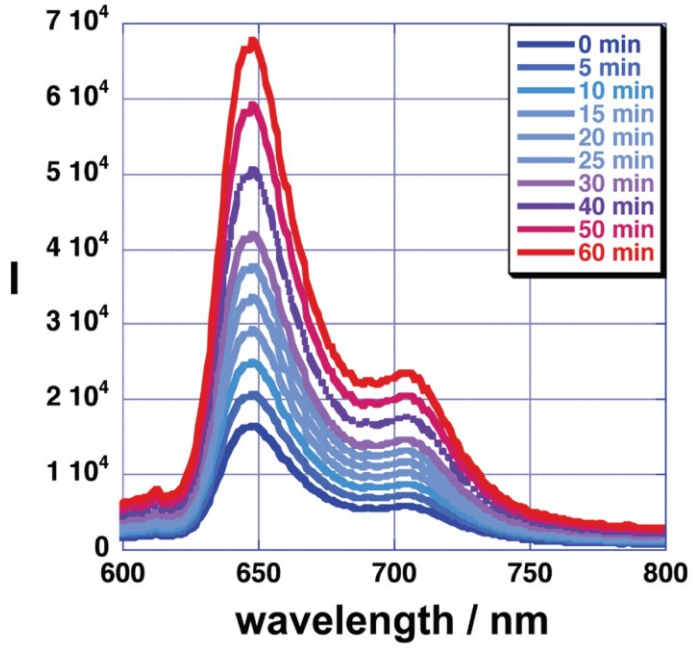


**Figure 50: "Light-Switch Effect" of the Fe/Fe3O4-nanoplatform for detecting MMP-13: fluorescence increase as a function of reaction time under standard conditions at 25 °C after addition of 1.0 x 10−12 mol L−1 of MMP-13; I: fluorescence intensity** (Taken with permission from Royal Society of Chemistry[122])

## 4.2 Relative Error from 10 Independently Performed Protease Measurements

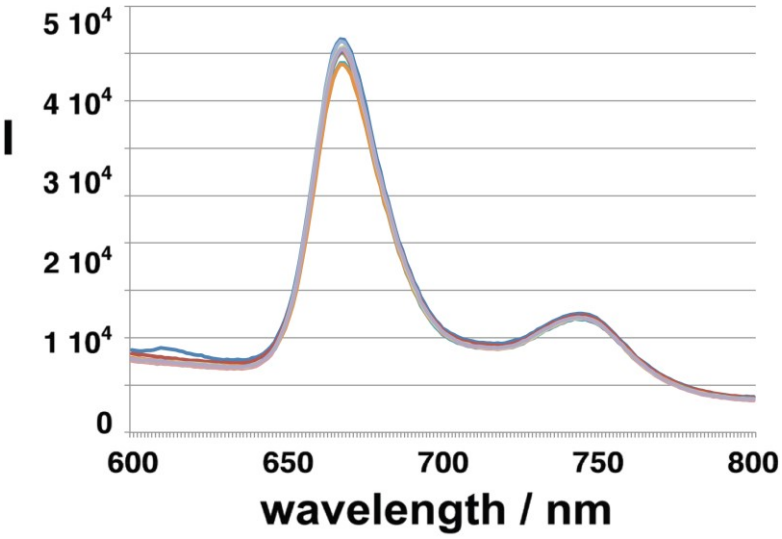


**Figure 51: 10 independent repetitions of measuring the activity of the Fe/Fe3O4-nanoplatform for detecting MMP-13 under standard conditions at 25 °C after addition of 1.0 x 10−13 mol L−1 of MMP13. The relative error was determined to be 2 percent. I: fluorescence intensity**

## 4.3 Cross-Sensitivity of the Nanobiosensors

"In order to determine the cross-sensitivities of the nanoplatforms, the following control experiments were conducted: The nanoplatforms for MMP 1, 2, 3, 7, 9, 13, uPA, and CTS B, L were (separately) incubated with 1.0 x $10^{-10}$ mol $l^{-1}$ of MMP 1 under standard conditions. After 60 min. of incubation at 25 °C, the fluorescence spectra of all nanoplatforms were recorded. The next set of experiments consisted of incubating the nanoplatforms for MMP 1, 2, 3, 7, 9, 13, uPA, and CTS B, L with 1.0 x $10^{-10}$ mol $l^{-1}$ of MMP 2 under standard conditions. This is followed by MMP 3, 7, 9, 19, uPA and CTS B, and L. In Figure 52, the normalized results for this set of experiments are summarized. The normalization procedure consists of dividing each set of integrated fluorescence data for each enzyme by the fluorescence recording for the correct match in the entire set of nine nanoplatforms.

Set 1: integrated fluorescence recordings for all nine nanoplatforms incubated with MMP-1 (1.0 x $10^{-10}$ mol $l^{-1}$), divided by the integrated fluorescence signal obtained with the nanoplatform for MMP-1 in the presence of MMP-1;

Set 2: integrated fluorescence recordings for all nine nanoplatforms incubated with MMP-2 (1.0 x $10^{-10}$ mol $l^{-1}$), divided by the integrated fluorescence signal obtained with the nanoplatform for MMP-2 in the presence of MMP-2

Sets 3 to 8 have been recorded accordingly for MMP-3, -7, -9, -13, uPA and CTS B.

Set 9: integrated fluorescence recordings for all nine nanoplatforms incubated with CTS L (1.0 x $10^{-10}$ mol $l^{-1}$), divided by the integrated fluorescence signal obtained with the nanoplatform for CTS L in the presence of CTS L."[122] (Taken with permission from Beilstein Journal of Nanotechnology).

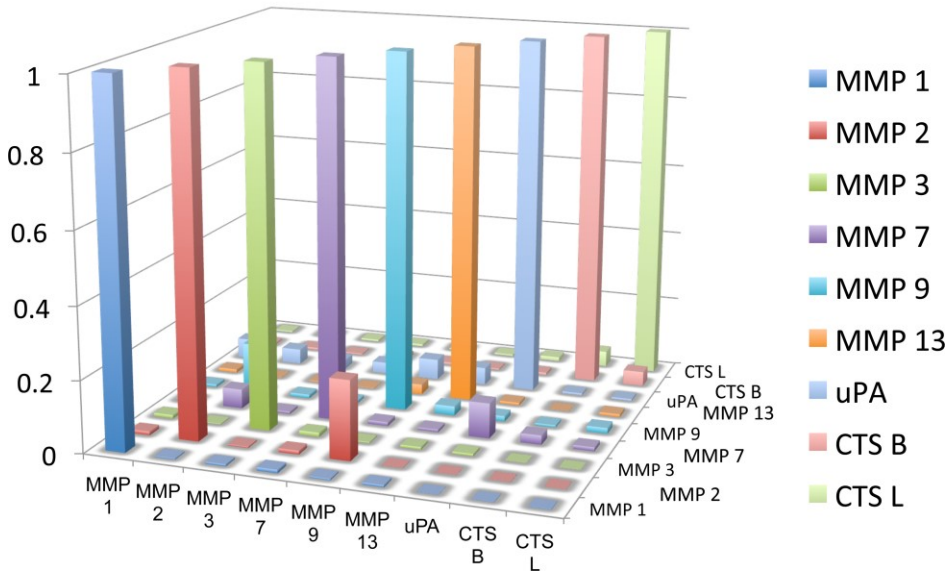


**Figure 52: "Cross-sensitivities of the nanobiosensors used in this study. Further explanations are provided above."[81]** (Taken with permission of Reference[81])

## 4.4 Means, Standard Deviations, and Average Protease Activities for Each Protease and Stage

**Table 10: Means, Standard Deviations, and Average Protease Activities in Serum for Cathepsin B (CTS B)**

| Stages | Means | SD | Average Protease Activity in Serum (mol $L^{-1}$) |
|---|---|---|---|
| H | 1.360853 | 0.07226045 | $2.4 \times 10^{-16}$ |
| 1 | 1.356708 | 0.0532257 | $2.2 \times 10^{-16}$ |
| 2 | 2.312725 | 0.1794251 | $1.2 \times 10^{-13}$ |
| 3 | 2.417865 | 0.2105544 | $3.5 \times 10^{-13}$ |

**Table 11: Means, Standard Deviations, and Average Protease Activities in Serum for Cathepsin L (CTS L)**

| Stages | Means | SD | Average Protease Activity in Serum (mol $L^{-1}$) |
|---|---|---|---|
| H | 1.923536 | 0.40659660 | $1.8 \times 10^{-15}$ |
| 1 | 2.525293 | 0.0836583 | $2.5 \times 10^{-15}$ |
| 2 | 2.873535 | 0.2741506 | $1.4 \times 10^{-13}$ |
| 3 | 3.049788 | 0.3474912 | $1.2 \times 10^{-12}$ |

**Table 12: Means, Standard Deviations, and Average Protease Activities in Serum for urokinase-type Plasminogen Activator (uPA)**

| Stages | Means | SD | Average Protease Activity in Serum (mol $L^{-1}$) |
|---|---|---|---|
| H | 0.9848335 | 0.025264087 | $1.3 \times 10^{-15}$ |
| 1 | 0.9921240 | 0.023313962 | $1.2 \times 10^{-15}$ |
| 2 | 0.8921566 | 0.034226941 | $2.8 \times 10^{-11}$ |
| 3 | 0.8868113 | 0.021102354 | $7.4 \times 10^{-11}$ |

**Table 13: Means, Standard Deviations, and Average Protease Activities in Serum for Matrix Metalloproteinase 1 (MMP-1)**

| Stages | Means | SD | Average Protease Activity in Serum (mol $L^{-1}$) |
|---|---|---|---|
| H | 1.314616 | 0.23507424 | $1.6 \times 10^{-15}$ |
| 1 | 2.4499240 | 0.13775162 | $8.3 \times 10^{-8}$ |
| 2 | 2.3424636 | 0.21967214 | $3.1 \times 10^{-9}$ |
| 3 | 2.3840819 | 0.11741315 | $4.5 \times 10^{-9}$ |

**Table 14: Means, Standard Deviations, and Average Protease Activities in Serum for Matrix Metalloproteinase 2 (MMP-2)**

| Stages | Means | SD | Average Protease Activity in Serum (mol $L^{-1}$) |
|---|---|---|---|
| H | 1.551050 | 0.2210302 | $4.0 \times 10^{-15}$ |
| 1 | 1.778842 | 0.1615579 | $7.0 \times 10^{-13}$ |
| 2 | 1.797345 | 0.2712342 | $8.8 \times 10^{-13}$ |
| 3 | 1.917671 | 0.1823691 | $9.1 \times 10^{-13}$ |

**Table 15: Means, Standard Deviations, and Average Protease Activities in Serum for Matrix Metalloproteinase 3 (MMP-3)**

| Stages | Means | SD | Average Protease Activity in Serum (mol $L^{-1}$) |
|---|---|---|---|
| H | 1.276774 | 0.10293781 | $3.4 \times 10^{-16}$ |
| 1 | 1.387032 | 0.05586801 | $8.2 \times 10^{-15}$ |
| 2 | 1.670378 | 0.13738547 | $1.2 \times 10^{-14}$ |
| 3 | 1.789161 | 0.19236757 | $9.3 \times 10^{-14}$ |

**Table 16: Means, Standard Deviations, and Average Protease Activities in Serum for Matrix Metalloproteinase 7 (MMP-7)**

| Stages | Means | SD | Average Protease Activity in Serum (mol $L^{-1}$) |
|---|---|---|---|
| H | 1.265858 | 0.08413963 | $6.4 \times 10^{-16}$ |
| 1 | 1.353391 | 0.05112853 | $9.2 \times 10^{-16}$ |
| 2 | 1.352708 | 0.09032285 | $9.1 \times 10^{-15}$ |
| 3 | 1.365533 | 0.11891228 | $9.5 \times 10^{-15}$ |

**Table 17: Means, Standard Deviations, and Average Protease Activities in Serum for Matrix Metalloproteinase 9 (MMP-9)**

| Stages | Means | SD | Average Protease Activity in Serum (mol $L^{-1}$) |
|---|---|---|---|
| H | 0.9622952 | 0.011980785 | $8.6 \times 10^{-13}$ |
| 1 | 0.94443 | 0.012026643 | $1.3 \times 10^{-10}$ |
| 2 | 0.941885 | 0.011387601 | $1.4 \times 10^{-10}$ |
| 3 | 0.940606 | 0.010589256 | $2.6 \times 10^{-10}$ |

**Table 18: Means, Standard Deviations, and Average Protease Activities in Serum for Matrix Metalloproteinase 13 (MMP-13)**

| Stages | Means | SD | Average Protease Activity in Serum (mol $L^{-1}$) |
|---|---|---|---|
| H | 2.402871 | 0.6767673 | $3.2 \times 10^{-15}$ |
| 1 | 2.426960 | 0.5062057 | $7.7 \times 10^{-15}$ |
| 2 | 2.443162 | 0.5665877 | $7.8 \times 10^{-15}$ |
| 3 | 2.690081 | 1.1047931 | $9.7 \times 10^{-15}$ |

# References


(1) Kerr, J. F.; Winterford, C. M.; Harmon, B. V. *Cancer* **1994**, *73*, 2013.

(2) http://www.cancerinstitute.org.au/patient-support/what-i-need-to-know/about-cancer/what-are-the-different-stages-of-cancer.

(3) Kos, J.; Sekirnik, A.; Kopitar, G.; Cimerman, N.; Kayser, K.; Stremmer, A.; Fiehn, W.; Werle, B. *British journal of cancer* **2001**, *85*, 1193.

(4) Siegel, R. L.; Miller, K. D.; Jemal, A. *CA: a cancer journal for clinicians* **2016**, *66*, 7.

(5) Schmitt, M.; Sturmheit, A. S.; Welk, A.; Schnelldorfer, C.; Harbeck, N. *Breast cancer research protocols* **2006**, 245.

(6) Wang, J. *Biosensors and Bioelectronics* **2006**, *21*, 1887.

(7) Harvey, J. M.; Clark, G. M.; Osborne, C. K.; Allred, D. C. *Journal of clinical oncology* **1999**, *17*, 1474.

(8) Xu, S.; Liu, Y.; Wang, T.; Li, J. *Analytical chemistry* **2011**, *83*, 3817.

(9) Bubendorf, L.; Kononen, J.; Koivisto, P.; Schraml, P.; Moch, H.; Gasser, T. C.; Willi, N.; Mihatsch, M. J.; Sauter, G.; Kallioniemi, O.-P. *Cancer research* **1999**, *59*, 803.

(10) Wang, H.; Udukala, D. N.; Samarakoon, T. N.; Basel, M. T.; Kalita, M.; Abayaweera, G.; Manawadu, H.; Malalasekera, A.; Robinson, C.; Villanueva, D. *Photochemical & Photobiological Sciences* **2014**, *13*, 231.

(11) Udukala, D. N.; Wang, H.; Wendel, S. O.; Malalasekera, A. P.; Samarakoon, T. N.; Yapa, A. S.; Abayaweera, G.; Basel, M. T.; Maynez, P.; Ortega, R. *Beilstein Journal of Nanotechnology* **2016**, *7*, 364.

(12) Sahoo, H. *Journal of Photochemistry and Photobiology C: Photochemistry Reviews* **2011**, *12*, 20.

(13) Malalasekera, A. P.; Wang, H.; Samarakoon, T. N.; Udukala, D. N.; Yapa, A. S.; Ortega, R.; Shrestha, T. B.; Alshetaiwi, H.; McLaurin, E. J.; Troyer, D. L. *Nanomedicine: Nanotechnology, Biology and Medicine* **2016**.

(14) Mandhare, M.; Patil, P.; Jagdale, D.; Kadam, V. *Int. J. Pharm. Sci. Rev. Res* **2012**, *12*, 27.

(15) López-Otín, C.; Matrisian, L. M. *Nature Reviews Cancer* **2007**, *7*, 800.

(16) Coussens, L. M.; Werb, Z. *Chemistry & biology* **1996**, *3*, 895.

(17) Bergers, G.; Brekken, R.; McMahon, G.; Vu, T. H.; Itoh, T.; Tamaki, K.; Tanzawa, K.; Thorpe, P.; Itohara, S.; Werb, Z. *Nature cell biology* **2000**, *2*, 737.

(18) Cantero, D.; Friess, H.; Deflorin, J.; Zimmermann, A.; Bründler, M.; Riesle, E.; Korc, M.; Büchler, M. *British journal of cancer* **1997**, *75*, 388.

(19) John, A.; Tuszynski, G. *Pathology oncology research* **2001**, *7*, 14.

(20) Matrisian, L. M. *Trends in Genetics* **1990**, *6*, 121.

(21) Rooprai, H.; McCormick, D. *Anticancer research* **1996**, *17*, 4151.

(22) Celentano, D. C.; Frishman, W. H. *The Journal of Clinical Pharmacology* **1997**, *37*, 991.

(23) McKenna, G. J.; Meneghetti, A.; Chen, Y. L.; Mui, A. L.; Ong, C.; Scudamore, C. H.; McMaster, W. R.; Owen, D. A.; Chung, S. W. *Journal of surgical oncology* **2005**, *90*, 239.

(24) Seki, N.; Kodama, J.; Hongo, A.; Miyagi, Y.; Yoshinouchi, M.; Kudo, T. *International journal of oncology* **1999**, *15*, 781.

(25) Parks, W. C.; Shapiro, S. D. *Respiratory research* **2000**, *2*, 1.

(26) Gialeli, C.; Theocharis, A. D.; Karamanos, N. K. *FEBS journal* **2011**, *278*, 16.

(27) Tan, G.-J.; Peng, Z.-K.; Lu, J.-P.; Tang, F.-Q. *World* **2013**, *4*, 91.

(28) Kuester, D.; Lippert, H.; Roessner, A.; Krueger, S. *Pathology-Research and Practice* **2008**, *204*, 491.

(29) Mohamed, M. M.; Sloane, B. F. *Nature Reviews Cancer* **2006**, *6*, 764.

(30) Joyce, J. A.; Hanahan, D. *Cell cycle* **2004**, *3*, 1516.

(31) Henneke, I.; Greschus, S.; Savai, R.; Korfei, M.; Markart, P.; Mahavadi, P.; Schermuly, R. T.; Wygrecka, M.; Stürzebecher, J. r.; Seeger, W. *American journal of respiratory and critical care medicine* **2010**, *181*, 611.

(32) Rakash, S.; Rana, F.; Rafiq, S.; Masood, A.; Amin, S. *Biotechnology and Molecular Biology Reviews* **2012**, *7*, 90.

(33) Nakamura, K.; Hongo, A.; Kodama, J.; Abarzua, F.; Nasu, Y.; Kumon, H.; Hiramatsu, Y. *Anticancer research* **2009**, *29*, 1685.

(34) Saleem, M.; Adhami, V. M.; Zhong, W.; Longley, B. J.; Lin, C.-Y.; Dickson, R. B.; Reagan-Shaw, S.; Jarrard, D. F.; Mukhtar, H. *Cancer Epidemiology Biomarkers & Prevention* **2006**, *15*, 217.

(35) Imamura, T.; Kitamoto, Y. *American Journal of Physiology-Gastrointestinal and Liver Physiology* **2003**, *285*, G1235.

(36) Yamamoto, H.; Iku, S.; Adachi, Y.; Imsumran, A.; Taniguchi, H.; Nosho, K.; Min, Y.; Horiuchi, S.; Yoshida, M.; Itoh, F. *The Journal of pathology* **2003**, *199*, 176.

(37) Tang, C.-H.; Wei, Y. *Cellular and Molecular Life Sciences* **2008**, *65*, 1916.

(38) http://www.enzolifesciences.com/cancer/serine-proteases-and-cancer.

(39) Shin, E. J.; Canto, M. I. *Gastroenterology Clinics of North America* **2012**, *41*, 143.

(40) Gullo, L.; Tomassetti, P.; Migliori, M.; Casadei, R.; Marrano, D. *Pancreas* **2001**, *22*, 210.

(41) Connolly, G. N. *Tobacco Control* **1995**, *4*, 73.

(42) Horner, M.; Ries, L.; Krapcho, M.; Neyman, N.; Aminou, R.; Howlader, N.; Altekruse, S.; Feuer, E.; Huang, L.; Mariotto, A. 2009.

(43) Keleg, S.; Büchler, P.; Ludwig, R.; Büchler, M. W.; Friess, H. *Molecular cancer* **2003**, *2*, 1.

(44) Neoptolemos, J.; Dunn, J.; Stocken, D.; Almond, J.; Link, K.; Beger, H.; Bassi, C.; Falconi, M.; Pederzoli, P.; Dervenis, C. *The Lancet* **2001**, *358*, 1576.

(45) Gress, T.; Müller-Pillasch, F.; Lerch, M.; Friess, H.; Büchler, M.; Adler, G. *International Journal of Cancer* **1995**, *62*, 407.

(46) Gress, T.; Müller-Pillasch, F.; Lerch, M.; Friess, H.; Büchler, M.; Beger, H.; Adler, G. *Zeitschrift fur Gastroenterologie* **1994**, *32*, 221.

(47) Bramhall, S.; Stamp, G.; Dunn, J.; Lemoine, N.; Neoptolemos, J. *British journal of cancer* **1996**, *73*, 972.

(48) Lee, C. S.; Montebello, J.; Georgiou, T.; Rode, J. *International journal of experimental pathology* **1994**, *75*, 79.

(49) Mollenhauer, J.; Roether, I.; Kern, H. *Pancreas* **1987**, *2*, 14.

(50) World Health Organization. International Agency for Research on Cancer, 2012.

(51) National Center for Health Statistics: Centers for Disease Control and Prevention, 2016.

(52) U.S. National Institutes of Health. National Cancer Institute, 1975-2013.

(53) Palmisano, W. A.; Divine, K. K.; Saccomanno, G.; Gilliland, F. D.; Baylin, S. B.; Herman, J. G.; Belinsky, S. A. *Cancer research* **2000**, *60*, 5954.

(54) Team, N. L. S. T. R. *N Engl J Med* **2011**, *2011*, 395.

(55) Ma, J.; Ward, E. M.; Smith, R.; Jemal, A. *Cancer* **2013**, *119*, 1381.

(56) Kohler, B. A.; Ward, E.; McCarthy, B. J.; Schymura, M. J.; Ries, L. A.; Eheman, C.; Jemal, A.; Anderson, R. N.; Ajani, U. A.; Edwards, B. K. *Journal of the National Cancer Institute* **2011**.

(57) Siegel, R.; Naishadham, D.; Jemal, A. *CA: a cancer journal for clinicians* **2012**, *62*, 10.

(58) Bolon, I.; Gouyer, V.; Devouassoux, M.; Vandenbunder, B.; Wernert, N.; Moro, D.; Brambilla, C.; Brambilla, E. *The American journal of pathology* **1995**, *147*, 1298.

(59) Bolon, I.; Devouassoux, M.; Robert, C.; Moro, D.; Brambilla, C.; Brambilla, E. *The American journal of pathology* **1997**, *150*, 1619.

(60) Robert, C.; Bolon, I.; Gazzeri, S.; Veyrenc, S.; Brambilla, C.; Brambilla, E. *Clinical cancer research* **1999**, *5*, 2094.

(61) Kodate, M.; Kasai, T.; Hashirnoto, H.; Yasumoto, K.; Iwata, Y.; Manabe, H. *Pathology international* **1997**, *47*, 461.

(62) Urbanski, S.; Edwards, D.; Maitland, A.; Leco, K.; Watson, A.; Kossakowska, A. *British journal of cancer* **1992**, *66*, 1188.

(63) Tokuraku, M.; Sato, H.; Murakami, S.; Okada, Y.; Watanabe, Y.; Seiki, M. *International journal of cancer* **1995**, *64*, 355.

(64) Muller, D.; Breathnach, R.; Engelmann, A.; Millon, R.; Bronner, G.; Flesch, H.; Dumont, P.; Eber, M.; Abecassis, J. *International journal of cancer* **1991**, *48*, 550.

(65) Kos, J.; Lah, T. T. *Oncology reports* **1998**, *5*, 1349.

(66) http://www.cancer.org/cancer/pancreaticcancer/detailedguide/pancreatic-cancer.

(67) Silverman, D. T. *Teratog., Carcinog., Mutagen.* **2001**, *21*, 7.

(68) Peery, A. F.; Crockett, S. D.; Barritt, A. S.; Dellon, E. S.; Eluri, S.; Gangarosa, L. M.; Jensen, E. T.; Pasricha, S.; Runge, T.; Schmidt, M.; Shaheen, N. J.; Sandler, R. S.; Lund, J. L. *Gastroenterology* **2015**, *149*, 1731.

(69) Kuroki, T.; Eguchi, S. *Surg. Today* **2016**, Ahead of Print.

(70) Feig, C.; Gopinathan, A.; Neesse, A.; Chan, D. S.; Cook, N.; Tuveson, D. A. *Clin. Cancer Res.* **2012**, *18*, 4266.

(71) Yamada, H.; Hirano, S.; Tanaka, E.; Shichinohe, T.; Kondo, S. *HPB (Oxford)* **2006**, *8*, 85.

(72) Boeck, S.; Ankerst, D. P.; Heinemann, V. *Oncology* **2007**, *72*, 314.

(73) Elie, B. T.; Gocheva, V.; Shree, T.; Dalrymple, S. A.; Holsinger, L. J.; Joyce, J. A. *Biochimie* **2010**, *92*, 1618.

(74) Pancreas, A. J. C. o. C. E. a. E.; Springer: New York, NY, 2010; Vol. 7th Edition, p 241.

(75) Hinton, J.; Callan, R.; Bodine, C.; Glasgow, W.; Brower, S.; Jiang, S.-W.; Li, J. *Expert Rev. Mol. Diagn.* **2013**, *13*, 431.

(76) http://www.cancer.gov/cancertopics.

(77) http://www.personalgenome.com/.

(78) http://www.genomichealth.com/.

(79) https://www.myriad.com/.

(80) Malalasekera, A. P.; Wang, H.; Samarakoon, T. N.; Udukala, D. N.; Yapa, A. S.; Ortega, R.; Shrestha, T. B.; Alshetaiwi, H.; McLaurin, E. J.; Troyer, D. L.; Bossmann, S. H. *Nanomedicine (N. Y., NY, U. S.)* **2016**, *13*, 383.

(81) Udukala, D. N.; Wang, H.; Wendel, S. O.; Malalasekera, A. P.; Samarakoon, T. N.; Yapa, A. S.; Abayaweera, G.; Basel, M. T.; Maynez, P.; Ortega, R.; Toledo, Y.; Bossmann, L.; Robinson, C.; Janik, K. E.; Koper, O. B.; Li, P.; Motamedi, M.; Higgins, D. A.; Gadbury, G.; Zhu, G.; Troyer, D. L.; Bossmann, S. H. *Beilstein J. Nanotechnol.* **2016**, *7*, 364.

(82) Udukala, D.; Wendel, S.; Kalubowilage, M.; Wang, H.; Malalasekera, A. P.; Yapa, A. S.; Toledo, Y.; Ortega, R.; Maynez, P.; Bossmann, L.; Janik, K.; Gadbury, G.; Troyer, D. L.; Bossmann, S. H. *ACS Nanp* **2017**, *submitted*.

(83) http://www.cancer.gov/cancertopics/pdq/treatment/pancreatic.

(84) http://www.cancer.org/cancer/pancreaticcancer/detailedguide/pancreatic-cancer-key-statistics.

(85) Cooper, C. L.; O'Toole, S. A.; Kench, J. G. *Pathology* **2013**, *45*, 286.

(86) Morris-Stiff, G.; Taylor, M. A. *J. Gastrointest. Oncol.* **2012**, *3*, 88.

(87) Ozkan, H.; Kaya, M.; Cengiz, A. *Hepatogastroenterology* **2003**, *50*, 1669.

(88) Kinugasa, H.; Nouso, K.; Miyahara, K.; Morimoto, Y.; Dohi, C.; Tsutsumi, K.; Kato, H.; Matsubara, T.; Okada, H.; Yamamoto, K. *Cancer (Hoboken, NJ, U. S.)* **2015**, *121*, 2271.

(89) Locker, G. Y.; Hamilton, S.; Harris, J.; Jessup, J. M.; Kemeny, N.; MacDonald, J. S.; Somerfield, M. R.; Hayes, D. F.; Bast, R. C., Jr. *J. Clin. Oncol.* **2006**, *24*, 5313.

(90) Logsdon, C. D.; Lu, W. *Int. J. Biol. Sci.* **2016**, *12*, 338.

(91) Mason, S. D.; Joyce, J. A. *Trends Cell Biol* **2011**, *21*, 228.

(92) Quesada, V.; Ordonez, G. R.; Sanchez, L. M.; Puente, X. S.; Lopez-Otin, C. *Nucleic Acids Res.* **2009**, *37*, D239.

(93) Schmitt, M.; Harbeck, N.; Bruenner, N.; Jaenicke, F.; Meisner, C.; Muehlenweg, B.; Jansen, H.; Dorn, J.; Nitz, U.; Kantelhardt, E. J.; Thomssen, C. *Expert Rev. Mol. Diagn.* **2011**, *11*, 617.

(94) Mohamed, M. M.; Sloane, B. F. *Nat. Rev. Cancer* **2006**, *6*, 764.

(95) Rukamp, B.; Powers, J. C.; Taylor & Francis Ltd.: 2002, p 84.

(96) Gopinathan, A.; DeNicola, G. M.; Frese, K. K.; Cook, N.; Karreth, F. A.; Mayerle, J.; Lerch, M. M.; Reinheckel, T.; Tuveson, D. A. *Gut* **2012**, *61*, 877.

(97) Gocheva, V.; Zeng, W.; Ke, D.; Klimstra, D.; Reinheckel, T.; Peters, C.; Hanahan, D.; Joyce, J. A. *Genes Dev.* **2006**, *20*, 543.

(98) Dennemaerker, J.; Lohmueller, T.; Mayerle, J.; Tacke, M.; Lerch, M. M.; Coussens, L. M.; Peters, C.; Reinheckel, T. *Oncogene* **2010**, *29*, 1611.

(99) Lopez-Otin, C.; Matrisian, L. M. *Nat. Rev. Cancer* **2007**, *7*, 800.

(100) Kessenbrock, K.; Plaks, V.; Werb, Z. *Cell (Cambridge, MA, U. S.)* **2010**, *141*, 52.

(101) Choi, Y.; Kendziorski, C. *Bioinformatics* **2009**, *25*, 2780.

(102) https://www.ncbi.nlm.nih.gov/geo/.

(103) Coffey, C. S.; Cofield, S. S. *Biostatistics* **2006**, *15*, 223.

(104) Page, R. B.; Stromberg, A. J. *TheScientificWorldJournal* **2011**, *11*, 1383.

(105) Romero, P. A.; Stone, E.; Lamb, C.; Chantranupong, L.; Krause, A.; Miklos, A.; Hughes, R. A.; Fechtel, B.; Ellington, A. D.; Arnold, F. H.; Georgiou, G. *ACS Synth. Biol.* **2012**, *1*, 221.

(106) Di Costanzo, L.; Sabio, G.; Mora, A.; Rodriguez, P. C.; Ochoa, A. C.; Centeno, F.; Christianson, D. W. *Proc. Natl. Acad. Sci. U. S. A.* **2005**, *102*, 13058.

(107) Das, P.; Lahiri, A.; Lahiri, A.; Chakravortty, D. *PLoS Pathog.* **2010**, *6*, No pp. given.

(108) Mahmood, U.; Weissleder, R. *Mol. Cancer Ther.* **2003**, *2*, 489.

(109) Werle, B.; Kotzsch, M.; Lah, T. T.; Kos, J.; Gabrijelcic-Geiger, D.; Spiess, E.; Schirren, J.; Ebert, W.; Fiehn, W.; Luther, T.; Magdolen, V.; Schmitt, M.; Harbeck, N. *Anticancer Res.* **2004**, *24*, 4147.

(110) Vasiljeva, O.; Reinheckel, T.; Peters, C.; Turk, D.; Turk, V.; Turk, B. *Curr. Pharm. Des.* **2007**, *13*, 387.

(111) Platt, M. O.; Dumas, J. E.; CRC Press: 2013, p 297.

(112) http://www.signaling-gateway.org/molecule/query

(113) Hoyer-Hansen, G.; Lund, I. K. *Adv. Clin. Chem.* **2007**, *44*, 65.

(114) Beleva, E.; Grudeva-Popova, J. *J BUON* **2013**, *18*, 25.

(115) Ishida, T.; Tsukada, H.; Hasegawa, T.; Yoshizawa, H.; Gejyo, F. *Lung* **2006**, *184*, 15.

(116) Mehner, C.; Miller, E.; Radisky, E. S.; Radisky, D. C.; Nassar, A.; Bamlet, W. R. *Genes Cancer* **2015**, *6*, 480.

(117) Rieder, F.; Kessler, S. P.; West, G. A.; Bhilocha, S.; de la Motte, C.; Sadler, T. M.; Gopalan, B.; Stylianou, E.; Fiocchi, C. *Am. J. Pathol.* **2011**, *179*, 2660.

(118) Meyer-Hoffert, U.; Wiedow, O. *Curr. Opin. Hematol.* **2010**, *18*, 19.

(119) Welch, B. L. *Biometrika* **1947**, *34*, 28.

(120) Doucet, A.; Butler, G. S.; Rodriguez, D.; Prudova, A.; Overall, C. M. *Mol. Cell. Proteomics* **2008**, *7*, 1925.

(121) Rakashanda, S.; Rana, F.; Rafiq, S.; Masood, A.; Amin, S. *Biotechnol. Mol. Biol. Rev.* **2012**, *7*, 90.

(122) Wang, H.; Udukala, D. N.; Samarakoon, T. N.; Basel, M. T.; Kalita, M.; Abayaweera, G.; Manawadu, H.; Malalasekera, A.; Robinson, C.; Villanueva, D.; Maynez, P.; Bossmann, L.; Riedy, E.; Barriga, J.; Wang, N.; Li, P.; Higgins, D. A.; Zhu, G.; Troyer, D. L.; Bossmann, S. H. *Photochem. Photobiol. Sci.* **2014**, *13*, 231.

(123) Udukala, D. N.; Wang, H.; Wendel, S. O.; Malalasekera, A. P.; Samarakoon, T. N.; Yapa, A. S.; Abayaweera, G.; Basel, M. T.; Maynez, P.; Ortega, R.; Toledo, Y.; Bossmann, L.; Robinson, C.; Janik, K. E.; Koper, O. B.; Li, P.; Culbertson, C. T.; Gadbury, G.; Zhu, G.; Troyer, D. L.; Bossmann, S. H. *ACS Nano* **2016**, *submitted*.

(124) Lacroix, L.-M.; Frey Huls, N.; Ho, D.; Sun, X.; Cheng, K.; Sun, S. *Nano Lett.* **2011**, *11*, 1641.

(125) Wang, H.; Shrestha, T. B.; Basel, M. T.; Dani, R. K.; Seo, G.-M.; Balivada, S.; Pyle, M. M.; Prock, H.; Koper, O. B.; Thapa, P. S.; Moore, D.; Li, P.; Chikan, V.; Troyer, D. L.; Bossmann, S. H. *Beilstein J. Nanotechnol.* **2012**, *3*, 444.

(126) Xu, C.; Xu, K.; Gu, H.; Zheng, R.; Liu, H.; Zhang, X.; Guo, Z.; Xu, B. *J. Am. Chem. Soc.* **2004**, *126*, 9938.

(127) Sobczynski, J.; Toennesen, H. H.; Kristensen, S. *Pharmazie* **2013**, *68*, 100.

(128) Patsenker, L.; Tatarets, A.; Kolosova, O.; Obukhova, O.; Povrozin, Y.; Fedyunyayeva, I.; Yermolenko, I.; Terpetschnig, E. *Ann. N. Y. Acad. Sci.* **2008**, *1130*, 179.

(129) http://merops.sanger.ac.uk/

(130) Ben-Avraham, D.; Schulman, L. S.; Bossmann, S. H.; Turro, C.; Turro, N. J. *J. Phys. Chem. B* **1998**, *102*, 5088.

(131) Mody, V. V.; Siwale, R.; Singh, A.; Mody, H. R. *J. Pharm. BioAllied Sci.* **2010**, *2*, 282.

(132) Udukala, D. N.; Samarakoon, T.; Wang, H.; Higgins, D. A.; Gadbury, G.; Zhu, G.; Troyer, D. L.; Bossmann, S. H.; American Chemical Society: 2014, p ORGN.

(133) Coin, I.; Beyermann, M.; Bienert, M. *Nat. Protoc.* **2007**, *2*, 3247.

(134) http://www.cellgrow.com/heat-inactivation/.

(135) http://www.kucancercenter.org/patient-care/biospecimen-bank/staff.

(136) Piperi, C.; Papavassiliou, A. G. *Curr. Top. Med. Chem. (Sharjah, United Arab Emirates)* **2012**, *12*, 1095.

(137) Siegel, R.; Naishadham, D.; Jemal, A. *CA Cancer J Clin* **2013**, *63*, 11.

(138) Zhao, Y.; Valbuena, G.; Walker, D. H.; Gazi, M.; Hidalgo, M.; DeSousa, R.; Oteo, J. A.; Goez, Y.; Brasier, A. R. *Molecular & cellular proteomics : MCP* **2016**, *15*, 289.

(139) Veglia, F.; Vineis, P.; Overvad, K.; Boeing, H.; Bergmann, M.; Trichopoulou, A.; Trichopoulos, D.; Palli, D.; Krogh, V.; Tumino, R.; Linseisen, J.; Steindorf, K.; Raaschou-Nielsen, O.; Tjonneland, A.; Gonzalez, C. A.; Martinez, C.; Dorronsoro, M.; Barricarte, A.; Cirera, L.; Quiros, J. R.; Day, N. E.; Saracci, R.; Riboli, E. *Epidemiology* **2007**, *18*, 769.

(140) Mayor, S. *Bmj* **2009**, *338*, b981.

(141) Bach, P. B.; Jett, J. R.; Pastorino, U.; Tockman, M. S.; Swensen, S. J.; Begg, C. B. *JAMA* **2007**, *297*, 953.

(142) Hassanein, M.; Callison, J. C.; Callaway-Lane, C.; Aldrich, M. C.; Grogan, E. L.; Massion, P. P. *Cancer Prev Res (Phila)* **2012**, *5*, 992.

(143) Mutti, A. *Acta Biomed* **2008**, *79 Suppl 1*, 11.

(144) Wang, J.; Wang, K.; Xu, J.; Huang, J.; Zhang, T. *PLoS One* **2013**, *8*, e78070.

(145) Hirales Casillas, C. E.; Flores Fernandez, J. M.; Padilla Camberos, E.; Herrera Lopez, E. J.; Leal Pacheco, G.; Martinez Velazquez, M. *Future Oncol* **2014**, *10*, 1501.

(146) Trudgen, K.; Khattar, N. H.; Bensadoun, E.; Arnold, S.; Stromberg, A. J.; Hirschowitz, E. A. *PLoS One* **2014**, *9*, e87947.

(147) Ilie, M.; Hofman, V.; Long, E.; Bordone, O.; Selva, E.; Washetine, K.; Marquette, C. H.; Hofman, P. *Ann Transl Med* **2014**, *2*, 107.

(148) Carlsson, A.; Nair, V. S.; Luttgen, M. S.; Keu, K. V.; Horng, G.; Vasanawala, M.; Kolatkar, A.; Jamali, M.; Iagaru, A. H.; Kuschner, W.; Loo, B. W., Jr.; Shrager, J. B.; Bethel, K.; Hoh, C. K.; Bazhenova, L.; Nieva, J.; Kuhn, P.; Gambhir, S. S. *J Thorac Oncol* **2014**, *9*, 1111.

(149) Krebs, M. G.; Sloane, R.; Priest, L.; Lancashire, L.; Hou, J. M.; Greystoke, A.; Ward, T. H.; Ferraldeschi, R.; Hughes, A.; Clack, G.; Ranson, M.; Dive, C.; Blackhall, F. H. *J Clin Oncol* **2011**, *29*, 1556.

(150) Vachani, A.; Hammoud, Z.; Springmeyer, S.; Cohen, N.; Nguyen, D.; Williamson, C.; Starnes, S.; Hunsucker, S.; Law, S.; Li, X. J.; Porter, A.; Kearney, P. *Lung* **2015**, *193*, 1023.

(151) Ricard-Blum, S.; Vallet, S. D. *Biochimie* **2016**, *122*, 300.

(152) Pham, W.; Weissleder, R.; Tung, C.-H. *Angew. Chem., Int. Ed.* **2002**, *41*, 3659.

(153) Pham, W.; Choi, Y.; Weissleder, R.; Tung, C.-H. *Bioconjugate Chem.* **2004**, *15*, 1403.

(154) Zhao, M.; Josephson, L.; Tang, Y.; Weissleder, R. *Angew. Chem., Int. Ed.* **2003**, *42*, 1375.

(155) Funovics, M.; Weissleder, R.; Tung, C.-H. *Anal. Bioanal. Chem.* **2003**, *377*, 956.

(156) Bossmann, S. H.; Troyer, D. L. *Expert Rev. Mol. Diagn.* **2013**, *13*, 107.

(157) Liang, J.; Liu, H.; Huang, C.; Yao, C.; Fu, Q.; Li, X.; Cao, D.; Luo, Z.; Tang, Y. *Anal. Chem. (Washington, DC, U. S.)* **2015**, *87*, 5790.

(158) Gao, Y.; Lam, A. W. Y.; Chan, W. C. W. *ACS Appl. Mater. Interfaces* **2013**, *5*, 2853.

(159) Spindel, S.; Sapsford, K. E. *Sensors* **2014**, *14*, 22313.

(160) Udukala, D. N., Kansas State University, 2014.

(161) Jennings, T. L.; Singh, M. P.; Strouse, G. F. *J. Am. Chem. Soc.* **2006**, *128*, 5462.

(162) Selvin, P. R. *Nat. Struct. Biol.* **2000**, *7*, 730.

(163) Schulman, L. S.; Bossmann, S. H.; Turro, N. J. *J. Phys. Chem.* **1995**, *99*, 9283.

(164) Kang, K. A.; Wang, J.; Jasinski, J. B.; Achilefu, S. *J. Nanobiotechnol.* **2011**, *9*, 16.

(165) Bonomi, P. *Semin. Oncol.* **2002**, *29*, 78.

(166) Johnson, D. H.; Schiller, J. H. *Cancer Chemother. Biol. Response Modif.* **2002**, *20*, 763.

(167) Lalmanach, G.; Saidi, A.; Marchand-Adam, S.; Lecaille, F.; Kasabova, M. *Biol. Chem.* **2015**, *396*, 111.

(168) Thompson, J. M. *Anal. Proc. (London)* **1988**, *25*, 363.

(169) Gora, J.; Latajka, R. *Curr. Med. Chem.* **2015**, *22*, 944.

(170) Weston, M. A.; Patterson, M. S. *Photochem. Photobiol.* **2014**, *90*, 1359.

(171) Yu, X.; Wang, Y. *Xiandai Zhongliu Yixue* **2005**, *13*, 461.

(172) Radisky, D. C.; Przybylo, J. A. *Proc. Am. Thorac. Soc.* **2008**, *5*, 316.

(173) Rybakowski, J. K. *Cardiovasc. Psychiatry Neurol.* **2009**, No pp. given.

(174) Yuan, X.; Wu, H.; Han, N.; Xu, H.; Chu, Q.; Yu, S.; Chen, Y.; Wu, K. *J. Hematol. Oncol.* **2014**, *7*, 87/1.

# Appendix A - Data tables

**Table 19: Fluorescence intensity data and p-values for Arginase in Fig 24**

| Ductal Adenocarcinoma | | Neuroendocrine Tumor | | Metastatic Adenocarcinoma | | Metastatic Neuroendocrine | |
|---|---|---|---|---|---|---|---|
| Sample ID | patient | Sample ID | Patient | Sample ID | patient | Sample ID | Patient |
| 2720 | 308.7778 | 5327 | 102.2222 | 2689 | 290.5556 | 851 | 106.4444 |
| 4236 | 249.7778 | 5247 | 156.8889 | 2996 | 344.6667 | 7428 | 103.0000 |
| 4967 | 114.2222 | 7433 | 110.2222 | 3824 | 151.5556 | | |
| 7253 | 158.6667 | 9829 | 126.1111 | 5273 | 139.3333 | | |
| 8306 | 123.1111 | 10550 | 107.3333 | 5237 | 107.6667 | | |
| 9620 | 148.8889 | | | 5417 | 111.1111 | | |
| 9928 | 130.2222 | | | 6839 | 127.1111 | | |
| | | | | 7779 | 144.0000 | | |
| | | | | 8417 | 98.2222 | | |
| Sample ID | control | Sample ID | Control | Sample ID | control | Sample ID | Control |
| 17424 | 109.7778 | 21486 | 141.4444 | 2741 | 206.5556 | 5783 | 126.4444 |
| 17297 | 122.4444 | 17370 | 118.6667 | 17170 | 129.5556 | 17125 | 121.3333 |
| 9178 | 115.5556 | 17268 | 116.8889 | 3371 | 101.8889 | | |
| 4650 | 122.2222 | 20834 | 130.4444 | 3319 | 113.3333 | | |
| 8170 | 114.3333 | 17468 | 122.0000 | 3754 | 93.7778 | | |
| 6194 | 113.1111 | | | 9503 | 111.3333 | | |
| 20483 | 109.2222 | | | 8441 | 116.2222 | | |
| | | | | 4185 | 107.7778 | | |
| | | | | 17180 | 126.2222 | | |

**Table 20: Mean values and standard deviations of fluorescence intensities in Table 10**

| | Ductal Adenocarcinoma | | Neuroendocrine Tumor | | Metastatic Adenocarcinoma | | Metastatic Neuroendocrine | |
|---|---|---|---|---|---|---|---|---|
| | Control | Patient | Control | Patient | Control | Patient | Control | Patient |
| mean | 115.2381 | 176.2381 | 125.8889 | 120.5556 | 122.9630 | 168.2469 | 123.8889 | 104.7222 |
| SD | 5.3566 | 73.9566 | 10.1367 | 22.1850 | 33.2447 | 87.5471 | 3.6141 | 2.4356 |

**Table 21: Fluorescence intensity data and p-values for Cathepsin B in Fig 25**

| Ductal Adenocarcinoma | | Neuroendocrine Tumor | | Metastatic Adenocarcinoma | | Metastatic Neuroendocrine | |
|---|---|---|---|---|---|---|---|
| Sample ID | patient | Sample ID | Patient | Sample ID | patient | Sample ID | Patient |
| 2720 | 3638.7778 | 5327 | 3283.6667 | 2689 | 2804.6667 | 851 | 3567.3333 |
| 4236 | 3091.0000 | 5247 | 3794.0000 | 2996 | 1235.2222 | 7428 | 2976.5556 |
| 4967 | 2731.5556 | 7433 | 3630.5556 | 3824 | 3799.0000 | | |
| 7253 | 3220.0000 | 9829 | 3585.7778 | 5273 | 3424.5556 | | |
| 8306 | 3396.4444 | 10550 | 3916.1111 | 5237 | 3003.3333 | | |
| 9620 | 3686.2222 | | | 5417 | 2319.1111 | | |
| 9928 | 3086.2222 | | | 6839 | 3235.0000 | | |
| | | | | 7779 | 3677.2222 | | |
| | | | | 8417 | 2913.0000 | | |
| Sample ID | control | Sample ID | Control | Sample ID | control | Sample ID | Control |
| 17424 | 3954.3333 | 21486 | 3579.1111 | 2741 | 4300.5556 | 5783 | 3503.3333 |
| 17297 | 4264.6667 | 17370 | 2581.0000 | 17170 | 4208.5556 | 17125 | 3708.5556 |
| 9178 | 2573.6667 | 17268 | 3355.4444 | 3371 | 2717.3333 | | |
| 4650 | 3626.6667 | 20834 | 3970.7778 | 3319 | 3191.6667 | | |
| 8170 | 3555.2222 | 17468 | 3697.6667 | 3754 | 3170.5556 | | |
| 6194 | 3405.7778 | | | 9503 | 3321.4444 | | |
| 20483 | 4083.5556 | | | 8441 | 3506.7778 | | |
| | | | | 4185 | 4039.6667 | | |
| | | | | 17180 | 3614.1111 | | |

**Table 22: Mean values and standard deviations of fluorescence intensities in Table 11**

| | Ductal Adenocarcinoma | | Neuroendocrine Tumor | | Metastatic Adenocarcinoma | | Metastatic Neuroendocrine | |
|---|---|---|---|---|---|---|---|---|
| | Control | Patient | Control | Patient | Control | Patient | Control | Patient |
| mean | 3637.6984 | 3264.3175 | 3436.8000 | 3642.0222 | 3563.4074 | 2934.5679 | 3605.9444 | 3271.9444 |
| SD | 560.5072 | 337.4507 | 527.3634 | 239.7580 | 531.4033 | 784.0405 | 145.1140 | 417.7430 |

**Table 23: Fluorescence intensity data and p-values for Cathepsin D in Fig 26**

| Ductal Adenocarcinoma | | Neuroendocrine Tumor | | Metastatic Adenocarcinoma | | Metastatic Neuroendocrine | |
|---|---|---|---|---|---|---|---|
| Sample ID | patient | Sample ID | Patient | Sample ID | patient | Sample ID | patient |
| 2720 | 317.4444 | 5327 | 360.8889 | 2689 | 305.7778 | 851 | 248.2222 |
| 4236 | 196.0000 | 5247 | 397.6667 | 2996 | 257.7778 | 7428 | 234.0000 |
| 4967 | 282.8889 | 7433 | 283.4444 | 3824 | 328.6667 | | |
| 7253 | 258.8889 | 9829 | 269.1111 | 5273 | 281.2222 | | |
| 8306 | 266.6667 | 10550 | 253.8889 | 5237 | 223.2222 | | |
| 9620 | 296.4444 | | | 5417 | 250.5556 | | |
| 9928 | 316.2222 | | | 6839 | 254.4444 | | |
| | | | | 7779 | 315.5556 | | |
| | | | | 8417 | 202.6667 | | |
| Sample ID | control | Sample ID | Control | Sample ID | control | Sample ID | Control |
| 17424 | 264.7778 | 21486 | 291.7778 | 2741 | 315.0000 | 5783 | 281.7778 |
| 17297 | 270.0000 | 17370 | 273.3333 | 17170 | 298.3333 | 17125 | 240.0000 |
| 9178 | 239.3333 | 17268 | 270.6667 | 3371 | 219.4444 | | |
| 4650 | 259.8889 | 20834 | 286.1111 | 3319 | 299.0000 | | |
| 8170 | 264.8889 | 17468 | 253.1111 | 3754 | 224.5556 | | |
| 6194 | 212.7778 | | | 9503 | 250.1111 | | |
| 20483 | 282.2222 | | | 8441 | 253.6667 | | |
| | | | | 4185 | 242.3333 | | |
| | | | | 17180 | 260.4444 | | |

**Table 24: Mean values and standard deviations of fluorescence intensities in Table 14**

| | Ductal Adenocarcinoma | | Neuroendocrine Tumor | | Metastatic Adenocarcinoma | | Metastatic Neuroendocrine | |
|---|---|---|---|---|---|---|---|---|
| | Control | Patient | Control | Patient | Control | Patient | Control | Patient |
| mean | 256.2698 | 276.3651 | 275.0000 | 313.0000 | 262.5432 | 268.8765 | 260.8889 | 241.1111 |
| SD | 23.0948 | 41.9918 | 15.0468 | 62.7608 | 34.1110 | 42.4310 | 29.5413 | 10.0566 |

**Table 25: Fluorescence intensity data and p-values for Cathepsin E in Fig 27**

| Ductal Adenocarcinoma | | Neuroendocrine Tumor | | Metastatic Adenocarcinoma | | Metastatic Neuroendocrine | |
|---|---|---|---|---|---|---|---|
| Sample ID | patient | Sample ID | patient | Sample ID | patient | Sample ID | patient |
| 2720 | 12948.2222 | 5327 | 11465.1111 | 2689 | 11646.1111 | 851 | 10322.4444 |
| 4236 | 7478.5556 | 5247 | 14530.3333 | 2996 | 2637.7778 | 7428 | 10493.1111 |
| 4967 | 10721.7778 | 7433 | 8826.6667 | 3824 | 8623.0000 | | |
| 7253 | 10101.2222 | 9829 | 11112.3333 | 5273 | 9005.4444 | | |
| 8306 | 10857.8889 | 10550 | 11283.6667 | 5237 | 8618.0000 | | |
| 9620 | 9654.3333 | | | 5417 | 5787.0000 | | |
| 9928 | 5719.2222 | | | 6839 | 11375.0000 | | |
| | | | | 7779 | 8508.0000 | | |
| | | | | 8417 | 8964.1111 | | |
| Sample ID | control | Sample ID | control | Sample ID | control | Sample ID | Control |
| 17424 | 10449.3333 | 21486 | 12870.0000 | 2741 | 10783.7778 | 5783 | 12284.8889 |
| 17297 | 10298.3333 | 17370 | 10947.6667 | 17170 | 11149.6667 | 17125 | 11509.1111 |
| 9178 | 10247.4444 | 17268 | 10526.5556 | 3371 | 9004.2222 | | |
| 4650 | 9936.2222 | 20834 | 10784.7778 | 3319 | 11528.4444 | | |
| 8170 | 12849.7778 | 17468 | 9984.0000 | 3754 | 10559.2222 | | |
| 6194 | 10483.1111 | | | 9503 | 10829.1111 | | |
| 20483 | 10118.6667 | | | 8441 | 10719.6667 | | |
| | | | | 4185 | 12375.5556 | | |
| | | | | 17180 | 14465.7778 | | |

**Table 26: Mean values and standard deviations of fluorescence intensities in Table 16**

| | Ductal Adenocarcinoma | | Neuroendocrine Tumor | | Metastatic Adenocarcinoma | | Metastatic Neuroendocrine | |
|---|---|---|---|---|---|---|---|---|
| | Control | Patient | Control | Patient | Control | Patient | Control | Patient |
| mean | 10626.1 | 9640.17 | 11022.60 | 11443.62 | 11268.3827 | 8351.6049 | 11897.0000 | 10407.7778 |
| SD | 998.387 | 2375.39 | 1095.4236 | 2031.750 | 1495.3726 | 2742.9787 | 548.5577 | 120.6796 |

**Table 27: Fluorescence intensity data and p-values for UpA in Fig 28**

| Ductal Adenocarcinoma | | Neuroendocrine Tumor | | Metastatic Adenocarcinoma | | Metastatic Neuroendocrine | |
|---|---|---|---|---|---|---|---|
| Sample ID | patient | Sample ID | patient | Sample ID | patient | Sample ID | patient |
| 2720 | 159.0000 | 5327 | 107.8889 | 2689 | 193.3333 | 851 | 130.1111 |
| 4236 | 143.8889 | 5247 | 117.7778 | 2996 | 353.6667 | 7428 | 91.1111 |
| 4967 | 114.1111 | 7433 | 93.0000 | 3824 | 100.7778 | | |
| 7253 | 111.2222 | 9829 | 152.8889 | 5273 | 164.1111 | | |
| 8306 | 109.3333 | 10550 | 107.5556 | 5237 | 148.6667 | | |
| 9620 | 130.6667 | | | 5417 | 106.3333 | | |
| 9928 | 152.0000 | | | 6839 | 111.1111 | | |
| | | | | 7779 | 121.8889 | | |
| | | | | 8417 | 219.2222 | | |
| Sample ID | control | Sample ID | control | Sample ID | control | Sample ID | control |
| 17424 | 110.8889 | 21486 | 104.1111 | 2741 | 118.0000 | 5783 | 108.1111 |
| 17297 | 108.0000 | 17370 | 77.6667 | 17170 | 102.6667 | 17125 | 104.1111 |
| 9178 | 87.5556 | 17268 | 108.5556 | 3371 | 97.0000 | | |
| 4650 | 102.4444 | 20834 | 138.3333 | 3319 | 104.7778 | | |
| 8170 | 110.8889 | 17468 | 100.0000 | 3754 | 98.8889 | | |
| 6194 | 118.2222 | | | 9503 | 99.4444 | | |
| 20483 | 117.4444 | | | 8441 | 118.5556 | | |
| | | | | 4185 | 112.8889 | | |
| | | | | 17180 | 129.6667 | | |

**Table 28: Mean values and standard deviations of fluorescence intensities in Table 18**

| | Ductal Adenocarcinoma | | Neuroendocrine Tumor | | Metastatic Adenocarcinoma | | Metastatic Neuroendocrine | |
|---|---|---|---|---|---|---|---|---|
| | Control | Patient | Control | Patient | Control | Patient | Control | Patient |
| mean | 107.9206 | 131.4603 | 105.7333 | 115.8222 | 109.0988 | 168.7901 | 106.1111 | 110.6111 |
| SD | 10.4816 | 20.5572 | 21.7599 | 22.5272 | 11.2358 | 80.4713 | 2.8284 | 27.5772 |

**Table 29: Fluorescence intensity data and p-values for MMP-1 in Fig 29**

| Ductal Adenocarcinoma | | Neuroendocrine Tumor | | Metastatic Adenocarcinoma | | Metastatic Neuroendocrine | |
|---|---|---|---|---|---|---|---|
| Sample ID | patient | Sample ID | patient | Sample ID | patient | Sample ID | patient |
| 2720 | 647.7778 | 5327 | 431.2222 | 2689 | 611.6667 | 851 | 583.4444 |
| 4236 | 592.1111 | 5247 | 328.6667 | 2996 | 494.6667 | 7428 | 293.0000 |
| 4967 | 483.3333 | 7433 | 291.2222 | 3824 | 471.0000 | | |
| 7253 | 326.7778 | 9829 | 321.7778 | 5273 | 607.2222 | | |
| 8306 | 312.3333 | 10550 | 231.8889 | 5237 | 533.2222 | | |
| 9620 | 297.5556 | | | 5417 | 325.5556 | | |
| 9928 | 323.4444 | | | 6839 | 305.0000 | | |
| | | | | 7779 | 252.7778 | | |
| | | | | 8417 | 239.4444 | | |
| Sample ID | control | Sample ID | control | Sample ID | control | Sample ID | control |
| 17424 | 492.0000 | 21486 | 337.5556 | 2741 | 495.3333 | 5783 | 348.7778 |
| 17297 | 540.7778 | 17370 | 264.4444 | 17170 | 511.5556 | 17125 | 223.6667 |
| 9178 | 222.3333 | 17268 | 249.1111 | 3371 | 422.0000 | | |
| 4650 | 384.7778 | 20834 | 269.2222 | 3319 | 339.0000 | | |
| 8170 | 223.5556 | 17468 | 280.7778 | 3754 | 230.5556 | | |
| 6194 | 241.4444 | | | 9503 | 412.6667 | | |
| 20483 | 292.3333 | | | 8441 | 189.8889 | | |
| | | | | 4185 | 181.8889 | | |
| | | | | 17180 | 207.1111 | | |

**Table 30: Mean values and standard deviations of fluorescence intensities in Table 20**

| | Ductal Adenocarcinoma | | Neuroendocrine Tumor | | Metastatic Adenocarcinoma | | Metastatic Neuroendocrine | |
|---|---|---|---|---|---|---|---|---|
| | Control | Patient | Control | Patient | Control | Patient | Control | Patient |
| mean | 342.4603 | 426.1905 | 280.2222 | 320.9556 | 332.2222 | 426.7284 | 286.2222 | 438.2222 |
| SD | 132.1416 | 147.1088 | 34.0046 | 72.5186 | 133.3186 | 147.9377 | 88.4669 | 205.3752 |

**Table 31: Fluorescence intensity data and p-values for MMP-3 in Fig 30**

| Ductal Adenocarcinoma | | Neuroendocrine Tumor | | Metastatic Adenocarcinoma | | Metastatic Neuroendocrine | |
|---|---|---|---|---|---|---|---|
| Sample ID | patient | Sample ID | patient | Sample ID | patient | Sample ID | patient |
| 2720 | 94.8889 | 5327 | 60.1111 | 2689 | 89.8889 | 851 | 73.3333 |
| 4236 | 85.6667 | 5247 | 74.1111 | 2996 | 307.3333 | 7428 | 66.2222 |
| 4967 | 64.4444 | 7433 | 59.4444 | 3824 | 66.7778 | | |
| 7253 | 70.6667 | 9829 | 63.1111 | 5273 | 80.8889 | | |
| 8306 | 78.0000 | 10550 | 49.0000 | 5237 | 82.1111 | | |
| 9620 | 85.7778 | | | 5417 | 66.6667 | | |
| 9928 | 100.1111 | | | 6839 | 68.5556 | | |
| | | | | 7779 | 68.5556 | | |
| | | | | 8417 | 76.3333 | | |
| Sample ID | control | Sample ID | control | Sample ID | control | Sample ID | control |
| 17424 | 77.6667 | 21486 | 63.7778 | 2741 | 64.3333 | 5783 | 70.3333 |
| 17297 | 76.1111 | 17370 | 53.2222 | 17170 | 75.2222 | 17125 | 53.5556 |
| 9178 | 53.5556 | 17268 | 47.8889 | 3371 | 70.5556 | | |
| 4650 | 73.2222 | 20834 | 60.4444 | 3319 | 68.8889 | | |
| 8170 | 62.5556 | 17468 | 48.8889 | 3754 | 59.8889 | | |
| 6194 | 53.7778 | | | 9503 | 66.5556 | | |
| 20483 | 45.3333 | | | 8441 | 56.8889 | | |
| | | | | 4185 | 48.6667 | | |
| | | | | 17180 | 59.2222 | | |

**Table 32: Mean values and standard deviations of fluorescence intensities in Table 22**

| | Ductal Adenocarcinoma | | Neuroendocrine Tumor | | Metastatic Adenocarcinoma | | Metastatic Neuroendocrine | |
|---|---|---|---|---|---|---|---|---|
| | Control | Patient | Control | Patient | Control | Patient | Control | Patient |
| mean | 63.1746 | 82.7937 | 54.8444 | 61.1556 | 63.3580 | 100.7901 | 61.9444 | 69.7778 |
| SD | 12.7662 | 12.7154 | 7.0293 | 8.9923 | 8.0712 | 77.8792 | 11.8637 | 5.0283 |

**Table 33: Fluorescence intensity data and p-values for MMP-9 in Fig 31**

| Ductal Adenocarcinoma | | Neuroendocrine Tumor | | Metastatic Adenocarcinoma | | Metastatic Neuroendocrine | |
|---|---|---|---|---|---|---|---|
| Sample ID | patient | Sample ID | patient | Sample ID | patient | Sample ID | patient |
| 2720 | 174.1111 | 5247 | 229.6667 | 2689 | 271.1111 | 851 | 174.7778 |
| 4236 | 246.5556 | 7433 | 157.0000 | 2996 | 322.4444 | 7428 | 156.0000 |
| 4967 | 167.7778 | 9829 | 151.7778 | 3824 | 185.6667 | | |
| 7253 | 180.7778 | 10550 | 192.2222 | 5273 | 178.0000 | | |
| 8306 | 193.2222 | | | 5237 | 178.5556 | | |
| 9620 | 205.7778 | | | 5417 | 137.1111 | | |
| 9928 | 176.4444 | | | 6839 | 159.0000 | | |
| | | | | 7779 | 192.7778 | | |
| | | | | 8417 | 156.8889 | | |
| Sample ID | control | Sample ID | control | Sample ID | control | Sample ID | control |
| 17424 | 151.3333 | 21486 | 192.3333 | 2741 | 179.8889 | 5783 | 182.7778 |
| 17297 | 203.1111 | 17370 | 152.1111 | 17170 | 185.6667 | 17125 | 202.7778 |
| 9178 | 152.8889 | 17268 | 205.2222 | 3371 | 140.2222 | | |
| 4650 | 159.0000 | 20834 | 183.8889 | 3319 | 179.7778 | | |
| 8170 | 183.4444 | 17468 | 181.6667 | 3754 | 171.3333 | | |
| 6194 | 176.5556 | | | 9503 | 164.3333 | | |
| 20483 | 168.4444 | | | 8441 | 179.1111 | | |
| | | | | 4185 | 193.7778 | | |
| | | | | 17180 | 210.1111 | | |

**Table 34: Mean values and standard deviations of fluorescence intensities in Table 24**

| | Ductal Adenocarcinoma | | Neuroendocrine Tumor | | Metastatic Adenocarcinoma | | Metastatic Neuroendocrine | |
|---|---|---|---|---|---|---|---|---|
| | Control | Patient | Control | Patient | Control | Patient | Control | Patient |
| mean | 170.6825 | 192.0952 | 183.0444 | 183.6667 | 178.2469 | 197.9506 | 192.7778 | 165.3889 |
| SD | 18.6256 | 27.2097 | 19.6062 | 36.1165 | 19.3799 | 59.9038 | 14.1421 | 13.2779 |

**Table 35: Fluorescence intensity data and p-values for Neutrophil Elastase in Fig 32**

| Ductal Adenocarcinoma | | Neuroendocrine Tumor | | Metastatic Adenocarcinoma | | Metastatic Neuroendocrine | |
|---|---|---|---|---|---|---|---|
| Sample ID | patient | Sample ID | patient | Sample ID | patient | Sample ID | patient |
| 2720 | 3973.5556 | 5327 | 1767.2222 | 2689 | 3517.2222 | 851 | 2163.1111 |
| 4236 | 3367.7778 | 5247 | 2012.5556 | 2996 | 1038.7778 | 7428 | 1477.5556 |
| 4967 | 1811.1111 | 7433 | 1453.0000 | 3824 | 2700.5556 | | |
| 7253 | 1661.4444 | 9829 | 1650.0000 | 5273 | 1841.3333 | | |
| 8306 | 1664.6667 | 10550 | 1601.7778 | 5237 | 1978.6667 | | |
| 9620 | 1456.7778 | | | 5417 | 1138.1111 | | |
| 9928 | 1172.0000 | | | 6839 | 1491.1111 | | |
| | | | | 7779 | 1433.3333 | | |
| | | | | 8417 | 1655.2222 | | |
| Sample ID | control | Sample ID | control | Sample ID | control | Sample ID | control |
| 17424 | 2889.1111 | 21486 | 1794.6667 | 2741 | 2675.3333 | 5783 | 1638.4444 |
| 17297 | 1954.2222 | 17370 | 1329.4444 | 17170 | 2004.1111 | 17125 | 1778.8889 |
| 9178 | 1350.0000 | 17268 | 1694.8889 | 3371 | 1587.4444 | | |
| 4650 | 1559.2222 | 20834 | 1436.6667 | 3319 | 1571.3333 | | |
| 8170 | 1982.7778 | 17468 | 1506.1111 | 3754 | 1636.7778 | | |
| 6194 | 1548.2222 | | | 9503 | 1496.4444 | | |
| 20483 | 1497.2222 | | | 8441 | 1691.0000 | | |
| | | | | 4185 | 1699.4444 | | |
| | | | | 17180 | 2033.5556 | | |

**Table 36: Mean values and standard deviations of fluorescence intensities in Table 26**

| | Ductal Adenocarcinoma | | Neuroendocrine Tumor | | Metastatic Adenocarcinoma | | Metastatic Neuroendocrine | |
|---|---|---|---|---|---|---|---|---|
| | Control | Patient | Control | Patient | Control | Patient | Control | Patient |
| mean | 1825.8254 | 2158.1905 | 1552.3556 | 1696.911 | 1821.7160 | 1866.037 | 1708.6667 | 1820.3333 |
| SD | 525.0757 | 1067.2386 | 189.8962 | 209.3554 | 370.2063 | 792.3547 | 99.3092 | 484.7610 |